REPORT NO.
UCB/EERC-95/11
OCTOBER 1995

EARTHQUAKE ENGINEERING RESEARCH CENTER

STUDIES IN STEEL MOMENT RESISTING BEAM-TO-COLUMN CONNECTIONS FOR SEISMIC-RESISTANT DESIGN

by

BRENT BLACKMAN
EGOR P. POPOV

A report to: National Science Foundation
American Institute of Steel Construction

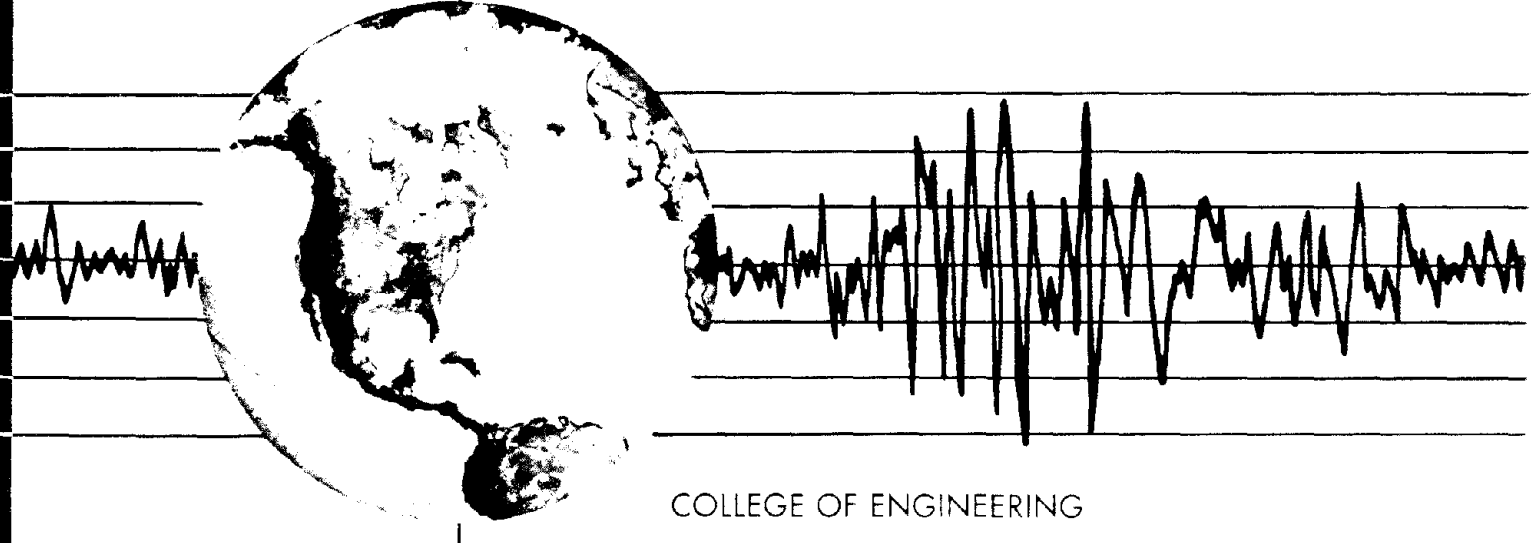

COLLEGE OF ENGINEERING

UNIVERSITY OF CALIFORNIA AT BERKELEY

STUDIES IN
STEEL MOMENT RESISTING BEAM-TO-COLUMN CONNECTIONS
FOR SEISMIC-RESISTANT DESIGN

by

Brent Blackman

and

Egor P. Popov

UCB/EERC-95/11
Earthquake Engineering Research Center
College of Engineering
University of California at Berkeley

October, 1995

ABSTRACT

Prior to the January 17, 1994 Northridge Earthquake, special moment resisting framed buildings constructed of steel were considered the best in seismic-resistant design. Although some researchers suggested that the welded beam-to-column connections used in such structures were potentially fallible, structural engineers, steel erectors, and building officials entrusted this type of structural system because of its perceived ability to absorb earthquake energy. After the earthquake, however, brittle failures were discovered in over 150 buildings, many which were designed and constructed according to contemporary standards. As a result, this report explores the primary reasons for such unexpected failures and attempts to provide methods of economically improving the performance of new connections.

First, a historical chapter presents background information regarding the development of earthquake-resistant design standards in building codes as well as the evolution of moment resisting beam-to-column connections used in areas of high seismicity in the United States. An emphasis is placed in how San Francisco responded to repeated earthquakes during the late 19th and early 20th centuries and how the advancement of technology in steel construction led to the welded steel structures of today. In addition, the deficiencies that were reported in unbraced steel framed structures following the 1906 San Francisco Earthquake are discussed. Then, three contemporary, full-scale subassemblages are examined to determine the underlying causes of poor performance during the Northridge Earthquake. These specimens, which were tested under the SAC Joint Venture Program, utilized materials, member sizes, and details representative of connections damaged during the earthquake. After these specimens were tested, two new connections were experimentally investigated in an attempt to improve the ductility and energy absorption capacities of such joints. The first incorporated of an all-welded, reinforced connection with a separated continuity plate configuration and "relief" holes and the second consisted of an I-beam to box-column connection with external tee stiffeners in place of internal continuity plates.

The first and second pre-Northridge specimens experimentally reproduced the brittle column flange fractures that were observed in structures that experienced the Northridge

Earthquake. The third pre-Northridge test duplicated another type of brittle failure reported in damaged structures; the beam flange-to-column flange welds cracked. It is believed that the brittle modes of failure can be partially attributed to the artificial cracks between the backup bars and column flange and the direction of crack propagation is most likely dependent on the strength of beam material used as well as the amount of panel zone activity. In comparison to these results, the all-welded, reinforced connection performed slightly better, however, it did not meet the criteria for successful performance provided by other researchers (namely Engelhardt and Sabol, 1994). It is believed that the slight improvement was attributed to the welded web detail as well as the removal of backup bars and subsequent placement of reinforcing fillet welds at the beam flange-to-column flange groove welds. Nevertheless, the "relief" holes drilled in the web of the column are believed to be the primary cause of brittle failure. Next, the I-beam to box-column specimen performed rather well, meeting the plastic rotation and energy dissipation goals. Similar to the all-welded connection, the removal of backup bars and placement of reinforcing fillet welds appeared to improve the ductility. Although a brittle failure occurred as a result of a premature fillet weld tear, it is believed that a ductile mode of failure can be achieved with simple design modifications. Thus, removing backup bars, placing reinforcing fillet welds, and providing an all-welded, reinforced connection will improve the performance of standard beam-to-column connections. However, drilling "relief" holes in the column web is not suggested. Likewise, the use of external stiffeners promises to be a valuable technique for improving the performance and economy of I-beam to box-column connections.

ACKNOWLEDGEMENTS

This report was completed with the support of the National Science Foundation (NSF) under the grant entitled *Re-evaluation of Conventional Seismic Beam-to-Column Flange Steel Connections* (CMS-9416457). Supplementary funding and arrangements for donations of structural steel were provided by the American Institute of Steel Construction (AISC). Drs. S.-C. Liu and M. P. Sing monitored the project for NSF, and Mr. Nestor Iwankiw for AISC. Mr. Fred Long of PDM Strocal and Mr. Roger Ferch of the Herrick Corporation provided fabrication services at no charge. This report is filed by the first author in fulfillment of the requirements for the degree of Master of Engineering (M. Eng). As part of the same program, a second report is being finalized for a doctoral dissertation by Mr. Tzong-Shuoh Yang.

Professor Stephen A. Mahin and Mr. James O. Malley of the SAC Joint Venture are sincerely thanked for coordinating the pre-Northridge tests. Likewise, the Department of Civil Engineering at the University of California at Berkeley is recognized for providing free hours of shop labor at Davis Hall as part of the Master's program. Special thanks are offered to Professor Mahin for serving as the second advisor. The assistance provided by Professor Stephen Tobriner and Mr. Duc Tran in preparing the historical chapter and figures, respectively, and by Kathryn Cunningham for editing the draft of this report are sincerely appreciated.

The following individuals are acknowledged for their assistance in instrumenting the specimens: Ms. Hana Mori, Professor Bozidar Stojadinovic, Dr. Chiao-Tung Chang, Mr. Tzong-Shuoh Yang, Dr. Lev Stepanov, Mr. Shih-Po Chang, and Mr. Edgar Castro.

The following shop personnel are also acknowledged for their assistance: Dr. Marcial Blondet, Principal Development Engineer, Mr. Larry Baker, Shop Superintendent; Mr. Todd Merport and Mr. Chris Moy, Electronic Engineers; as well as Mr. Jon Asselanis and Mr. Bill MacCracken, who assisted in the execution and video taping of experiments, respectively.

TABLE OF CONTENTS

page

ABSTRACT i
ACKNOWLEDGEMENTS iii
TABLE OF CONTENTS iv
1. INTRODUCTION 1
1.1 General 1
1.2 Moment Resisting Frames 4
1.3 Beam-to-Column Connections 5
1.4 The 1994 Northridge Earthquake 6
1.5 Research Program 7
2. BACKGROUND 9
2.1 Earthquake-Resistant Design in the Codes 9
2.1.1 The First Steps 9
2.1.2 Acceptance and Consensus 10
2.1.3 Implementation 11
2.2 Evolution of Beam-to-Column Connections of Unbraced Steel Framed Buildings 13
2.2.1 Building Design Before the 1906 San Francisco Earthquake 13
2.2.2 Results of the 1906 Earthquake 15
2.2.3 1930s 15
2.2.4 1950s - 1960s 16
2.2.5 1980s 17

3. STANDARD PRE-NORTHRIDGE CONNECTION 19
3.1 The SAC Joint Venture 19
3.2 Description of Test Specimens 20
3.3 Execution of Experiment 21
3.4 Experimental Results 22
3.4.1 Specimen PN1 23
3.4.2 Specimen PN2 24
3.4.3 Specimen PN3 26
3.5 Summary of Findings 27
4. NEW CONNECTIONS 30
4.1 Experimental Program 30
4.2 Experimental Setup, Instrumentation, and Loading Sequence 30
4.3 NSF Specimen #1 31
4.3.1 Fabrication and Inspection 32
4.3.2 Experimental Results 34
4.4 NSF Specimen #6 37
4.4.1 Recent Experimental Research 38
4.4.2 Design 39
4.4.3 Experimental Results 45
4.5 Summary of Findings 48
4.5.1 NSF Specimen #1 48
4.5.2 NSF Specimen #6 48
5. CONCLUSION 51
5.1 Pending Research 51
5.2 Suggestions for Further Research 52
5.3 The Limitations of Codes and Experimental Findings in Design 52
APPENDIX A. SNUBBER PLATES FOR TEST SETUP 53
APPENDIX B. FAILURE OF NSF SPECIMEN #1 62
TABLES 65
FIGURES 67
REFERENCES 132

1. INTRODUCTION

1.1 General

The intent of contemporary building codes is to provide minimum design standards that maintain safety for the building's occupants during all levels of earthquake ground motion. Although much of the public believes that these codes, if followed, produce "earthquake-proof" buildings, the term "earthquake-proof" is a misnomer; no structure may be designed with such a guarantee. Rather, engineers and architects merely use these standards to design buildings that are earthquake-resistant, meaning they will not collapse. For this purpose, gravity and seismic forces in structures must be transferred to the ground through a continuous load path, which consists of both a vertical and lateral force resisting system. Thus, the fundamental concern addressed in the codes is to insure that buildings will be designed to prevent collapse.

The *Recommended Lateral Force Requirements and Commentary* [1], published in 1990 by the Seismology Committee of the Structural Engineers Association of California, hereafter SEAOC, summarizes the design objectives of building codes. Chapter 1, Section 1A.1 of the Commentary, states that:

> "[S]tructures...should, in general, be able to:
> 1. Resist a minor level of earthquake ground motion without damage;
> 2. Resist a moderate level of earthquake ground motion without structural damage, but possibly experience some nonstructural damage;
> 3. Resist a major level of earthquake ground motion having an intensity equal to the strongest either experienced or forecast for the building site, without collapse, but possibly with some structural damage as well as nonstructural damage [1]."

Furthermore, "these Recommendations are intended to provide the minimum required resistance to earthquake ground shaking. It is not the intent of the Recommendations, however, to limit damage, maintain functions, or provide for easy repair [1]."

Prior to designing a structure that prevents catastrophic failure and loss of life, the size and configuration of the seismic forces must be defined. Since the current approach used to determine these forces relies on inelastic behavior, or damage, as an energy dissipating technique, buildings are not designed to be strong enough to remain elastic during the highest level earthquake expected at the site. Experience has shown that a reduction of the estimated earthquake force transmitted to the building is sufficient to design safe and cost-effective

structures. Therefore, it is standard practice to design for a reduced force, referred to as the seismic design force. This force is dependent on the type of material and lateral force resisting system that is chosen for the building as well as the seismicity of the region [2].

The structural design of most buildings that are located in the active seismic areas of the United States is currently governed by the 1994 Edition of the *Uniform Building Code*, commonly referred to as the UBC [3]. There are two basic procedures used to define seismic design force: the equivalent static force procedure, and the dynamic lateral force procedure. Although static forces do not represent the true dynamic nature of earthquake response, buildings are typically analyzed by this static procedure without the proof of dynamic response data. The consensus is that the static procedure adequately represents the dynamic behavior of regular structures, which have a reasonably uniform distribution of mass and stiffness [4].

Nevertheless, for irregular structures that do not fit into this category, the static lateral force procedure may not achieve accurate results. Thus, a dynamic analysis is required. For the purpose of this report, however, only the static lateral force procedure will be discussed in more detail. For an excellent discussion of both response spectrum analysis (RSA) and response history analysis (RHA) the reader is referred to Anil K. Chopra's book *The Dynamics of Structures* [2].

The static lateral force procedure requires that structures be designed to resist a reduced static lateral force applied to the building, referred to as the base shear. With an estimate of the fundamental natural period of the structure, formulas are specified for the base shear and distribution of lateral force over the height of the building [2]. The 1994 UBC has adopted the SEAOC recommended formulas to calculate the base shear and appropriately distribute this force to the various floor levels. The static lateral force procedure is summarized below.

The design base shear is:

$$V_b = \frac{Z I C}{R_w} W \tag{1-1}$$

where: Z is the seismic zone factor
I is the importance factor
W is the total seismic dead load of the building
R_w is the structural system coefficient
and C is a numerical coefficient that is equal to:

$$C = 1.25 S / T^{2/3} \tag{1-2}$$

where: S is the site coefficient for soil characteristics
and T is the fundamental period of vibration, which is equal to:

$$\mathbf{T = C_t\, h_n^{3/4} \leq 2.75} \tag{1-3}$$

where: C_t = 0.035 for steel moment frames
0.030 for reinforced concrete moment frames and eccentric braced frames
0.020 for all other buildings
h_n = height, in feet, above the base to level n

Then, once the base shear is determined, it is distributed to each floor as:

$$F_x = \frac{(V_b - F_t)\, w_x h_x}{\sum_{i=1}^{n} w_i h_i} \tag{1-4}$$

The force at the top floor is:

$$\begin{aligned} \mathbf{F_t} &= \mathbf{0} && \textbf{for } T \leq 0.7 \\ & \quad \mathbf{0.07\, T\, V_b} && \textbf{for } 0.7 < T < 3.6 \\ & \quad \mathbf{0.025\, V_b} && \textbf{for } T \geq 3.6 \end{aligned} \tag{1-5}$$

The seismic zone map of the United States (Figure 1-1) shows the five areas of seismic activity. Each zone is based on the maximum peak ground acceleration of the area in question. In most cases, the site's proximity to active faults and the measured accelerations from that region determine the seismic zone. A comparison of the fault locations in California (Figure 1-2) and the seismic zone map of California (Figure 1-3) shows that zone 4 encompasses all major active faults that have been discovered in the state. The maximum earthquake ground motion that seismologists determine is expressed in the UBC as the seismic zone factor Z and the numerical coefficient C. Once the seismic zone factor is defined, it is used to scale the response spectrum represented by C, where C is dependent on the local soil conditions and the period of the structure. The factor I distinguishes the importance of facilities and adds a 25 percent factor of safety for those considered essential and hazardous. Hospitals and fire stations, for example, have an importance factor of 1.25, whereas, the factor is 1.0 for single family homes. Thus, if the designer uses the value Z C multiplied by the weight of the building (W) for the design base shear, then the structure is expected to have a 90 percent chance of suffering no structural damage (remain elastic) during a 50 year period.

The code specified forces of the static lateral force procedure, however, are lower than those that the structure would experience during a moderate or major level earthquake [4]. That is, the design base shear is not only dependent on the seismicity of the region (Z and C), but also on the performance of the structural system (R_w). The value of R_w is dependent on the ductility capacity and inelastic performance of the material used in the structure [2]. Depending on the system chosen, the coefficient can be as high as 12, which results in the lowest design forces. For this reason, it is expected that properly designed structures will dissipate the energy of an earthquake through either inelastic deformation or damage, depending on the intensity of the earthquake.

1.2 Moment Resisting Frames

The two most common configurations used to resist seismic forces in steel buildings are braced frames and unbraced frames. Braced frames are those which the lateral stability of the building is provided by diagonal bracing. Depending on where the braces are connected to the beams, braced frames are considered either concentric or eccentric. Concentrically braced frames have braces that are connected only at locations where beams and columns intersect, whereas, the braces in eccentrically braced frames do not all connect at beam-column intersections. Unbraced frames, on the other hand, do not rely on braces for lateral stability. Rather, they depend on the flexural rigidities of the beams and columns, which are joined at moment resisting connections. For this reason, unbraced frames are commonly referred to as moment resisting frames.

For most of the last twenty five years, steel moment resisting frames have been the most popular structural systems chosen for office buildings because of their architectural flexibility and economy. Aesthetically, building owners prefer the accessibility of the large spanned, open bays that moment resisting frames can provide. More recently, through the use of larger members and increased strength, fewer columns are used to support such buildings, resulting in additional architectural appeal.

For the engineers who design these structures, however, beauty and convenience are not as meaningful. Engineers need to have confidence in the structure's ability to perform well in earthquakes. This confidence is reflected in structural system coefficient R_w, which is defined as 12 for "special" moment resisting frames. The term "special" refers to the reliability in the ductile behavior of the structural system. For this reason, R_w equals 12 for special moment

resisting frames, corresponding a design for only 1/12, or approximately eight percent of the maximum expected ground acceleration at the site. As a result of the widespread acceptance between owners, architects, and engineers, there are currently thousands of special moment resisting framed buildings in California alone.

1.3 Beam-to-Column Connections

Special moment resisting frames must possess proper strength, stiffness, and ductility to provide resistance to lateral earthquake forces. In the design of these structures, it is common practice to limit inelastic deformation of the system to the beams and, in some cases, to the area of the column web between the continuity plates, or panel zone. It is this inelastic deformation, commonly referred to as plastic hinging, that is so important in contemporary seismic-resistant design because its ability to dissipate earthquake energy within in the structure. Usually, preventing plastic hinges from forming in columns is desirable since it tends to improve the lateral stability of the structure. This strong column-weak beam collapse mechanism is commonly used to calculate the lateral stability of structures through a push-over analysis.

Of equal importance, are connections between beams and columns. These beam-to-column connections must allow large beams rotations to occur so that plastic hinges can form within the beams. Figure 1-4 shows the performance of four types of moment connections subjected to a seismic force. A simple measure of performance is the area contained within the force-displacements loops, which defines the amount of energy dissipated. As a "rule-of-thumb," poor connections either lack ductility (Figure 1-4b), strength (Figure 1-4c), or stiffness (Figure 1-4d). Whereas a desirable connection, shown in Figure 1-4a, dissipates the largest of the amount of energy. Thus, connections must have sufficient ductility, strength, and stiffness.

In order to achieve proper performance in an economical manner, the majority of moment-resistant steel structures in the United States consist of I-shaped beam and column members that are rigidly connected at intersections. The free body diagram for such connections subjected to load reversals is shown in Figure 1-5. Typical beam-to-column connections, which allow a reduction of $R_w = 12$, are required to develop the plastic moment capacity of the beam M_p, where:

$$\mathbf{M_p = Z\ F_y} \qquad (1\text{-}6)$$

Z is the plastic section modulus (in^3) and F_y is the yield strength of the beam material (ksi). The

resulting beam flange forces, defined as T_p, can be calculated by the equation:

$$T_p = M_p / 0.95\, d_b \qquad (1\text{-}7)$$

where d_b is the depth of the beam (in). Figure 1-6 depicts common configurations for both strong and weak-axis connections in the United States. Until recently, the most popular connection consisted of full penetration welds from the beam flanges to the column (to develop T_p) and a beam web-to-column connection (to transmit the shear force V). Evidence of this connection's popularity lies in its prequalification, or predetermined adequacy, in the UBC as well as in both of the most recent publications of the American Institute of Steel Construction (AISC): *Allowable Stress Design* (ASD) and *Load and Resistance Factor* Design (LRFD).

1.4 The 1994 Northridge Earthquake

Over the last twenty five years, the engineering profession has placed an increasing amount of confidence in the *expected* ductile behavior of special moment resisting frames. It was believed that laboratory tests over the years confirmed the performance of prequalified connections used in such structures. But on January 17, 1994, the welds of over 150 steel buildings failed when a Magnitude 6.8 earthquake hit Northridge, California. Considered a moderate level earthquake by most standards, the type of damage to these connections was completely *unexpected* - the connections simply "unzipped."

At first, inspectors scanning the city for damage thought that special moment resisting frames had suffered no damage because none had collapsed. In the weeks and months to follow, however, a permanent drift, or leaning was observed in these buildings and at that point, engineers knew something had gone wrong. After removing the cladding and fire proofing, inspectors discovered that fractures had occurred around the beam-to-column connection welds. Over 75 percent of the buildings inspected thus far suffered such damage and it is believed that closer examination will detect even more buildings. But, this is not just a Los Angles problem, it is also a nation-wide and international problem. Similar damage has been discovered in buildings located near the Landers Earthquake, the Big Bear Earthquake (Big Bear Lake City Hall damaged), and although it has not been proven, it is even believed that steel moment framed buildings that experienced the Hyogoken-Nanbu (Kobe) Earthquake may also have suffered similar damage.

The numerous brittle fractures that plagued special moment resisting frames affected all building types: old, new, tall, and short. As a result, the prequalified connections of the UBC and AISC design codes were invalidated and emergency ordinances were passed to stop construction and design of moment resisting connections. Thus, a dilemma had arisen for the owners and engineers of special moment resisting frames. What was to be done with damaged buildings, undamaged buildings, and the design of new buildings?

Currently, Los Angeles only requires that damaged connections be repaired to the strength prior to the earthquake. There is no requirement to reconfigure the connection. But if building owners are interested in protecting their investments against damage in future earthquakes, it is clear that much more must be done. Although recent tests at the University of Texas as well as other universities have shown promise, the amount of knowledge available is insufficient - there is no "quick fix" [5]. Furthermore, the structural engineering profession has not reached a consensus regarding these connections.

1.5 Research Program

The amount of damage encountered by special moment frames during the 1994 Northridge Earthquake and more recent earthquakes has raised several questions that require immediate response. As a result, SAC Joint Venture, the National Science Foundation (NSF), and the American Institute of Steel Construction (AISC) are funding research programs in an attempt to answer these questions. The SAC Joint Venture, which consists of SEAOC, the Applied Technology Council (ATC), and the California Universities for Research in Earthquake Engineering (CUREE), was established following the Northridge Earthquake in an attempt to address immediate as well as long term needs of the steel construction industry. In addition, the NSF and AISC are also funding other research efforts with similar goals. In total, millions of dollars will be directed toward solving steel moment frame problems.

The research discussed in this report consists of two parts, both under the supervision of Professor Egor P. Popov, principal investigator and my research advisor. All research discussed in this report was conducted at the Davis Hall Testing Facility, which is located on the campus of the University of California at Berkeley. The objective and scope of the first part, which is funded by SAC, is to determine why the standard connection that was commonly used prior to the Northridge Earthquake had performed inadequately during the earthquake, and how the

damage can be repaired. These specimens, which are discussed in Chapter 3 of this report, are referred to as PN1, PN2, and PN3 - where PN stands for pre-Northridge.

The objective of the second part of this research, which is discussed in Chapter 4 of this report, is to find connections for use in new buildings or as retrofit for existing undamaged buildings. Funded by the NSF and AISC, nine connections in all will be tested at the Davis Hall Testing Facility. The scope of this report, however, is to provide a detailed discussion of the design, experimentation, and results of Specimen #1 and Specimen #6. The discussion of most other specimens will be included in the dissertation of T-S. Yang [28].

2. BACKGROUND

2.1 Earthquake-Resistant Design in the Codes

The addition of earthquake-resistant design to building codes in the United States took place over several decades from the late 19th to early 20th century. Following the San Francisco earthquakes of 1865 and 1868, almost all architects and engineers were opposed to the change since few if any understood the technical nature of earthquakes. Although some attempts were made to design "earthquake-proof" buildings prior to the 1906 earthquake, there was no standardized method to define seismic forces. Architects and engineers believed that a 30 pounds per square foot (psf) wind resistance was more than adequate, even in San Francisco. But after observing the widespread damage that occurred as a result of the 1906 earthquake, resistance to change within the engineering community rapidly diminished. For policy makers, however, the transition was much more gradual since business interests were involved. Finally, in 1927, the first seismic-resistant design requirements appeared in the Uniform Building Code, 175 years after the first seismic code in Europe [6].

2.1.1 The First Steps

During the late 19th Century, there was little concern about the damaging effects of earthquake ground motion in the United States, even though damage occurred as a result of several earthquakes in the country's history (Boston, 1755; New Madrid, 1812; and Charleston, 1886). Since very few people had experienced them, most architects and engineers in the United States believed that "the effects of earthquakes would scarcely seem to warrant much consideration [7]." At the time, the only requirement for lateral force-resistance in the United States was to design for a wind pressure of 30 psf on the windward side of tall buildings in Chicago, a standard also adopted in San Francisco.

The debate over the adequacy of wind-resistant versus the need for earthquake-resistant design of structures emerged following two major earthquakes that hit the Bay Area, the first in 1865 and the second in 1868. In most cases, structural failures that occurred as a result of these earthquakes were blamed on improper construction and/or defective materials. Although this may have been true to some extent, an engineer named Henry H. Quimby was not a complete believer. In a paper titled "Wind Bracing for Tall Buildings," he warned that wind-resistant design may

be insufficient to protect against damage caused by seismic activity [8]. Nevertheless, San Francisco did not establish requirements for earthquake-resistant design. The consensus was that buildings designed for 30 psf wind resistance were "amply provided to withstand earthquakes [7]."

Possibly even more important than the lack of a consensus among engineers, however, the City of San Francisco feared the economic impact of being "singled out" from the rest of the country. First of all, if word got out that San Francisco was a dangerous area because of earthquakes, then tourists and workers from the East Coast might be reluctant to come. Second, more stringent design standards would require larger investments to construct new buildings, possibly preventing building owners from coming to San Francisco. Finally, if existing structures needed improvement, many business owners would be forced to leave because of the high cost of retrofitting. As a result of such fears, politicians and ultimately policy makers were very hesitant to make changes. Thus some evidence suggests that San Francisco made an attempt to hide its earthquake predicament for economic reasons - a choice that would soon backfire.

2.1.2 Acceptance and Consensus

Following the widespread destruction that occurred in the 1906 San Francisco Earthquake, the controversy of wind versus earthquake-resistant design was all but over. At this point, engineers who had experienced the shock began to realize the fundamental difference between wind and earthquake force. As one engineer put it "[A] pile of brick may be laid so that it will resist wind pressure, but will fail on account of the acceleration caused by an earthquake [9]." As a result, R. S. Chew presented a new theory at a meeting of the American Society of Civil Engineers (ASCE) on March 4, 1908 [10]. He suggested that the force a building experiences from an earthquake is proportional to the mass of the building and the acceleration of the ground at the base of the building. The mass is:

$$\mathbf{m = W / g} \qquad (2\text{-}1)$$

where: W is the weight of the building in pounds and
g is the acceleration due to gravity or 32.2 ft/sec^2

The correlation to Newton's Second Law of Motion (F = m a) gave building designers a basis to specify forces.

Many engineers were not comfortable with this new concept. In the discussion following Chew's paper, one engineer said: "[I]n nature we see resistances increasing with the size and weight of objects; if this idea can be carried out by buildings, we but obey the mathematical laws which govern the stability of all things composed of matter. The heavier the building the more horizontal resistance it will naturally have... [9]." Ironically, the speaker in this case was the same person who had also said, "[A] pile of brick may be laid so that it will resist wind pressure, but will fail on account of the acceleration caused by an earthquake." Needless to say, he was not in the Bay Area during the earthquake of 1906.

On the other hand, those who experienced the earthquake seemed to have an amazingly good sense of dynamic response. An engineer who was in the quake described his experience of resonance: "[I]f it (the building) should have a natural period that synchronizes with that of the applied force, a resonant vibration of very large amplitude would be set up, causing extreme stress [11]." Likewise, another engineer described the concept of base isolation: "[I]f the foundation of the building were divided into two horizontal parts, with roller or ball bearings between the parts, the earth vibration could pass through without materially affecting the upper structure, whether heavy or light, the only vibration being the friction of the bearings [9]."

2.1.3 Implementation

It was more than 20 years after the 1906 San Francisco Earthquake, however, that a requirement of earthquake-resistant design appeared in the codes. In 1927, the Uniform Building Code contained a discussion of provisions to be used in earthquake prone regions that stated:

> "[T]he following provisions are suggested for inclusion in the Code of cities located within an area subject to earthquake shocks. The design of the buildings for earthquake shocks is a moot question but the following provisions will provide adequate strength when applied in the design of buildings or structures.
>
> (a) LATERAL BRACING
> Every building and every portion thereof, except Type IV and V buildings and all one story buildings which are less than twenty (20) feet in height shall be designed and constructed with bracing to resist the stresses produced by lateral forces as provided in this Section. The stresses shall be calculated as the effects of a force applied horizontally to each floor or roof level above the foundation, such force to be proportional to the total dead plus live load of the building above any given plane and shall be considered as concentrated at each floor of roof level. Where the design live load specified in Section 2304 for a particular building or portion thereof is fifty (50) pounds per square foot or less, such live load may be disregarded in the computation of the lateral forces required

in this Section. The full value of all live loads specified in Section 2304 more than fifty (50) pounds per square foot shall be used in such computation. The force shall be assumed to come from a direction at right angles to any elevation of the building.

The factors to be employed to fix the total lateral force shall vary with the character of the foundation material and shall be as follows:

1. When the foundation rests upon material upon which a load of two (2) or more tons per square foot is allowed, the horizontal force to be applied at any plane shall be assumed as seven and one-half percent ($7\ ^1/_2$ %) of the dead load plus live load of the building above that plane.
2. When the foundation rests upon material upon which a load of less than two (2) tons per square foot is allowed, the horizontal force to be applied at any plane shall be assumed as ten percent (10 %) of the dead load plus live load of the building above that plane. All buildings on pile foundations shall be included in this class [12]."

The 1927 UBC required simple calculations to determine seismic design forces. Since then, the complexity of such calculations has generally increased with each new code. Over the past 68 years, additional criteria has improved the representation of structural response in a rational manner. As a result, confidence in the ability to design for *predicted* earthquakes has risén. To bolster this faith, the advent of the computer has increased the accuracy of analysis. Ironically, however, the magnitude of these forces has not necessarily increased during this period. So should engineers be confident in their designs? Although earthquakes are *not predictable*; the response of a structure is. Therefore, the best an engineer can do is design for the maximum *expected* earthquake, which is determined by seismologists (and maybe policy makers), then wait to see how it performs in the next "big one." In the meantime, research attempts to find solutions to the most important unanswered questions.

2.2 Evolution of Beam-to-Column Connections of Unbraced Steel-Framed Buildings

Technical innovation in materials and earthquake-resistant design over the last 100 years has led engineers to the special moment-resisting steel framed structures of today. Historically, however, economics has had an equally important role in the development of building design. From the late 19th century to today, the driving concern of investors has been economic -- to construct buildings in order to make a profit. Thus, since many owners do not appreciate the intent of building codes they rarely consider earthquake-resistant design beyond the code minimum. As a result, they are not protecting their investments from damage as well as they could. Meanwhile, the disconcerting structural failures that have occurred as a result of earthquakes have driven engineers to use more reliable materials and configurations in their designs. The transition from mild steel bolts, to rivets, to high strength bolts, and finally to welding for beam-to-column connections of moment resisting frames is a perfect example of this. As a result of such changes, steel buildings are more cost-effective than ever before.

2.2.1 Building Design Before the 1906 San Francisco Earthquake

Beginning in the early 1880s, the emergence of tall buildings in Chicago led to the first partial steel-framed structure. Designed by an architect named William Le Baron Jenney, the Home Insurance Building was a precedent in American building design - it was one of the first "skyscrapers" [13]. In the years to follow, dozens of structures with a greater percentage of steel were built in New York and Chicago since it had superior strength and ductility to both wrought and cast iron. Amazingly, the Home Insurance Building, which was unbraced, had a single mild steel bolt connecting the web of each beam to a bracket cast with the iron columns (Figure 2-1). Because of its lack of lateral resistance, the building was demolished in 1931.

Although Jenney was trained in architecture and engineering at a French technical school, he was not aware of the need for lateral force-resistant design, whether it be wind or earthquake. The criteria he established for the Home Insurance Building was to "design to meet the most rigorous functional requirements... maximum durability and fire-resistance, utmost economy of construction, maximum admission of natural light, and open interior space for maximum freedom in arrangement of internal elements [14]." But Joseph Kendall Freitag, an engineer, had lateral stability on his mind. In his book *Architectural Engineering* (1895), he said that the need for wind bracing is "undoubtedly reduced through... the dead weight of the structure itself, the

resistance to lateral strains offered in the stiff riveted connections between the floor systems and the columns, the stiffening effects of partitions (if continuously and strongly built), and linings. But, in view of the uncertainty in regard to the efficiency of these considerations, they may not be relied upon, and are therefore disregarded in the calculations [7]." He then gave four examples of proper wind bracing "that must reach some solid connection at the ground": the sway rod (two), portal, and knee bracing systems (Figures 2-2 a, b, c, and d).

Accordingly, a new trend in tall building design was established by two Chicago structural engineers named Wade and Purdy. The Rand McNally Building, built from 1889 to 1890, was the first structure that was constructed of an entire steel frame in the United States [14]. Rather than having load-bearing exterior walls that supported the steel, the steel supported the masonry. With this new technique, the steel frame could be erected prior to the masonry walls, thus reducing the cost of erection. Another advantage of Wade and Purdy's structure was that rivets instead of bolts were used in the beam-to-column connections. Wade and Purdy's structure, in comparison to Jenney's, had multiple rivets "rigidly" fastening the beams to columns. Moreover, diagonal bracing provided redundant lateral resistance.

Through Freitag's advice, Wade and Purdy, as well as many other designers, made large strides in lateral force resistant design. The codes that were recently developed in Chicago, Boston, and New York, however, did not specify how lateral forces (wind at the time) could be resisted. Designers were typically free to choose the forces to be resisted, the strength of the materials employed, and the most efficient details of construction [7]. Consequently, some buildings were braced and some were not. Two examples of such diversity are buildings, both constructed in Chicago on the same block in 1895 [7]. The first building was a 200 ft. tall and 60 ft. wide office building with a lateral-force resisting system consisting of 2.25 in. thick clay tile partitions. The second building used 15 in. channels, which were connected to 6 in. eye-bars, for diagonal bracing. It should be noted that the second building had equal height but two and one-half times the width of the first. Thus, in the late 19th century each individual designed to his or her own specifications.

2.2.2 Results of the 1906 Earthquake

After the 1906 San Francisco Earthquake, the performance of steel buildings was evidence that Freitag, Wade, and Purdy were correct. Although it is believed that only one steel framed building collapsed as a result of the earthquake, the majority of reported damage occurred in unbraced steel frames with top and bottom flange angle connections [15]. In his damage report on March 4, 1908, Chew noted that "after the shock of April 18 (1906), a number of cases the connection of beams to columns had failed by the rivets shearing off [10]." Chew demonstrated that the force couple at an unbraced frame connection caused rivets to fail in shear. After noting these failures, Chew advised against the use of unbraced frames and his opinion soon gained widespread acceptance. Accordingly, the 1927 UBC required that all tall steel buildings subject to earthquakes be braced to resist lateral forces [12].

Besides the UBC requirement, unbraced buildings faced another challenge in the 1920s. Steel mills, at that time, produced a limited selection of standard shapes including angles, channels, I-beams, and plates. The lack of economic connections and the high cost of built-up members created little interest in unbraced frames. An example of the complexity required to provide proper strength and rigidity in a riveted beam-to-column connection of these shapes is shown in Figure 2-3. For comparative reasons, the estimated cost factor is normalized to 1.00 for contemporary connections (see Figure 2-6).

Although fully restrained (FR), or rigid, connections were not economically feasible after the turn of the century, partially restrained (PR) connections were. Architects and engineers actually relied on PR connections in braced buildings because of their economic benefits. The purpose was not to supply lateral resistance (since braces were provided) but rather to reduce the design moments and deflections of beams under gravitational forces. In effect, PR connections "take out" a portion of the midspan moment, which is equal to the moment resistance provided by the connection.

2.2.3 1930s

The addition of earthquake-resistant design to the codes in the late 1920s and early 1930s compelled engineers to be economical and safe in their designs. Prior to this requirement, steel had already become very popular since it had greater strength and stiffness than any other building material. But a limited number of shapes were produced in a single-roll process. This

was a very inefficient way of producing larger shapes since it prevented the thinning of the webs [16]. In response, the steel industry developed a new milling process that allowed several rolls to be situated one after another. This step signified the birth of wide-flange members, which are still used today. The increase in availability of shapes and sizes resulted in the demise of built-up members. Figure 2-4 shows a typical seated shear connection in one direction (braced) and a moment-resisting connection of shop-riveted and field-bolted tees.

It should be noted that a large number of extremely tall buildings, such as the Empire State Building in New York, were constructed during the 1930s. Since few of these "true skyscrapers" were built during the '20s, riveting in the field created few noise complaints. But during the '30s, steel structures were going up at a rapid rate in all major cities of the United States. Due to the disturbance created by riveting during office hours, an immediate substitute for field riveting was needed. The only available substitute at the time was the mild steel bolt which was widely used at the turn of the century.

2.2.4 1950s - 1960s

The most important step that signified the obsolescence of riveting, however, was the development of high-strength bolts during the '30s, '40s, and '50s. Riveting, which required a crew of four or five experienced persons and rigid inspection (especially preheat requirements), was a labor-intensive process. Although it was time consuming, the overall cost of riveting was less than bolting until the 1950s. At that time, the reduced labor cost for installing bolts offset the higher material cost [17].

Meanwhile, some designers and fabricators recognized the advantages of welding over mechanical connectors such as bolts or rivets. Not only was welding quiet, it was fast, it provided continuity, it would require less material to provide the same strength, and it looked "clean." Figure 2-5 shows a typical beam-to-column connection of the '50s and '60s. It consisted of a cover plate at each beam flange and a shear tab at the beam web, which were shop-welded to the column and field-bolted to the beam. This type of connection became the norm for steel framed construction of the era since it achieved added efficiency in the use of materials and dramatically reduced the time (and thus cost) of fabrication. Yet, prior to gaining widespread acceptance, the quality and consistency of welds needed to improve; a step that required improvement in steel properties.

From the turn of the century to the 1960s, the majority of structural steel used in building construction was A-7. In some instances, rolled A-7 shapes had poor chemical composition - a characteristic that presented welding problems. Consequently, there was a need to produce a structural steel of superior quality. After extensive metallurgical research, a stronger and improved steel was created. Commonly referred to as A-36 because of its minimum required yield strength (F_y =36 ksi), A-36 hit the market in 1960. It is a low carbon (C <0.2%) alloy of excellent strength, ductility, and weldability. Because of its economy, availability, and properties, A-36 has become the most popular material in steel moment resisting buildings. Along with the more recently developed A-572, Grade 50 (F_y = 50 ksi), the theoretical performance of a steel structures could be determined based on material properties and connection design. The only major obstacle left for special moment resisting frames was a method of economically joining members in the field.

2.2.5 1980s

Following the development of weldable steel, advancements in welding techniques resulted in economical, field welding processes. Although some methods of welding, such as submerged arc welding (SAW) and electroslag welding (ESW), are best suited for the shop, many others are easily transportable into the field. Shielded metal arc welding (SMAW), or stick welding, for example, is a popular field welding method. The equipment is highly portable, costs less than other types, and electrode sticks are readily available. However, the method has two major disadvantages: first, if the flux that covers the wire is exposed to water, then a poor quality weld may result, and second, the amount of weld material available in one pass is limited to the size of the stick. Flux-cored arc welding (FCAW), on the other hand, provides a seemingly never-ending supply of wire through feed rolls. As a result, FCAW typically has approximately twice the deposition rate of SMAW. Also, FCAW protects the flux within the core of a wire tube (i.e. flux-cored), which reduces the possibility of embrittlement. Even though a major drawback of FCAW is the large spool of wire that makes the equipment more bulky than SMAW, FCAW is still the process of choice because of its high deposition rate.

During the 1980s, the most popular beam-to-column connection of special moment resisting framed buildings consisted of the welded flange-bolted web field erection shown in Figure 2-6. Several tests of this configuration were performed during the '70s and '80s [18-23].

As a result of the adequate performance of these tests (plastic hinging beams and shear yielding of column panel zones), this connection became prequalified in the ASD and LRFD Manuals of Steel Construction as well as the UBC. More recently, however, the attractiveness of such connections has diminished as a result of the 1994 Northridge Earthquake - the connections could not "survive" the earthquake without brittle failure.

3. STANDARD PRE-NORTHRIDGE CONNECTION

The 1994 Northridge Earthquake, which hit approximately 20 miles northwest of Los Angeles, was one of the first earthquakes with high accelerations to affect a large number of steel framed buildings in the United States [24]. Although the earthquake was considered moderate based on the amount of energy released, hundreds of special moment resisting framed buildings that were recently constructed of steel experienced over 0.30g ground acceleration. As a result, thousands of beam-to-column connections of special moment resisting frame buildings failed during this severe cyclic test. In very few cases, however, did joints perform in the ductile manner intended. Rather, the majority of connections failed in a brittle fashion at or near the complete penetration groove welds between the column and beam flanges. Failure modes included:

1. failure of the beam bottom flange weld;
2. divot of the column flange (at face) that pulled away with the beam and weld material;
3. fracture of the column flange and/or web;
4. failure of the beam top flange weld;
5. fracture of the beam flanges in the heat affected zone;
6. failure of the shear tab bolts and/or failure of the shear tab plate [24].

3.1 The SAC Joint Venture

Although several tests have supported the ductile performance of special moment resisting frame connections in the past, there is currently little data available on the effectiveness of contemporary connections. For this reason, the Northridge Earthquake was the first "test" to reveal a large number of flaws in current seismic resistant design of steel moment frames. According to some estimates, the cost to repair each damaged connection ranges between $6,000 and $20,000 (*ENR*, April 17, 1995). As a result, the SAC Joint Venture was established to experimentally investigate the causes of brittle failures that resulted from the Northridge Earthquake and develop economical and reliable methods of repair and/or retrofit of existing damaged buildings.

3.2 Description of Test Specimens

Three full-scale subassemblages of a W36x150 cantilevered beam connected to the strong axis of a W14x257 column were designed to the standards in use prior to the Northridge Earthquake. Each specimen was representative of a perimeter column (one-sided) of a mid-rise, special moment resisting frame building that was recently constructed of steel in Los Angeles. Member lengths were chosen to correspond to locations of inflection points that would develop in the event of an earthquake; that is, at mid-span of the beam and at mid-story heights of the column. Figure 3-1 shows the overall dimensions of Specimens PN1, PN2, and PN3 (where the PN stands for pre-Northridge).

The intent of the pre-Northridge tests was to reproduce the failures which occurred in buildings that experienced the earthquake. Accordingly, the materials, welding procedure, and fabrication sequence were representative of pre-Northridge specifications. All beam and column material requested was ASTM A-36 and A-572, Grade 50, respectively. However, Specimens PN1 and PN2 were mistakenly fabricated of A-572, Grade 50 beam material rather than the A-36 requested. (It should be noted that this substitution is not currently regulated; this practice is very common with the advent of dual grade steel). Complete joint penetration groove welds were of E70T-4 Lincoln filler metal applied by the self-shielded FCAW welding process. Fillet welds were also of the self-shielded FCAW welding process, but the filler metal was E71T-8 Lincoln wire. Preheat and interpass temperatures were regulated by Section 4.2 of the American Welding Society (AWS) D1.1-94: "Structural Welding Code - Steel." Furthermore, details included those suspected to contribute to poor performance. Specifically, backup bars and runoff tabs were not removed. Figures 3-2 and 3-3 show the connection and end plate details. The fabrication sequence was as follows:

1. weld continuity plates to the column;
2. weld shear tab to the column;
3. attach beam to shear tab with bolts and fully tension all web bolts using the turn-of-nut method;
4. weld beam top flange to the column;
5. weld beam bottom flange to the column alternating weld layers from one side of the web to the other until the weld was complete;
6. after the beam flange welds had cooled, make required fillet welds between the shear tab and beam web.

3.3 Execution of Experiment

Each specimen was tested by applying cyclic loads to the end of the cantilevered beam located at a distance of 134.5 in. away from the face of the column. The experiment was conducted in the horizontal plane under a displacement-controlled loading history that monotonically increased over time. Table 1 lists the peak deformation, number of cycles, displacement rate, and number of data points recorded for each load step. Figure 3-4 is a plan of the test setup that shows support and loading locations. Photographs of the overall setup with a specimen in place are shown in Figures 3-5 and 3-6. The setup facilitated viewing of the specimens during testing.

Forces were transmitted from the column to the strong floor through built-up I-sections, concrete blocks, snubbers, and stress rods that were designed to allow rotation but prevent slip at support locations. Three I-shaped stubs, which separate the column from the concrete reaction blocks, were constructed of 1.5 in. thick steel plates at the west supports and a W14x455 member at the south. To allow rotation, the web of each stub was oriented so it could bend in flexure. Four 1.25 in. diameter high-strength rods (F_y = 112 ksi) were used to prestress the specimen at each support, thus preventing movement between the column and concrete blocks. Furthermore, a guide frame was constructed near the end of the cantilever to provide lateral support for the beam. Figures 3-7, 3-8, 3-9, and 3-10 show column supports with stress rods in place and the lateral guide frame, respectively. To prevent movement of the concrete blocks relative to the floor, snubbers constructed of 1.25 in. thick steel plates were grouted and prestressed to the floor at either side of each concrete block. The snubbers were designed to provide a minimum of 350 kips friction resistance (μ_s = 0.30). Also, each block was prestressed to the floor to prevent overturning. See Appendix A for snubber design and prestressing rod locations.

The hydraulic actuator used for the test was capable of delivering 350 kips of force at a displacement rate of 0.20 in. per second. The maximum stroke of the actuator was approximately $\pm$6 in. Force was transmitted from the actuator to the cantilevered beam through the clevis shown in Figure 3-11. One 5 in. diameter pin transferred force from the actuator to the clevis, whereas four 1.25 in. and four 2.25 in. diameter A325 bolts transferred force from the clevis to the end plate of the beam. In addition, two small tabs were welded to the end plate of each specimen to limit slip between the clevis and beam. Figure 3-12 shows the clevis attached to the actuator and beam end plate.

Each specimen was instrumented with displacement potentiometers, linear strain gages, and three-direction rosettes to determine response during the test. Global displacements were measured at the column panel zone, at the cantilevered beam tip, at the beam flanges near the connection, and at various locations of the column opposite the side of the connection. Displacements were measured to an accuracy of a thousandth of an inch. In addition, force was measured to the hundredth of a kip in a calibrated load cell that was mounted on the actuator. Lime whitewash was painted on the exposed side of each specimen to give an indication where inelastic behavior occurred. Local response was measured by linear strain gages at the beam flanges, at the column flanges near the connection, and at the continuity plates. Rosettes were used to determine the state of plane strain in the panel zone, on the edge of the column flange neighboring the beam, and on the column flange faces near the beam flange and continuity plate welds. All strains were measured to the tenth of a microstrain ($\mu\epsilon$). Proper instrumentation of each specimen was verified during a calibration and low-amplitude test on the day prior to each experiment.

3.4 Experimental Results

As previously mentioned, Specimens PN1 and PN2 were constructed of A-572, Grade 50 beam and column material, whereas Specimen PN3 was built of A-36 beam and A-572, Grade 50 column material. Table 2 lists the mill certificate mechanical properties for each specimen. For all three specimens, the beam yield strengths reported were considerably higher than those for the column, especially for Specimens PN1 and PN2. Tensile coupon tests, which are currently being conducted on all material, are not complete. Thus, since mill certificate coupon specimens were taken from the web of each member, the actual yield strength of the flange will be assumed to be approximately 5 percent lower than that of the web. This is primarily due to cold working of the web during the rolling process. As a result, the beam flange material of all three specimens was stronger than that of the column; the specimens did not meet the strong column-weak beam intent of the design.

3.4.1 Specimen PN1

Specimen PN1 was tested to failure on February 9, 1995. Force measured at the actuator (**P**) versus displacement at the beam tip (Δ_{total}) is plotted in Figure 3-13. Moment at the column face versus plastic rotation, where the moment is equal to the force times 134.5 inches, and:

$$\theta_p = \frac{1}{L}(\Delta_{total} - \Delta_{elastic}) = \frac{1}{L}(\Delta_{total} - P/k) \qquad (3\text{-}1)$$

where: L = 134.5 inches, and
k = elastic stiffness of the connection (kips/in),

is plotted in Figure 3-14. In general, the specimen failed in an abrupt manner near the end of the first 3-in. displacement cycle. The maximum plastic rotation and energy dissipated at failure were 0.94 percent and 1770 kip-in., respectively. Figure 3-15 shows the joint after the test.

Based on the imposed displacements, the performance of the specimen was characterized by an elastic, yield point, and inelastic response. Up to and including the 1-in. displacement cycles, the connection behaved elastically. The average stiffness of the connection was 138 kips/in. The strain distribution across the beam flanges adjacent to the complete penetration groove welds was generally uniform. No measured strains exceeded yield values.

In the first excursion of the 2-in. displacement cycles, a reduction of connection stiffness defined the onset of yielding. At this time, flaking of the lime whitewash was observed in the panel zone, but none was observed on the beam flanges. Sizable yielding in the panel zone was confirmed by the principal strains computed from rosette readings at the center of the panel zone. The maximum principal strain at this location was approximately 8 times that of the assumed yield strain (based on mill certificate tests). Gross inelastic behavior was observed throughout the panel zone, leading to a large amount of panel zone rotation. Beam flange strains, which were measured 2.5 in. from the face of the column, increased to approximately 9.5 times the anticipated yield strain. The distribution was slightly bell-shaped across both flanges. It should be noted that the maximum beam flange strains were misleading since measurements were limited to a small area on the outer fiber of the beam adjacent to the column; this is an area of high stress concentration. Based on the amount of whitewash spalling, observable inelastic deformation did not occur in the beam.

During the following 2-in. displacement cycles, loud noises were heard as the shear tab bolts slipped. Each slip is discernible in the hysteresis loops as a slight reduction in force near zero displacement. In addition, slight yielding occurred on the face of the column flange bordering to the beam flange welds. Yielding was suspected to occur where whitewash flaked off the east face (see Figure 3-4) of the column flange opposite to the continuity plates. However, this cannot be confirmed since strain gages were not placed at these locations. No significant yielding occurred in other locations of the joint nor did the connection strength degrade.

The specimen failed near the end of the first 3-in. displacement cycle by brittle fractures in the column flange and panel zone neighboring the bottom beam flange. The failure was associated with a loud noise and sudden loss of approximately 150 kips of connection strength. The crack initiated at the backup bar that was left in place after the bottom beam flange was welded. The crack extended across the column flange width and crossed diagonally through its thickness into the panel zone. In the panel zone, the crack propagated approximately 10 in. vertically up the column k-region and 8 in. horizontally along the continuity plate. The test concluded subsequent to the column fracturing. Figures 3-16 through 3-19 show damaged locations following the test. Table 3 summarizes the performance of Specimen PN1. It should be noted that this is the first time a column flange failure was reproduced in a laboratory experiment.

3.4.2 Specimen PN2

Specimen PN2 was tested to failure on February 16, 1995. The mode of failure and performance were very similar to that of Specimen PN1. Force measured at the actuator versus displacement at the beam tip and moment at the column face versus plastic rotation are plotted in Figures 3-20 and 3-21, respectively. The specimen suddenly failed during the second 2-in. displacement cycle. The maximum plastic rotation and energy dissipated at failure were 0.35 percent and 510 kip-in., respectively. Figure 3-22 shows the joint after the test.

The elastic performance of the joint was nearly identical to that of Specimen PN1. Up to and including the 1-in. displacement cycles, the connection behaved elastically, with an average stiffness of 143 kips/in. The strain distribution across the beam flanges was more erratic than Specimen PN1 but was generally uniform. No measured strains exceeded yield values.

In the first excursion of the 2-in. displacement cycles, a reduction of the connection stiffness defined the onset of yielding. Similar to Specimen PN1, flaking of the whitewash was not observed on the beam flanges, whereas flaking did occur throughout the panel zone and on the east face of the column flange opposite the continuity plates. After yield, the principal strain computed in the center of the panel zone was approximately 6 times that of the mill certificate yield strain. The large amount of panel zone activity led to local kinks that developed in the column flanges, thus causing the whitewash to spall. The beam flange strains increased to 4 times the assumed yield strain and the distribution was slightly bell-shaped across both flanges. As was true with Specimen PN1, Specimen PN2 beam flange strain measurements did not indicate that large inelastic deformation occurred in the beam; the yielding was limited to a very small area of high stress concentration. During the following 2-in. displacement cycle, a noise was heard as the shear tab bolts slipped. Slight yielding also occurred on the face of the column flange bordering to the beam flange welds. No significant yielding occurred at other locations of the joint.

Similar to Specimen PN1, Specimen PN2 failed by brittle fractures in the column flange and panel zone neighboring the bottom beam flange. However, failure occurred earlier in the experiment. A loud noise and sudden loss of approximately 150 kips of connection strength occurred near the end of the second 2-in. displacement cycle. Once again, the crack initiated at the bottom beam flange backup bar, extended across the column flange width, and crossed diagonally through its thickness into the panel zone. In the panel zone, the crack propagated approximately 10 in. up the column k-region. Following the loading that created bottom flange failure, the specimen was loaded in the opposite direction. The connection strength degraded approximately 4 percent without any other noticeable effects in performance. Then the specimen was loaded in the same direction that produced failure to determine the amount of strength lost. The post-failure behavior is plotted as a dashed line in Figures 3-20 and 3-21. The joint reached a load of approximately 50 kips, close to one-quarter the strength before failure. A second crack, approximately 4 in. long, formed along the continuity plate. Figures 3-23 and 3-24 show the damage to the column and permanent separation between the bottom backup bar and column face. Table 3 summarizes the performance of Specimen PN2.

3.4.3 Specimen PN3

Specimen PN3 was tested to failure on February 28, 1995. Force measured at the actuator versus displacement at the beam tip and moment at the column face versus plastic rotation are plotted in Figures 3-25 and 3-26, respectively. The specimen suddenly failed during the second 3-in. displacement cycle. The maximum plastic rotation and energy dissipated at failure were 1.12 percent and 2530 kip-in., respectively. Figure 3-27 shows the joint after the test.

The elastic performance of the joint was similar to that of Specimens PN1 and PN2. Up to and including the 1-in. displacement cycles, the connection behaved elastically, with an average stiffness of 136 kips/in. The slight reduction in connection stiffness can be attributed to weaker beam material. The strain distribution across both beam flanges was generally uniform. Although the hysteresis loops did not indicate inelastic behavior, beam flange strains exceeded the anticipated yield value when the beam tip displacement reached 0.80 in. The most probable explanation was that local stress concentrations, similar to those in Specimens PN1 and PN2, developed at this location. Nonetheless, observable yielding did not occur in the joint.

During the first leg of the 2-in. displacement cycles, a reduction of the connection stiffness defined the onset of yielding. Unlike Specimens PN1 and PN2, significant flaking of the beam flange whitewash was observed early in the 2-in. displacement cycles, whereas, flaking was not observed in the panel zone. After yield, beam flange strains dramatically increased over yield with an erratic distribution across each flange. The maximum strains measured were approximately 16.5 times the anticipated yield value, far more than Specimens PN1 and PN2. The region of beam flange yielding extended from approximately 10 in. to 18 in. away from the face of the column. Although no flaking of the whitewash was observed in the panel zone, the principal strain computed at its center was approximately 5 times the mill certificate yield strain. Similarly, noises were heard as the shear tab bolts slipped. Slight yielding was also observed on the face of the column flange bordering to the beam flange welds and in the top and bottom corners of the shear tab plate and adjacent beam web. No significant yielding occurred at other locations of the joint.

Unlike Specimens PN1 and PN2, the failure of Specimen PN3 occurred in the beam flange-to-column weld. During the second 3-in. displacement cycle, a brittle fracture occurred along the weld-column interface of the bottom beam flange. The fracture immediately propagated across the weld width. As a result, the bottom beam flange force was transferred to the shear tab,

causing it to tear along the bolt line for 6 in. and shear the next three bolts. The connection lost nearly all of its strength in this direction. Following this failure, the joint was tested 3 in. in the opposite direction. This portion of the response is plotted as a dashed line in Figures 3-25 and 3-26. Near zero displacement, the bottom beam flange weld and shear tab cracks closed. When the displacement reached approximately -2.25 in., the top beam flange weld began to tear along the weld-beam flange interface. As the displacement increased, the crack slowly propagated across the flange resulting in a tear at the top 4-in. weld return (supplemental weld) between the shear tab and beam web. At the target 3-in. displacement, the crack length reached 9 in. and the connection resistance was approximately two-thirds that of the maximum strength. Figures 3-28 through 3-32 show damaged locations after the test and Table 3 summarizes the performance of Specimen PN3.

3.5 Summary of Findings

Three contemporary special moment resisting connections, which were prequalified in the UBC, did not perform well in the laboratory experiments executed at the University of California at Berkeley. For comparative purposes, the same criteria that were used to judge the University of Texas at Austin tests were employed to assess the performance of the three pre-Northridge specimens. The three factors that Engelhardt and Sabol [25] used to describe performance were:

1. the amount of maximum beam plastic rotation prior to failure, goal of 3 percent
2. the nature of the failure, goal to prevent sudden loss of strength
3. the amount of energy dissipated prior to failure, goal of 20 percent of the beam plastic moment capacity (M_p).

Based on these criteria, the performance of all three specimens was poor.

Specimens PN1 and PN2 both reproduced the brittle column flange and web failures that occurred in the Northridge Earthquake. The amount of plastic rotation and energy dissipation that Specimen PN1 achieved prior to failure were on the order of one-third and one-fourth that of the performance goals, respectively. Likewise, Specimen PN2 reached a plastic rotation and energy dissipation that were on the order of one-tenth and one-twelfth that of the performance goals, respectively. Specimen PN3, on the other hand, performed slightly better; it attained a plastic rotation and energy dissipation that were both on the order of one-third that of the performance goals (prior to failing in a brittle fashion).

For Specimens PN1 and PN2, Figure 3-33a shows how the crack formed near the bottom beam flange and how it propagated into the panel zone. The crack initiated at the unfused interface between the backup bar and column face. Due to the strong beam material used for both specimens (F_y = 62.6 ksi), a large amount of panel zone rotation led to a localized kinks in the column flange. As a result of the concentrated tensile stresses at this location, the crack propagated toward the panel zone. Similarly, Figure 3-33b shows how the crack initiated at the bottom backup bar of Specimen PN3. However, the crack did not propagate toward the panel zone. Rather, the crack spread along the weld-column flange interface, the primary reason being that Specimen PN3 was constructed of weaker beam material (F_y = 56.8 ksi). Consequently, the amount of panel zone rotation was approximately 25 percent less than that of Specimens PN1 and PN2, which led to smaller kinks and ultimately smaller tensile stresses along the column flange. As a result, the crack propagated along the weld-base metal interface.

Due to the initiation of a crack at the unfused interface between the backup bar and column face, it is recommended that the backup bar be removed and a reinforcing fillet weld be applied under the root pass of the groove weld. The University of Texas at Austin tests showed promise that this practice will reduce the likelihood a brittle fracture [25]. On the other hand, since most the failures did not occur at the top groove weld, removal of the top backup bar may not be cost-effective. Furthermore, removing the top backup bar may cause more harm than good since the beam web creates an interference. Therefore, the benefits of removing the top backup bar are questionable - its effects are not yet fully understood.

Earlier tests performed at the University of California at Berkeley [18-20], however, may provide an answer to this problem. In these tests, it is believed that a sealing fillet weld was placed under many of the backup bars (without their removal) and when tested, most specimens did not fail in a brittle fashion. The theory, which is based on fracture mechanics, is that a crack will not propagate if it is small and internal. Thus, it is possible that a standard backup bar may be left in place if a fillet weld is applied to seal the crack. This is a subject of pending research at the University of California at Berkeley. With the current state of knowledge, it is recommended that the removal of backup bars and application of reinforcing fillet welds is an adequate alternative.

The amount of column flange failures that occurred in the Northridge Earthquake brings up an important trend in the mechanical properties of structural steels produced over the years. The first moment resisting connections, which were tested from 1968 to 1972 at the University of California at Berkeley [18-20], met contemporary performance goals. In the majority of tests, plastic hinges formed in the beams because their yield strengths ranged from 37 to 39 ksi with little variation [26]. In comparison, the mean yield strength of A-36 steel today is 49 ksi with a standard deviation of approximately 6 ksi [27]. As a result, the American Society for Testing and Materials (ASTM) is currently working with the Structural Shape Producers Council (SSPC) to develop a new specification that places tighter restrictions on mechanical properties. Until then, it is recommended that a conservative value of 55 ksi, which is based on the mean plus one standard deviation, be assumed for A-36 beam yield strengths.

In conclusion, although some evidence has suggested that welding and inspection practices were to blame for the poor performance of special moment resisting frame connections in Northridge, it is needless to say that proper implementation ***and*** design are key to reliable performance.

4. NEW CONNECTIONS

4.1 Experimental Program

Primarily funded by the National Science Foundation (NSF) and the American Institute of Steel Construction (AISC), a total of six specimens, two of which are still pending, comprise the University of California at Berkeley research program. The goal of these tests is to improve the performance of special moment resisting connections by changing the configuration and improving the details. The design, fabrication, testing, and experimental results of two specimens are reported in this chapter. The performance of each specimen is compared to the pre-Northridge results as well as the performance goals provided by Engelhardt and Sabol [25]. Because of our project team's numbering system, the first specimen is referred to as NSF Specimen #1 and the second is referred to as NSF Specimen #6. In general, both specimens are intended for new construction rather than as repair and/or retrofit for existing buildings; that issue is addressed by the SAC Joint Venture. Furthermore, the NSF experimentation makes no attempt to change or control the material properties of the base metal since economics is a major concern.

4.2 Experimental Setup, Instrumentation, and Loading Sequence

NSF Specimens #1 and #6 were tested using the same setup utilized in the pre-Northridge experiments, shown in Figures 3-4 through 3-12. Originally, the setup was designed for use with the NSF specimens, but it was decided that a "first come - first serve" method would be exercised to determine the order of testing. Thus, since the fabricator of the first three NSF specimens was delayed in their delivery and the three pre-Northridge specimens had arrived, the pre-Northridge specimens were tested first. As illustrated in the previous chapter, a significant amount of information was acquired from the pre-Northridge tests, which ultimately aided in the design and testing of NSF specimens. Furthermore, a considerable amount analytical work, in the form of nonlinear finite element analysis and fracture mechanics, was performed by T-S. Yang [28].

Since "hot spots" were determined by the nonlinear finite element analysis (Yang, 1995), less instrumentation than that of pre-Northridge specimens was used to determine the response of NSF specimens. In general, linear or rosette strain gages were placed at these "hot spots." For NSF Specimen #6, in which no finite element analysis was performed, strain gages were placed at locations of expected yielding. To determine global displacements and rotations for both specimens, potentiometers were placed at the following locations: various points along the column, diagonal across the panel zone (NSF Specimen #1 only), at the beam tip, at the beam flanges outside the tee stiffeners (NSF Specimen #6 only), and at a distance of 134.5 in. from the face of the column (at the actuator). Proper instrumentation of each specimen was verified during a calibration and low-amplitude test on the day prior to each experiment.

NSF Specimens #1 and #6 were tested using the displacement-controlled loading history listed in Table 1. Cyclic loads were applied to the end of the cantilever with a hydraulic actuator capable of delivering 350 kips of force at 0.20 in. per second. The moment arm from the actuator to the face of the column was 134.5 in. Depending on the exact location where the beam was fabricated along the column, the maximum actuator stroke was approximately ± 6 in.

4.3 NSF Specimen #1

The basic intent of NSF Specimen #1 was to design an all-welded moment connection with a flexible panel zone so that the joint could sustain large inelastic deformations without brittle failure. Previous experimental research by Popov et al. [23, 29] has shown that all-welded connections show superior ductility and energy absorption capabilities over bolted web-welded flange connections. Likewise, since the current *SEAOC Recommendations* [1] allow inelastic shear deformation to occur in the panel zone, it was determined that a smaller column than those tested at the University of Texas at Austin (W14x455) would contribute additional ductility to the joint. In other words, the same size beam that was tested at the University of Texas at Austin (W36x150) with an all-welded attachment to a smaller column would increase the plastic rotation and energy absorption capacities of the connection. As a result, a W36x150 beam (A-36) was connected to the strong axis of a W14x211 column (A-572, Grade 50).

Besides the all-welded and flexible panel zone changes, it was decided that the configuration and details of the connection also needed improvement. First, continuity plates were moved away from the beam flange groove welds in order to prevent the build-up of residual stress in the heat-affected zones of the column flange. For symmetry, the number of "continuity" plates was doubled (to four per side of the column web) with each plate located 4 in. clear of the beam flanges. Second, following the performance that was observed in the pre-Northridge specimens, it was determined that the panel zone may be too supple; thus, it was reinforced with a 1/2 in. thick doubler plate. Third, details were improved to limit the likelihood of crack initiation and propagation at the beam flange groove welds. Top and bottom backup bars were subsequently removed and a reinforcing fillet weld was provided under each root pass. A notch tough welding wire (Lincoln NR-311 Ni) was used in an attempt to limit crack propagation. The self-shielded FCAW process was used throughout this portion of the fabrication.

Following fabrication of the specimen, a closer look at the beam mechanical properties raised doubt in the ability of the connection to provide adequate resistance at the beam flange-to-column welds. As a result, it was decided that cover plates would be added to reinforce the beam at these locations. Trapezoidal cover plates similar to those used on the top beam flanges of Specimens 7 and 8 in the University of Texas at Austin tests [25] were constructed of 1/2 in. thick plate. Identical in appearance, the cover plates were attached to the top and bottom beam flanges with fillet welds and to the column flange with single-bevel groove welds. As will be explained later, the SMAW process was used to add the cover plates. In effect, the plates increased the beam flange-to-column weld area by 37.5 percent. In addition, the connection was "softened" by drilling two 1 in. diameter holes in the column web opposite each beam flange. Since the holes were located a short distance apart, a short slit was cut between them with the intent of providing added flexibility. Figures 4-1, 4-2, and 4-3 show the overall dimensions, connection details, and detailed sections for NSF Specimen #1.

4.3.1 Fabrication and Inspection

On April 10, 1995, NSF Specimen #1 was constructed at a fabrication shop according to standard steel construction practices. Shop and field welds were applied simulating appropriate conditions; that is, shop welds were performed within a shop setting whereas field welds were executed outdoors. During the construction process, continuous visual inspection was provided

by an AWS Certified Welding Inspector from an independent testing laboratory. The inspector, who met ASNT Level II NDT qualifications, also provided ultrasonic testing services. Likewise, an experienced welding journeyman was obtained to erect the specimen. Strict adherence to the welding parameters provided in the AWS D1.1-94 "Structural Welding Code - Steel" were followed.

In order to simulate field conditions, the specimen was erected outside the fabrication shop, as shown in Figure 4-4. Flat, horizontal, vertical, and overhead welds were applied with approved wires in their respective positions. The welder used the same platform and equipment that would be used in the field. Furthermore, no protection from the weather was provided.

The field erection portion of the fabrication process was witnessed by the inspector, individuals from the University of California at Berkeley project team, as well as the quality control engineer from the fabrication shop. The fabrication sequence was as follows:

shop (not in any specific order):

1. weld "continuity" plates to column;
2. weld erection tab to column flange;
3. weld doubler plate to column panel zone;

field:

4. attach beam web to erection tab with bolts and fully tension all bolts using turn-of-nut method;
5. weld bottom beam flange to column flange alternating weld layers from one side of beam web to the other (until completed);
6. weld top beam flange to column flange (Figures 4-5 and 4-6);
7. weld beam web to column flange (Figure 4-7);
8. remove top and bottom backup bars with air carbon arc (Figure 4-8 and 4-9);
9. remove runoff tabs and grind to rounded fillets;
10. apply reinforcing fillet welds under root pass of top and bottom beam flange welds.

Following the completion and shipment of the specimen to the University of California at Berkeley, the Davis Hall shop personnel welded cover plates to the top and bottom beam flanges (and column) and drilled holes in the column web adjacent to each beam flange. It should be noted that the bottom cover plate was not welded in overhead position since the proper equipment and wire were not available. Rather, these welds were applied in the horizontal and flat positions after the specimen was flipped over.

4.3.2 Experimental Results

NSF Specimen #1 was constructed of A-36 and A-572, Grade 50 beam and column material, respectively. Table 2 lists the mill certificate test results for beam and column material. Based on this information, the column had a slightly higher yield strength than the beam; thus, the specimen met the strong column-weak beam intent of the design. Since independent tensile coupon tests have not been performed on the material, mill certificate data was used to determine anticipated yield strains. As previously mentioned, however, flanges tend to have yield strengths that are approximately 5 percent lower than those of the web, depending on the rolling process of the section. Thus, the anticipated yield strains corresponding to mill certificate data are as follows:

$\epsilon_y = (0.95)\,\sigma_y / E = (0.95)\,52.5 / 29{,}000 = 1720\ \mu$in/in (beam flanges)
$\epsilon_y = \sigma_y / E = 52.5 / 29{,}000 = 1810\ \mu$in/in (beam web)
$\epsilon_y = (0.95)\,\sigma_y / E = (0.95)\,54.0 / 29{,}000 = 1770\ \mu$in/in (column flanges)
$\epsilon_y = \sigma_y / E = 54.0 / 29{,}000 = 1860\ \mu$in/in (column web).

Likewise, cover plate yield strain was calculated based on the minimum yield strength of A-572, Grade 50 steel, which is used in contemporary detailing. The calculated yield strain happens to corresponds with the beam flange yield strain calculated above.

NSF Specimen #1 was tested to failure on April 21, 1995. Hysteretic loops of force vs. displacement and moment vs. plastic rotation are shown in Figures 4-10 and 4-11, respectively. In general, the specimen did not perform as intended due to sudden fractures in the column. Failure occurred during the seventh inelastic cycle at a beam tip displacement of 3.08 in. and an actuator force of 236 kips. The maximum plastic rotation and energy dissipated prior to failure were 0.95 percent and 3490 kip-in., respectively. Figure 4-12 shows the joint after the test.

Up to and including the 1-in. displacement cycles, the specimen behaved elastically with an average stiffness of 131 kips/in. The strain distributions across the cover plates and beam flanges were approximately uniform and bell-shaped, respectively. Similar to Specimen PN3, hysteresis loops did not indicate the onset of inelastic behavior but cover plate strain gage measurements exceeded the anticipated yield value. Measured at a distance of 1.25 in. from the face of the column, the maximum strain was approximately 4 times the yield strain calculated from mill certificate test data (1720 min/in). As previously mentioned, this is primarily due to local stress concentrations in a small area adjacent to the column; thus, global inelastic behavior was not observed. No other strains exceeded yield values.

In the first leg of the 2-in. displacement cycles, a reduction in the connection stiffness defined the onset of yielding. At this time, slight yielding was observed on the east face of the column flange opposite the outer most "continuity" plates. Yielding was not confirmed since no strain gages were placed at these locations. Continued yielding of the cover plates was confirmed, however, as the maximum strain reached approximately 6 times the calculated yield value. The principal strain calculated at the center of the column web was approximately 5.5 times the assumed yield; meanwhile, it was approximately 1.8 times the assumed yield at the center of the doubler plate (A572, Grade 50). No other strains exceeded yield values.

Prior to completing the first 2-in. displacement cycle, a noise was heard at a beam tip displacement of -1.80 in. and an actuator force of -209 kips. Upon stopping the actuator and visually inspecting the specimen, a small crack was discovered in the column web adjacent to the top beam flange, as shown in Figure 4-13. The crack was in-plane with the beam flange and extended from the column web hole nearest the panel zone to the k-region, or fillet, of the column. Since the amount of strength lost was small (approximately 10 kips), testing proceeded after taking photographs and measuring the crack length. Subsequently, during the following two 2-in. displacement cycles, the center panel zone whitewash continued to spall (Figure 4-14) with the principal strains on the column web and doubler plate both reaching approximately 3.75 times the assumed yield values.

During the first 3-in. displacement cycle, the column web crack adjacent to the top beam flange propagated into the column flange, as shown in Figure 4-15. The length of the crack was approximately 6 in. from the k-region to its end. The extent of the column flange damage on the bottom side of the specimen could not be readily determined due to the lack of access. Next, the two 3-in. displacement cycles caused x-shaped yield patterns to develop on the cover plates as flaking of the whitewash occurred (see Figure 4-18). Continued yielding of the panel zone also occurred as the computed principal strain approximately reached 5.5 and 4.75 times the assumed yield of the column web and doubler plate, respectively. All other strains remained below yield values.

During the first 4-in. displacement cycle, specimen failed at a displacement and force of 3.08 in. and 236 kips, respectively. Overall, a loud noise was accompanied by a loss of approximately 125 kips of connection strength. At this time, the column flange fractured adjacent to the bottom beam flange, as shown in Figures 4-16 and 4-17. It is believed that the crack, as discussed later, initiated at the column web "relief" hole nearest the panel zone and immediately propagated into the column flange and across its width. Following this failure, the specimen was loaded in the opposite direction without a significant amount of strength degradation. As shown in Figure 4-18, the column flange crack adjacent to the top beam flange propagated through the column flange thickness into the beam flange and cover plate weld-to-column area.

As mentioned above, NSF Specimen #1 failed from a brittle fracture in the column adjacent to the bottom beam flange. Figure B-1 (in Appendix B) is a free-body diagram of the column at failure. Based on the associated bending moment diagram and calculations in Appendix B, the maximum tensile bending stress in the column at the "relief" holes exceeded the tensile strength of the column material. These calculations and Figure 4-13 (crack in the column adjacent to the top beam flange) give supporting evidence that the crack initiated at the edge of the "relief" hole nearest the extreme fiber and propagated into the column flange. Hence, drilling of the "relief" holes was the most likely cause of premature failure. Table 3 summarizes the performance of NSF Specimen #1.

4.4 NSF Specimen #6

A common configuration of lateral force resisting systems in the design of contemporary steel framed buildings is one that has moment resisting frames in both directions of a building's plan. Commonly referred to as a rigid space frame, this type of structural system has been widely used in areas of high seismicity for several reasons. As previously mentioned, both owners and architects prefer rigid space frames since they provide greater architectural versatility than any other type of framing system. Braced frames or shear walls, for example, interrupt the large-spanned, open bays that moment frames can provide. Likewise, as a result of several recent testing programs, many engineers have regained some confidence in the ability of special moment resisting connections to perform well in severe earthquakes. However, special moment resisting connections between wide flange beams (I-beams) and box-columns have not been the subject of recent tests in the United States.

Due to certain strength and stiffness limitations of a wide flange, some designers specify box-columns rather than standard wide flange sections for rigid space frames. Box-columns are typically constructed by one of two methods: either by welding plates to the sides of a wide flange member (Figure 4-19) or by welding four individual plates to form a box. The advantages of box-columns over wide flange columns are that box-columns provide more economical use of material, increased strength and stiffness (especially in the weak axis), greater torsional strength, and increased shear resistance. On the other hand, the higher cost of fabrication, which is primarily due to the difficulty in providing internal continuity plates (Figure 4-20), has prevented many engineers from using internal continuity plates.

When faced with this economic dilemma, engineers have been forced to oversize columns and/or side plates in order to satisfy the design equations. Nevertheless, numerous special moment resisting framed buildings have been erected of box-columns in areas of high seismicity. There are also two known hospitals in the Los Angeles area that propose this framing system in replacement structures that were damaged during the Northridge Earthquake. Yet, contemporary I-beam to box-column connections have not been tested in response to the earthquake. Based on the lack of sufficient experimental information, NSF Specimen #6 was chosen to investigate an economical method of connecting an I-beam to a box-column in a manner consistent with the performance goals provided by Engelhardt and Sabol [25].

4.4.1 Recent Experimental Research

Recent research performed by S-L. Lee, N. E. Shanmugam, and L-C. Ting at the University of Singapore [31, 32] has suggested that I-beam to box-column connections can be successfully stiffened by external structural tees, hereafter external tee stiffeners, rather than internal continuity plates. By finite element analysis and experimentation of several two-way and four-way connections, the researchers concluded that the configuration shown in Figure 4-21a provided sufficient strength, sufficient rotational capacity, adequate stiffness, ease of erection, and economical fabrication. Loads were monotonically and cyclically applied to the centerline of 1 m long tubular box-column stubs (sizes ranging from 200x200x12 mm to 300x300x20 mm) which had either two or four 1.5 m long I-beams (sizes ranging from 254x102x22.32 kg/m to 457x191x67 kg/m) each connected to the column at one end and supports at the other. All steel was Grade 43, which had a coupon yield strength ranging from 275 to 312 kPa (39.9 to 45.2 ksi). The size of stiffeners was determined by finite element analysis and resulted in tees that ranged from 102x102x12 kg/m of length 50 mm to 127x76x13 kg/m of 140 mm length. All beam flanges and webs were connected to the box-columns by full penetration groove welds. Full penetration welds were also used to attach the tee webs to the beam flanges, whereas vertical fillet welds were used to connect the tee flanges to the column.

The hysteretic loops for two cyclically loaded specimens are shown in Figures 4-22a and 4-22b. It can be seen that these two specimens appear to have met the strength, stiffness, and rotational demands placed on special moment resisting connections subjected to seismic load reversals. However, it should be mentioned that in comparison to the full-scale specimens previously discussed in this report, these specimens were not only very small they were also constructed of a low yield strength steel similar to A-36 steel used during the 1970s in the United States. Furthermore, the specimens were not tested under the same displacement controlled loading history listed in Table 1 of this report. The Singapore specimens were only subjected to a single cycle at each displacement increment (Figure 4-21b). Thus, it is not suggested that the criteria used for selection of tees be extrapolated for implementation in contemporary design of buildings constructed in the United States. Instead, this research suggests that external tee stiffeners can replace internal continuity plates with significant benefits to the connection's cost and performance.

4.4.2 Design

The intent of NSF Specimen #6 was to improve the economy and performance of modern I-beam to box-column special moment resisting connections by placing external tee stiffeners in a configuration similar to specimens recently tested at the University of Singapore [31, 32]. Typically, box-columns must be reinforced adjacent to the connecting beam flanges due to a lack of strength and/or stiffness in this region; the concentrated forces that develop can lead to local damage. At the beam tension flange attachment to the column, for instance, the column flange may require stiffener plates if local bending impairs the column's strength [17]. Likewise, the compressive beam flange force may require reinforcement to prevent local yielding, crippling, and buckling of the column web.

For box-columns, the placement of stiffener plates within the box-section (internal continuity plates) is a laborious and expensive process. First, internal continuity plates are prepared for placement with backup bars along each of the four edges as shown in Figure 4-20. Standard size backup bars are tack welded along three edges of the continuity plate, whereas one edge requires backup bars that are stacked several thick. Prior to adding a side plate (or fourth plate) to the column, each continuity plate is welded to the box-column along three sides. Standard sized backup bars are used for these complete penetration groove welds, which are typically applied by the FCAW process. After the side plate (or fourth plate) is welded to close the box-column, access to weld the stiffener plate to the side plate (or fourth plate) is limited. In most cases, a weld access hole is created by removing a circular piece of the column flange (or plate) material. Then, the electroslag welding (ESW) process is used to deposit weld material between the stiffener and side plate (or fourth plate) of the column. An extremely thick backup bar is required beneath this weld because of the high temperatures that develop. Finally, the piece of column flange (or wall) that was removed for weld access must be replaced.

Overall, this is an expensive process that provides a continuity plate of questionable quality, especially at the connection provided by the ESW process. Since high porosity is a common problem in these welds, they must be qualified by test [16]. On the other hand, it is believed that the current cost of furnishing structural tees and welding them at the proper locations will result in a connection of reduced cost. For these reasons, NSF Specimen #6 was equipped with external tee stiffeners designed to satisfy the equations for preventing local yielding, crippling, and buckling of the column web(s) and local bending of the column flange(s).

With a large number of box-columns currently being constructed of plated I-sections similar to the one shown in Figure 4-19, it was decided that NSF Specimen #6 would represent an I-beam to plated I-column connection characteristic of rigid space framed buildings recently constructed in areas of high seismicity. The choice of member sizes was a difficult process since typical members were too large for the testing equipment at the Davis Hall Testing Facility. As a result, the specimen needed to be scaled down slightly.

In general, the specimen consisted of a W36x135 (A-36) beam connected to a plated I-column (or box-column). The box-column was constructed of a W14x233 (A-572, Grade 50) member with two 1-1/4 in. thick by 16 in. wide side plates (A-572, Grade 50) over the height of the column. The column was oriented such that three webs provided shear resistance. The side plates were connected to the column flanges by full-height partial penetration groove welds. A welded flange-bolted web connection was used between the beam and the column. The shear connection consisted of ten 1 in. diameter high-strength bolts (A490) in conjunction with supplemental welds along three sides of the tab.

In addition to the goal of verifying the acceptability of replacing internal continuity plates with external tee stiffeners, the tees were also intended to provide additional strength, ductility, and redundancy at the connection for improved performance and reliability. Based on the performance of the University of Singapore tests, it was possible that the brittle failures observed near beam flange-to-column flange welds could be avoided by reinforcing the beam with structural tees at the connection. With such a configuration, the ductile performance basically relied upon plastic hinging behavior, which included both yielding and buckling, at the unreinforced section of the beam prior to the occurrence of a brittle failure at the beam flange-to-column welds. The size, configuration, and connection of tees was determined by the following criteria:

1. transfer an adequate amount of the beam flange forces in order to satisfy the requirements for omitting internal continuity plates;
2. provide sufficient beam reinforcement to limit the through-thickness stress in the column flange to 40 ksi (based on anisotropic properties of column flange);
3. provide beam reinforcement for a length adequate to move the plastic hinge to an area $d_b / 2$ to d_b away from the face of the column (d_b = the depth of the beam);
4. establish a reliable load path to transfer the amount of each beam flange force, which was calculated in criterium 1, to the side plates.

From these criteria, four WT5x44 (A-36) tees were selected and cut to the dimensions shown in Figures 4-24 and 4-26. For added economy, this tee section was chosen such that a W10x88 could be cut in half. Also, the top side of each tee flange was trimmed to provide 45 degrees access for the application of down-hand fillet welds between the tee webs and beam flanges. Finally, the tee flanges were tapered to reduce the amount of interference that would occur if a formed steel deck and concrete slab were placed above the beam. The tee flanges were also tapered below the beam for symmetry. However, it should be noted that the top tee flanges would not likely interfere with a formed steel deck and/or concrete slab if the ribs of the deck were parallel to the axis of the beam (depending on the depth of the ribs).

Figures 4-23 through 4-26 show the overall dimensions, connection details, configuration, and detailed sections for NSF Specimen #6. As mentioned, backup bars and run-off tabs were removed and reinforcing fillet welds were provided at the beam flange-to-column flange groove welds. A "side strap" detail was adopted to connect the flange of the tees to the column side plates. The intent of this configuration was to provide greater reliability than the butt joint used in the University of Singapore specimens. The fillet welds connecting the beam flanges to the tee webs and the tee flanges to the column side plates were sized according to criteria listed above and the strength of each connection was matched. Furthermore, although it did not govern in this case, a calculation was made to check the shear flow between the tees and the beam.

In theory, criterium 1 would be satisfied by limiting the maximum beam flange forces at the face of the column to the design strength of the column for concentrated loads (i.e. local web yielding, web crippling, compression buckling of the web, or local flange bending). Assuming a conservative value of 50 ksi for the column yield strength (capacity) of A-572, Grade 50 steel [27], the design strength of the column adjacent to the compression flange of the beam using LRFD was governed by either local web yielding or local web crippling. For local web yielding, the design strength of the column was:

$$\mathbf{P_{bf} = \phi\ (5k + t_{fb})\ F_{yc}\ t_{wc}} \qquad (4\text{-}1)$$

where P_{bf} = factored beam flange force
ϕ = resistance factor = 1.0
t_{fb} = thickness of the flange of the beam = 0.79 in.
F_{yc} = yield strength capacity of the column = 50 ksi
t_{wc} = thickness of the web of the column = 1.07 in.

$= 1.0\ [(5)\ (2.375) + 0.79]\ (50)\ (1.07)$

$= 678$ kips

For local web crippling, the design strength of the column was:

$$P_{bf} = \phi\ 135\ t_{wc}^2\ [1 + 3\ (t_{fb} / d_c)\ (t_{wc} / t_{fc})^{1.5}]\ (F_{yc}\ t_{fc} / t_{wc})^{0.5} \quad (4\text{-}2)$$

where ϕ = resistance factor = 0.75
d_c = overall depth of the column = 16.04 in.
t_{fc} = thickness of the flange of the column = 1.72 in.

$$= (0.75)\ (135)\ (1.07)^2\ [1 + 3\ (0.79 / 16.04)\ (1.07 / 1.72)^{1.5}]\ [(50)\ (1.72) / 1.07]^{0.5}$$

$$= 1115 \text{ kips}$$

Since the connection was one-sided, the local buckling limit state of the column web need not be checked, but for two-sided connections this limit state could govern [17]. It was also assumed that local column flange bending (at the beam flange tension force) would not be a concern since side plates were provided along the column. In the calculations of local web yielding and crippling, however, it was assumed that the column side plates did not provide added resistance. Thus, the expected capacity of the column web was 678 kips, which was governed by local web yielding.

Assuming a conservative value of 55 ksi for the beam flange yield strength (demand) of A-36 steel [27], the plastic moment at the unreinforced section of the beam was:

$$M_p = \alpha_{sh}\ (Z_x)\ (F_y) \quad (4\text{-}3)$$

where α_{sh} represents a strain hardening factor of the beam at the plastic hinge. Since the beam chosen had a slenderness ratio of:

$$\lambda = b / [(2)\ (t_{bf})] \quad (4\text{-}4)$$

$$= 12 / [(2)\ (.79)] = 7.6$$

for flange local buckling and the compact section limit was:

$$\lambda_p = 65 / (F_{yb})^{0.5} \quad (4\text{-}5)$$

$$= 65 / (55)^{0.5} = 8.8$$

it was determined that the beam had a slight propensity to buckle prior to significant strain hardening. For this reason, a strain hardening factor of 1.0 was used. From equation 4-3, the plastic moment of the beam was:

$$M_p = 1.0\ (509)\ (55) = 28{,}000 \text{ k-in.}$$

The location of expected plastic hinging was at a distance equal to the width of the beam flange divided by two (b_f / 2) beyond the end of the tees. From Figure 4-26, it can be seen that this distance was 33.5 in. (27.5 + 12 / 2) from the face of the column. However, if a plastic hinge was to form at this location, the moment at the column face would be proportional to the distances from the actuator to the column face (134.5 in.) and from the actuator to the plastic hinge (101 in.). The expected moment demand at the face of the column was:

$$\mathbf{M_{col} = (134.5 / 101)\, M_p = 1.33\, M_p} \qquad (4\text{-}6)$$
$$= 1.33\,(28{,}000) = 37{,}300 \text{ k-in.}$$

and the corresponding beam flange forces were:

$$\mathbf{T_{col} = C_{col} = M_{col} / [(0.95)\,(d_b)]} \qquad (4\text{-}7)$$
$$= 37{,}300 / [(0.95)\,(35.6)] = 1100 \text{ kips}$$

Thus, if internal continuity plates were to be omitted, each tee would be responsible for transferring a force of:

$$\mathbf{P_{tee} = (C_{col} - P_{bf}) / 2} \qquad (4\text{-}8)$$
$$= (1100 - 678) / 2 = 211 \text{ kips}$$

to the column side plates.

The tee connections were subsequently designed for this force. Each tee web was connected to a beam flange by one 1/2 in. fillet weld for a length of 24 in., whereas each tee flange was connected to a column side plate by two 3/4 in. fillet welds, each 8 in. long. The strength of each of these connections was matched. The strengths were:

$$\mathbf{R_n = \phi\,(0.6)\,(F_{EXX})\,(0.707)\,(w)\,(l)} \qquad (4\text{-}9)$$
$$= 0.75\,(0.6)\,(70)\,(0.707)\,(1/2)\,(24) = 267 \text{ kips}$$
$$= 2\,[(0.75)\,(0.6)\,(70)\,(0.707)\,(3/4)\,(8)] = 267 \text{ kips}$$

267 kips > 211 kips therefore ok

Upon calculating the shear flow between the tees and the beam flanges, it was determined that the 1/2 in. fillet welds provided adequate strength.

In theory, criterium 2 would be satisfied by reinforcing the beam such that "divot" failures in the column flange would be prevented. The addition of tees adjacent to the face of the column effectively increased the moment of inertia of the reinforced section by approximately 2.75 times that of the unreinforced section of the beam. Thus, for the same bending moment, the maximum bending stress at the column face would be 35 percent of that expected at an unreinforced section. Using equation 4-6 and the reinforced moment of inertia, the resulting bending stress at the beam flange-to-column flange connection would be approximately 60 percent of the maximum bending stress calculated at the unreinforced section of the beam (based on $M_p = Z_x F_y$). This corresponded to a through-thickness stress of 33 ksi. Consequently, it was expected that a plastic hinge would form near the end of the tees prior to a brittle "divot" failure at the connection.

Finally, criteria 3 and 4 would be satisfied by extending the tees 27 in. from the face of the column ($3 d_b / 4$) and by connecting the tees to the column side plates by a "side strap" detail, which was intended to provide greater reliability than a butt joint.

It should be noted that the specimen was fabricated and inspected according standard steel construction practices. Field construction was simulated in a fabrication shop by positioning the column vertically and attaching a cantilevered beam which was shored at its free end. Fillet welds were applied by the FCAW process with Lincoln NR-232 wire. Complete penetration groove welds were also applied by the FCAW process, but with Lincoln NR-311 wire. The partial penetration groove welds connecting the side plates to the column were applied in the shop by the submerged arc welding process (SAW). See Section 4.3.1 for more information regarding fabrication and inspection practices.

4.4.3 Experimental Results

On September 25, 1995, NSF Specimen #6 was tested to failure according to the displacement-controlled loading history listed in Table 1. The force versus displacement and moment versus plastic rotation are plotted in Figures 4-27 and 4-28, respectively. In general, the specimen performed well; a plastic hinge formed in the beam at the end of the reinforced area. However, the gradual tearing of one tee web-to-beam flange weld led to a premature failure at the bottom beam flange-to-column flange connection. The mode of failure at this location was a "divot" of the column flange base metal material. Following this failure, the specimen sustained one complete 5-in. displacement cycle before the test was terminated. Before and after photographs of the specimen are shown in Figures 4-29 through 4-32.

Up to and including the 1-in. displacement cycles, the specimen responded elastically with an average stiffness of 184 kips/in. Slight flaking of the whitewash was observed in the top and bottom beam flanges adjacent to the end of the tees. Strain gage measurements confirmed that yielding had occurred near the end of the tees. It is suspected that yielding was primarily due to stress concentration. However, the overall force versus displacement hysteretic loops did not show any signs of yielding. No other strain gage measurements exceeded yield values.

In the first excursion of the 2-in. displacement cycles, a reduction of connection stiffness defined the onset of yielding. The yield displacement of 0.98 in. was not reached until the first 2-in.displacement cycle because of a slip that occurred between the clevis and beam end plate. The slip was approximately 10 percent of the total beam tip deflection. During this cycle, yielding was observed in both the top and bottom beam flanges and neighboring areas of the beam web. Figures 4-33 and 4-34 show the yield patterns at these locations. Yielding was confirmed by the strain gage measurements outside of the reinforced area of the beam which exceeded the anticipated yield value by a small amount. No other strain gage measurements exceeded yield values. The maximum principal strain in the center of the column side plate, for example, was only one-fifth of the anticipated yield value.

During the second inelastic cycle, a weld between one of the tee webs and the bottom beam flange fractured. At a force of 239 kips and a displacement of 1.80 in., a noise was heard as the weld tore to a length of approximately 3 in. Figure 4-35 shows the yield pattern and separation between the tee and beam flange. No significant loss of connection strength resulted from this weld tear.

During the first leg of the 3-in displacement cycles, another noise occurred as the weld tear propagated to a length of 7 in. Once again, no loss of connection strength was observed. Soon thereafter, slight buckling of the top beam flange was observed as the displacement neared its peak. Subsequent loading toward the bottom of the connection also caused buckling of the bottom beam flange as shown in Figure 4-36. During the second and third 3-in. displacement cycles, noises were heard as the weld tear propagated to lengths of 11 and 12 in., respectively. As buckling of the beam flanges continued to progress, the beam web began to buckle in double-curvature. However, buckling did not result in a loss of connection strength.

At 3.25 in. displacement, during the first 4-in. displacement cycle, a loud noise was heard as the weld tear, which occurred between the tee web and bottom beam flange, spread an additional 8 in. toward the column. At this time, the strength of the weld was essentially insignificant. Almost immediately following this fracture, a second noise was heard as a crack formed across the bottom beam flange-to-column weld. Figure 4-37 shows the fracture at this complete penetration groove weld. At first, it appeared as if this fracture was a "divot" type failure in the column flange base metal. Upon closer inspection, however, the fracture was only observable at the extreme fiber of the bottom beam flange; there was no sign of distress on the inside of the beam flange. For this reason, this phenomenon was classified as a partial "divot," which led to an immediate loss of approximately 10 kips of connection strength.

As the displacement neared its peak during the first 4-in. cycle, the top beam flange buckled a considerable amount causing one of the tee web-to-top beam flange welds to tear. Figure 4-38 shows the buckling, weld tear, and yield pattern at this location. During the subsequent 4-in. displacement cycle, both flanges continued to buckle in compression leading to a gradual deterioration of connection strength. It should be noted that the second 4-in. displacement cycle did not cause additional damage at the partial "divot."

During the first leg of the 5-in. displacement cycles, however, a loud noise was heard as the bottom beam flange-to-column connection failed. At 3.10 in. displacement, the connection lost approximately 70 kips of strength due to a complete "divot" at this location. But following this failure, the connection strength **increased** by nearly 20 kips as the displacement proceeded to 5 in. Since the connection possessed over 50 percent of its maximum strength at this time, the test was not terminated.

During the second 5-in. displacement cycle, all of the bottom beam flange tensile force was resisted by a single tee and the shear tab. The force in the actuator at the peak displacement of 5 in. was 157 kips, which corresponds to 60 percent of the maximum strength of the connection. Upon returning to zero displacement, the connection strength dramatically reduced. At this point, it was believed that the connection could not provide additional energy dissipation that was of significance and the test was terminated.

Figures 4-39 through 4-43 show the damaged connection after the test. Both top and bottom beam flanges yielded over a length of approximately 4 ft. from the column face. Yielding also occurred across the depth of the beam at the end of the tees. Likewise, both top and bottom beam flanges as well as the web buckled near the end of the reinforced area; a plastic hinge formed at this location. As discussed, two of the beam flange-to-tee web welds gradually tore during the experiment. One tear was apparently the result of the top beam flange buckling. On the other hand, the second tear, which prematurely unzipped at the bottom beam flange, was most likely due to a poor quality weld. Nonetheless, it is suggested that these welds be oversized near the end to the tees in an effort to accommodate local flange buckling of the beam. Another method to prevent peeling of the beam flanges from the tees would be to bolt the web of each tee to the beam flanges near the end of the reinforcement.

Secondary damage, which developed after the complete "divot" failure, occurred at the "side strap" and shear tab neighboring the bottom beam flange. Since a single tee was connected to the bottom beam flange at this time, the tensile resistance was eccentric to the beam. Hence, this tee bent upward during the second 5-in. displacement cycle causing the "side strap" to yield in bending. Damage near the bottom of the shear connection consisted of a 22 in. long fracture of a supplemental shear tab weld, shear failure of one shear tab-to-beam web bolt, and bearing failure in the shear tab and beam web material surrounding the bottom four bolts. It should also be noted that prior to the complete "divot" failure, the column showed no signs of local damage at the concentrated beam flange forces.

4.5 Summary of Findings

4.5.1 NSF Specimen #1

In general, NSF Specimen #1 behaved somewhat better than the comparable pre-Northridge specimen (Specimen PN3). Although the amount of plastic rotation was essentially the same as Specimen PN3, NSF Specimen #1 did not fail until the seventh inelastic cycle (as compared to the fourth for Specimen PN3). As a result, the total energy dissipated by the connection was nearly 40 percent larger than Specimen PN3. Nonetheless, the failure of NSF Specimen #1 was characterized by a sudden loss of approximately 125 kips of connection strength. For this reason the performance of NSF Specimen #1 was subjectively rated poor.

4.5.2 NSF Specimen #6

In general, NSF Specimen #6 met two of the three performance goals provided by Engelhardt and Sabol [25]. The peak beam plastic rotation achieved was **3.1 percent** and the amount of energy dissipated was **49 percent** of the plastic moment capacity of the beam. However, the gradual tearing of one fillet weld, which connected the web of a tee to the bottom beam flange, led to a "divot" failure of the bottom beam flange-to-column connection. Although this brittle fracture occurred, the specimen sustained another inelastic cycle (at 5 in.) in which the connection strength reached greater than **60 percent** of its maximum value. Consequently, the performance of NSF Specimen #6 was subjectively rated good.

It is very important to note that the maximum plastic rotation and energy dissipation occurred after the bottom beam flange-to-column failed by a "divot." Although this is a brittle failure, the primary reason for including the second 5-in. cycle was that the connection strength did not diminish a sizable amount. For clarification, however, the maximum plastic rotation and energy dissipation prior to the "divot" failure were 2.1 percent and 9810 k-in. (40 percent of M_p), respectively. Nonetheless, NSF Specimen #6 performed rather well. The external tee stiffeners successfully prevented damage to the column web; the resistance they provided was adequate for omitting internal continuity plates. Furthermore, it is believed that if the connection between the tee web and bottom beam flange had not failed at one of the tees, the "divot" would have been avoided. Although this connection shows promise, an effort should be made to improve the details of this connection in future experimental research.

For further exemplification, the overall performance of NSF Specimen #6 was compared to that of another reinforced connection recently tested at the Davis Hall Testing Facility. Funded by the U.S. Department of Energy, Forell/Elsesser Engineers of San Francisco designed a reinforced connection to be used in a laboratory complex located at the Lawrence Berkeley National Laboratory [33]. Two identical specimens were designed, constructed, and tested in a manner similar to those previously discussed in this report.

Each specimen consisted of a W30x90 (A-572, Grade 50) beam connected to a W14x283 (A-572, Grade 50) column. The column was sized to prevent inelastic activity from occurring in the column and panel zone. The beam was not directly connected to the column at any location. Rather, the beam was fillet welded along its flanges to trapezoidal top and bottom cover plates. Then, the cover plates were both connected to the column by single-bevel, complete penetration groove welds in which the backup bars were removed and reinforcing fillet welds were applied. The bottom cover plate was connected to the column in the shop and to the beam in the field whereas the top cover plate was connected to the beam in the shop and to the column in the field. This process allowed the welders to apply the bottom groove weld without the obstruction of the beam web. Also, two bolts were provided between the shear tab and beam web for erection purposes and a large trapezoidal shear tab (14 in. wide and 5/8 in. thick) was connected to the column by double-bevel groove welds and to the beam web by fillet welds along three edges of the tab. Continuity plates were provided in the column.

In general, the specimen performed very well. The maximum plastic rotation achieved was 3.9 percent (specimen 2) at a force of approximately 60 kips, which corresponds to a strength of approximately 40 percent of the maximum value (148 kips). During the beginning of the test, local buckling of the beam flanges was observed almost immediately following yield. This caused a significant loss of connection strength over the first three inelastic cycles of loading. By the third inelastic cycle, the connection no longer supplied the plastic moment capacity of the beam at the location of yielding. Following this significant loss of strength, the performance of each specimen was characterized by hysteretic loops that gradually deteriorated with each successive cycle. Both specimens achieved the performance goal of at least three cycles that result in beam plastic rotations of 3.0 percent; specimen 1 sustained three and specimen 2 sustained ten.

However, it should be noted that the beam section was inadvertently changed from a compact section (W30x99) to a potentially noncompact section (W30x90), depending on the exact yield strength of the beam flange material. Based on the independent lab tension test data for the beam flange, the slenderness ratio for flange local buckling of a W30x90 was:

$$\lambda = 10.4 / [(2)\ (.61)] = 8.5$$

and the compact section limit was:

$$\lambda_p = 65 / (50.3)^{0.5} = 9.2$$

Based on this criteria, the W30x90 beam was compact. However, if a conservative yield value of 58 ksi was used (for the A-572, Grade 50), as recommended in the *DSA/OSHPD Emergency Code Change for Steel Moment Frame Girder-to-Column Connection* [27], the compact section limit would be:

$$\lambda_p = 65 / (58)^{0.5} = 8.5$$

For this reason, the mode of failure of these specimens was local buckling of the beam flanges outside of the cover plates that resulted in a connection strength significantly lower than the plastic moment capacity of the beam. Because of the reduction in strength that occurs during local flange buckling, the SEAOC *Recommended Lateral Force Requirements and Commentary* require that all beam sections be compact [1] such that the plastic moment capacity of the section is exceeded for numerous cycles.

From the experimental results of the Forell/Elsesser specimens, the maximum force in the actuator was 148 kips, which corresponded to a moment at the location of buckling of:

$$M_b = (134.5 - 24 - 10.4 / 2)\ 148 = 15{,}600 \text{ k-in.}$$

Using the independent testing lab results for the beam flange yield strength, the plastic moment capacity of the beam at the location of buckling was:

$$M_p = Z_x F_y = (283)\ (50.3) = 14{,}200 \text{ k-in.}$$

Thus, the connection strength exceeded the plastic moment capacity of the beam by a slight amount. What is important, however, is the number of cycles that exceeded the plastic moment capacity of the beam. For both Forell/Elsesser specimens, only three cycles of inelastic loading reached the plastic moment capacity of the beam. Nearly all of the energy absorption of the beam was due to local buckling of the flange. NSF Specimen #6, on the other hand, completed 7 inelastic cycles above the force required to for a plastic hinge at the end of the tees. This is primarily due to the lower slenderness value of the beam flange.

5. CONCLUSION

5.1 Pending Research

There are currently several tests scheduled for completion in the near future at the University of California at Berkeley which directly relate to the experimental research discussed in this report. The research in progress consists of the following:

1. A full-sized tension test of a simulated beam flange-to-column connection consisting of two 1-3/8 in. thick plates connected to a W14x455 column stub. The intent of the test is to determine the adequacy of placing a sealing fillet weld over each artificial crack formed between the backup bar and column flange. It is believed that some of the original beam-to-column specimens tested during the 1970s may have successfully used this technique to reduce stress concentrations at the backup bar. Figure 5-1 shows the specimen and connection details. For more information regarding this method of connection, see the EERC report titled "Behavior of Pre-Northridge Moment Resisting Steel Connections" by T-S. Yang and E. P. Popov [34].

2. Two full-sized beam-to-column moment resisting connections each consisting of a W36x150 beam connected to the strong axis of a W14x455 column. The intent of these tests is to determine the adequacy of drilling holes in the beam flanges in order to weaken the beam away from the connection. Successful tests would form plastic hinges at the weakened sections prior to a brittle failure at the connection. Depending of the outcome of the tension test discussed in item 1 above, the sealing filled weld detail is also to be used in these specimens. Also, one connection had horizontal reinforcing ribs or "wings" at the beam flange-to-column flange connections, whereas the other had an unreinforced connection.

5.2 Suggestions for Further Research

Due to the good behavior exhibited by NSF Specimen #6, it is suggested that further research be preformed on I-beam to box-column moment resisting connections stiffened externally. Rather that tee stiffeners, however, it is suggested that angles be used to allow for moment-resisting connections at right angles. Another benefit of an angle as compared to a tee is that both legs have the same thickness. In effect, this would allow shorter stiffeners to be used, resulting in reduced stresses at the face of the column. It is also suggested that a welded web connection be employed since it typically provides greater ductility. Furthermore, in order to prevent the premature failures that were observed during the experimentation, it is recommended that the beam flange-to-angle welds be oversized to prevent a peeling separation of the beam flanges at the end of the reinforcement. For added redundancy, it is also suggested that two bolts connect each angle to the beam flanges in this vicinity. Figures 5-2 through 5-5 show the proposed improvements for the connection.

5.3 The Limitations of Codes and Experimental Findings in Design

The intent of the building codes is to provide analysis and design guidelines that engineers can follow to determine the *minimum* requirements that supply life-safety. As engineers, we must educate those who do not understand this intent. As stated in the SEAOC *Recommended Lateral Force Requirements and Commentary*: "[I]t is the responsibility of the engineer to interpret and adapt these principles to each structure using experience and good judgement [1]." Furthermore, it is imperative that engineers as well as owners of buildings understand that a relatively small up-front investment will provide conservatism in excess of the code minimums and will result in a significant reduction of seismic hazard. In areas of high seismicity, it is likely that this investment will lead to a life-cycle cost savings.

Unlike most mass-produced structural systems, the exact behavior of steel framed buildings when subjected to seismic forces is difficult if not impossible to determine. Entire buildings are rarely tested dynamically; usually earthquakes are the only true "tests" for buildings. Instead, pieces of buildings are tested individually in order to determine the expected response of entire structures. Furthermore, earthquake-resistant design is not only dependent on the materials, size, and configuration of each building, it is also site-specific. For these reasons, it is suggested that conservatism be used when interpreting the results of this report.

APPENDIX A. SNUBBER PLATES FOR TEST SETUP

A.1 Calculate the maximum reaction force at each concrete block

Based on the configuration of blocks (Figure 3-4), the maximum force that could develop at a reaction block is approximately equal to the maximum actuator force.

From statics, the maximum force that could develop at each reaction is the following:

northwest block: 350 (134.5) / 138.0 = 341 kips

southwest block: 350 (134.5) / 138.0 = 341 kips

south block: 350 kips

Therefore, design all reactions for 350 kips.

A.2 Design snubbers to transfer reaction forces from the blocks to the strong-floor

To insure proper surface contact, place high-strength grout between the following:

concrete reaction blocks and concrete strong-floor,

steel snubbers and concrete reaction blocks, and

steel snubbers and concrete strong-floor.

Assume 3000 psi concrete compressive strength for reaction blocks.

use 6 in. tall steel snubbers bearing against concrete blocks
(see Figures A-3 and A-4 for configuration)

surface area = 6 (48) = 288 in^2

allowable bearing = 288 (3) = 864 kips

864 kips > 350 kips therefore ok

Assume a static coefficient of friction of 0.30 between steel snubbers and concrete.

Based on the rod manufacturer's recommended tensioning, the table below gives the friction resistance for each rod diameter available.

rod diameter (in)	recommended tensioning (kips)	friction resistance (kips)
1-1/4	137	41.1
1-3/8	166	49.8
2	351	105.3

Design rods in snubber-to-floor connection to prevent sliding.

Based on availability, the rods required to develop 350 kips friction resistance are the following:

northwest and southwest supports:

two 1-1/4 in. diameter = 2 (41.1) = 82.2 kips
two 1-3/8 in. diameter = 2 (49.8) = 99.6 kips
two 2 in. diameter = 2 (105.3) = 210.6 kips

total = 392.4 kips > 350 kips therefore ok

south support:

three 1-1/4 in. diameter = 3 (41.1) = 123.3 kips
one 1-3/8 in. diameter = 1 (49.8) = 49.8 kips
two 2 in. diameter = 2 (105.3) = 210.6 kips

total = 392.4 kips > 350 kips therefore ok

Therefore, fabricate each snubber to be large enough for six rods at 18 in. center-to-center, as shown in Figure A-1 and configure as shown in Figure A-3.

Design rods in concrete block-to-floor connection to prevent overturning.

The maximum overturning moment (about the top of the south snubbers) is approximately:

maximum O. T. M. = 350 (12) = 4200 kip-in.

Use six 1-1/4 in. diameter rods from each block to strong-floor, as shown in Figure A-6. Assume three rods resist overturning.

O. T. M. resistance = 3 (137) (46.4) = 19,100 kip-in

19,100 kip-in > 4200 kip-in therefore ok

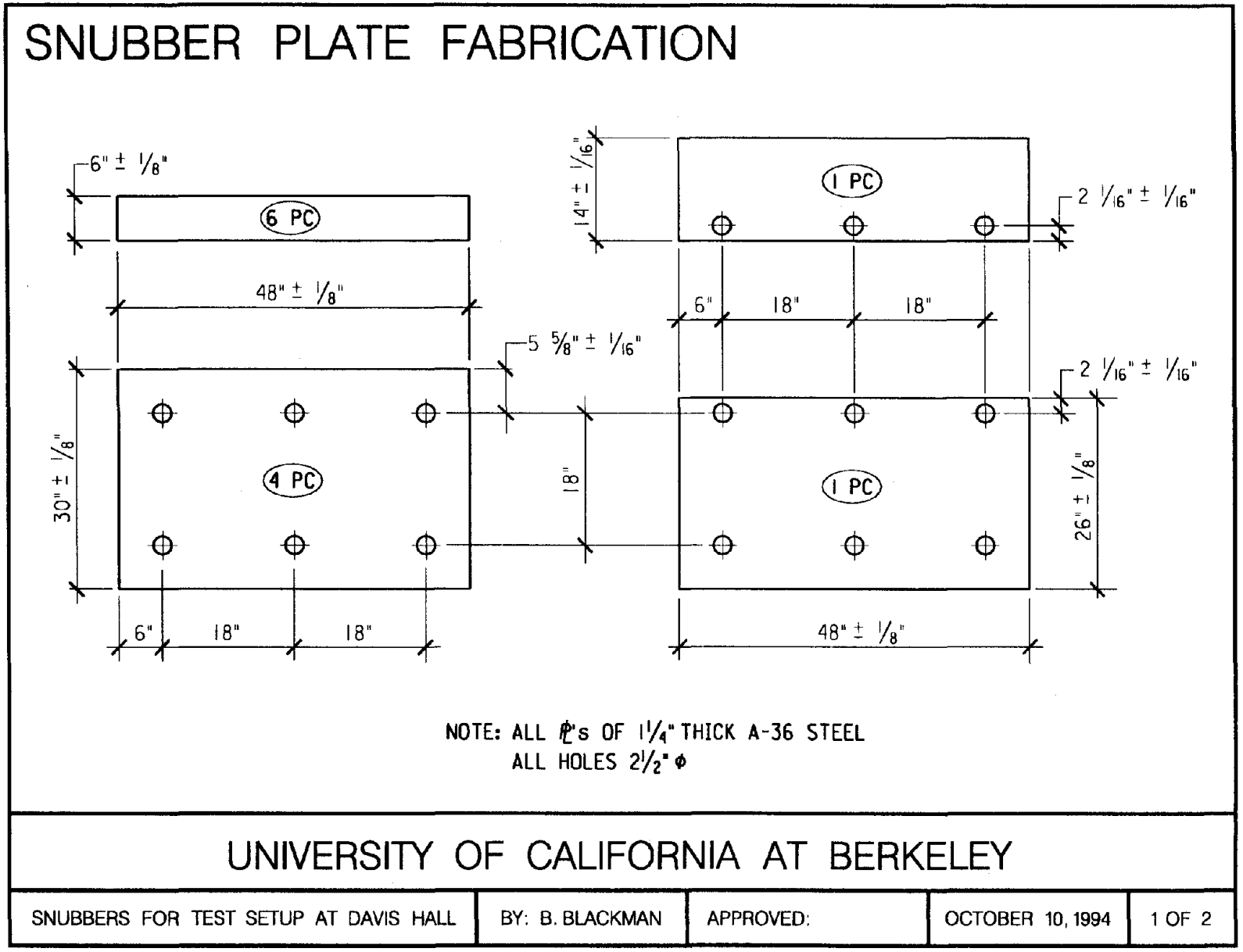

Figure A-1. Snubber Plate Fabrication

WASHER PLATE FABRICATION

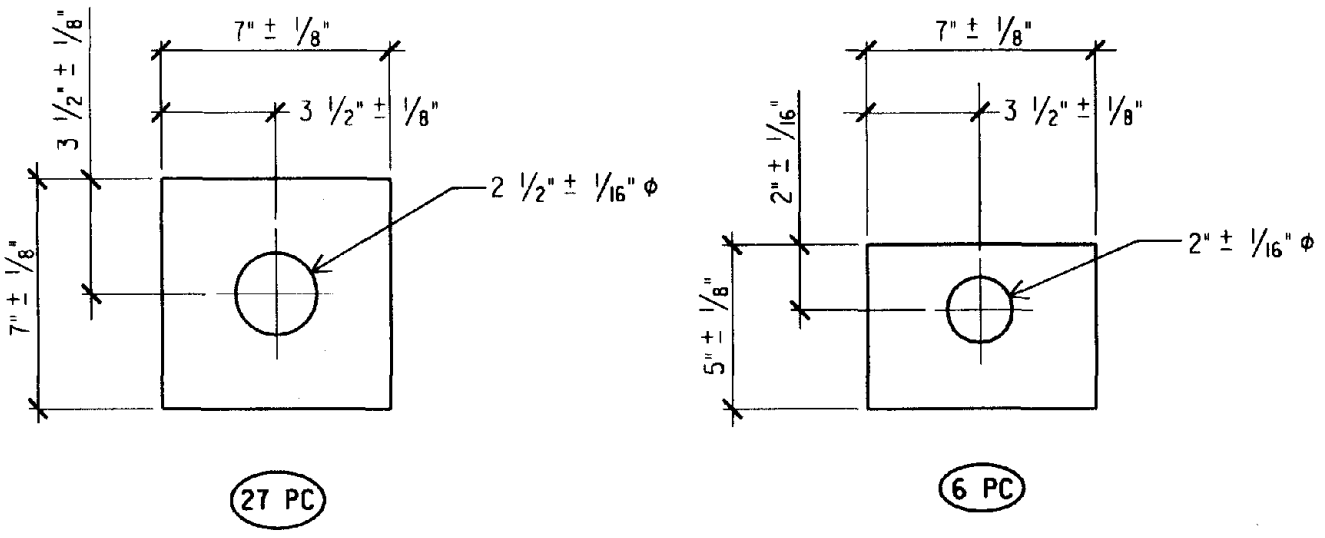

NOTE: ALL WASHER ℄'s 1¼" THICK A-36 STEEL

UNIVERSITY OF CALIFORNIA AT BERKELEY

SNUBBERS FOR TEST SETUP AT DAVIS HALL	BY: B. BLACKMAN	APPROVED:	OCTOBER 10, 1994	2 OF 2

Figure A-2. Washer Plate Fabrication

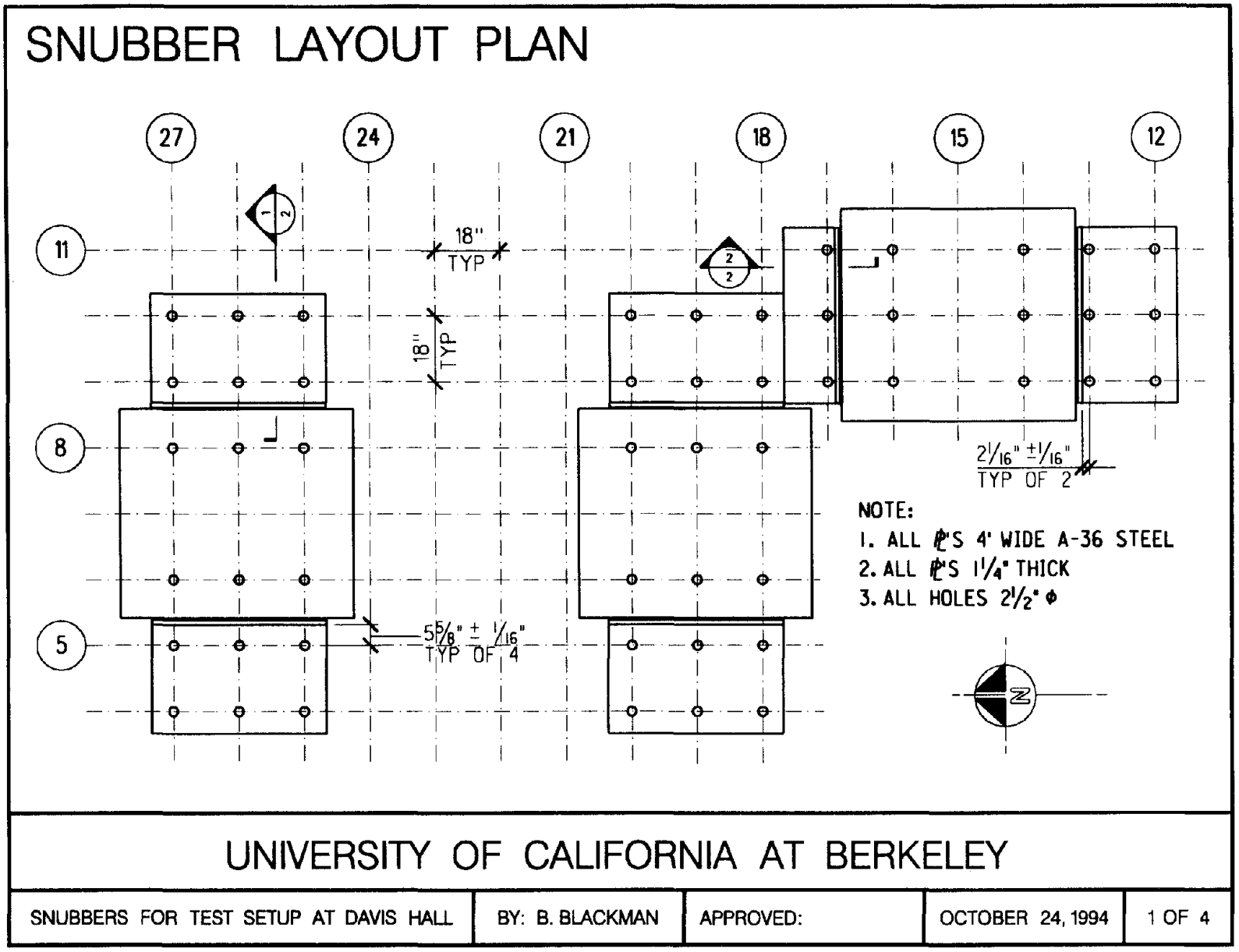

Figure A-3. Snubber Layout Plan

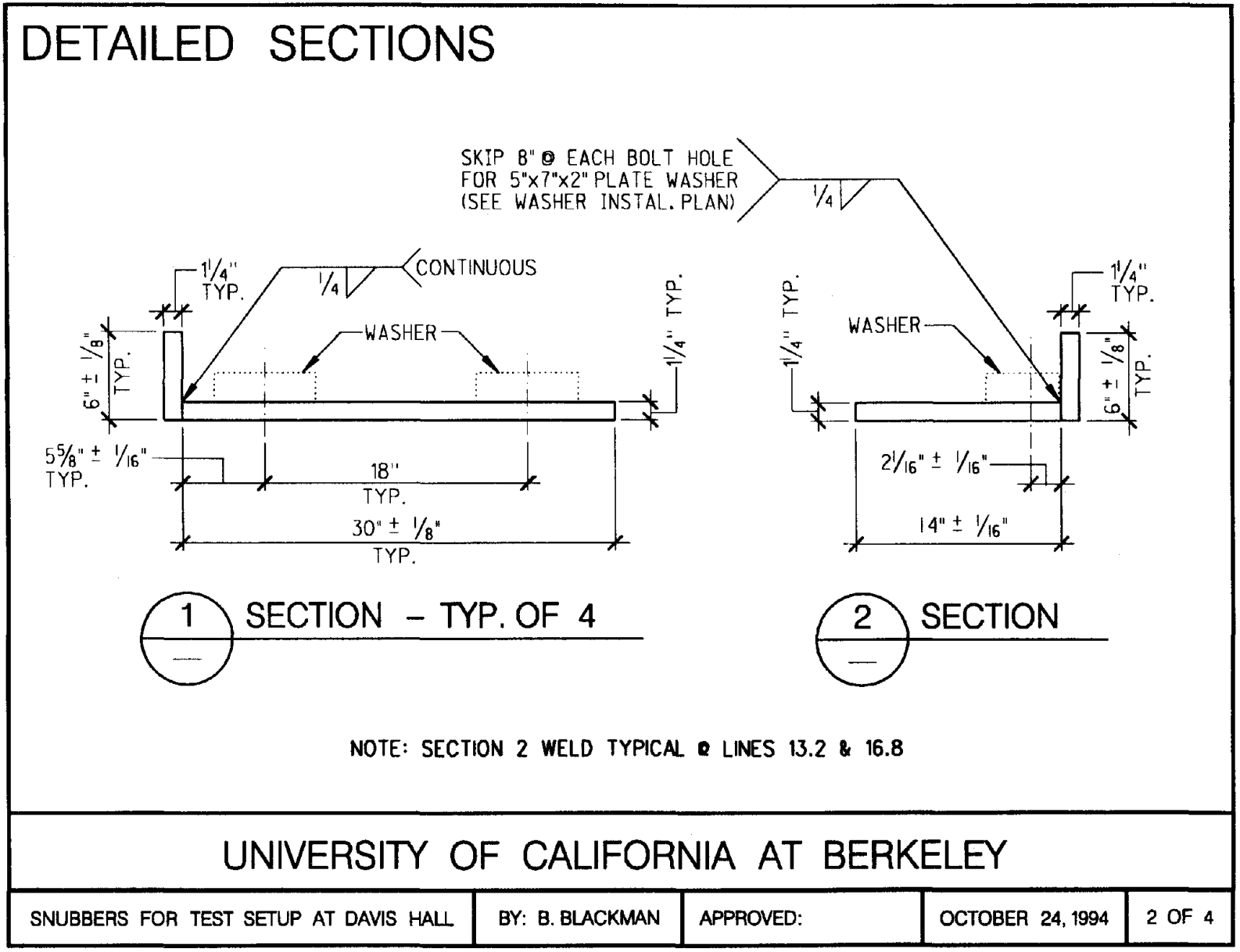

Figure A-4. Detailed Sections of Snubber Plates

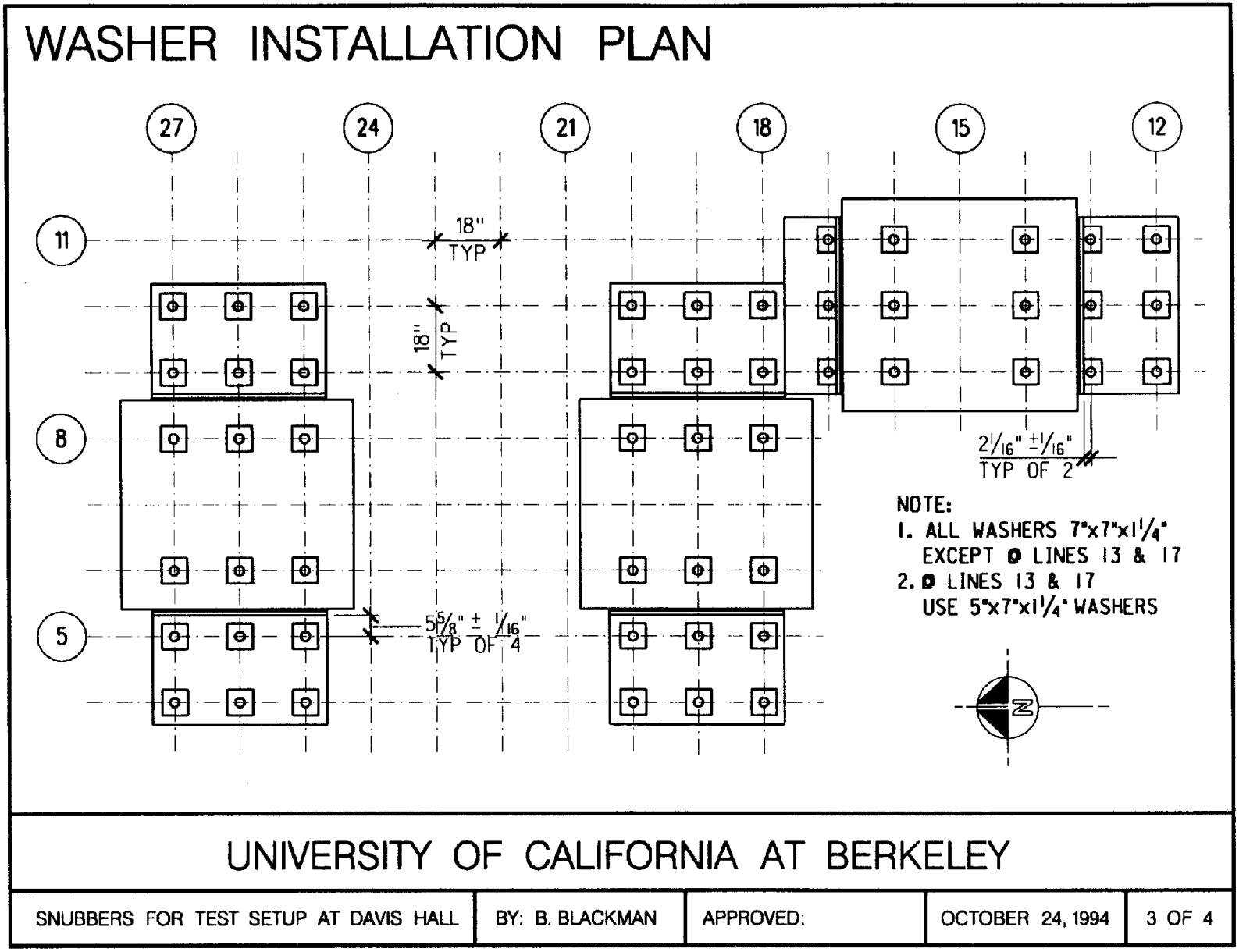

Figure A-5. Washer Installation Plan

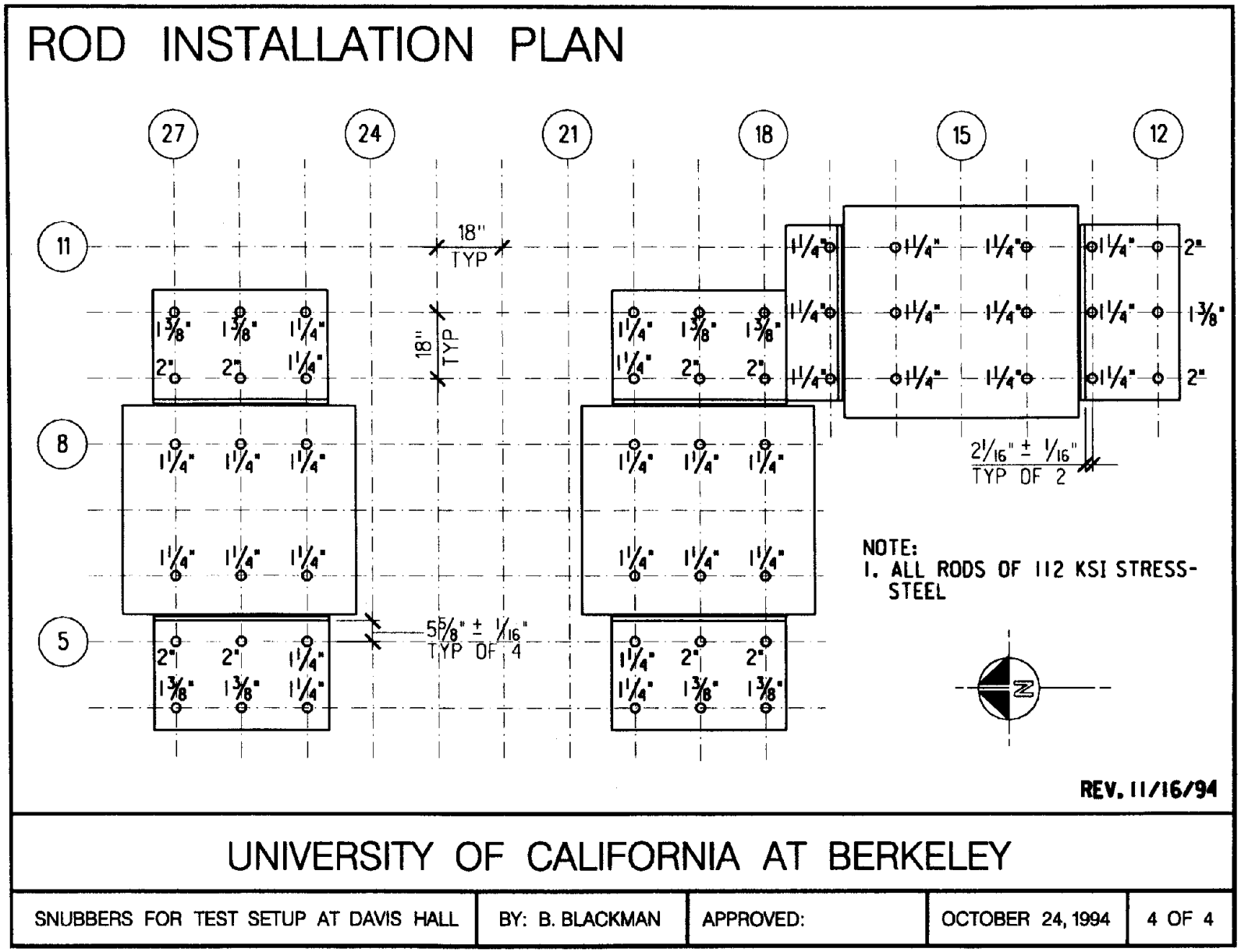

Figure A-6. Bolt Installation Plan

APPENDIX B. FAILURE OF NSF SPECIMEN #1

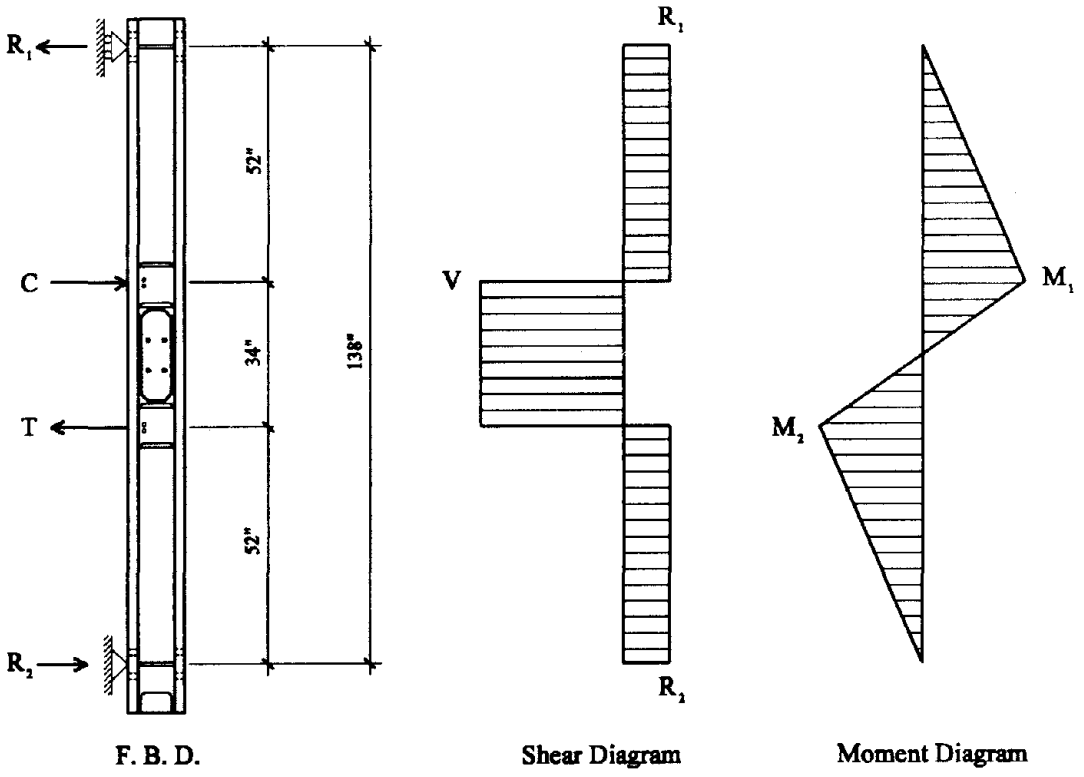

Figure B-1. Free-Body, Shear, and Moment Diagrams of NSF Specimen #1 Column at Failure

B.1 Calculate Moment in Column at Failure

force in actuator at failure = 236 kips

beam moment at column face = 236 (134.5) = 31,700 k-in

beam flange forces = T = C = 31,700 / 0.95 (35.85) = 931 kips

column reactions = R_1 = R_2 = 31,700 / 138.0 = 230 kips

column panel zone shear = V = 701 kips

column moments = M_1 = M_2 = 230 (52.0) = 12,000 k-in

B.2 Calculate Centroid and Moment of Inertia of Column at "Relief" Holes

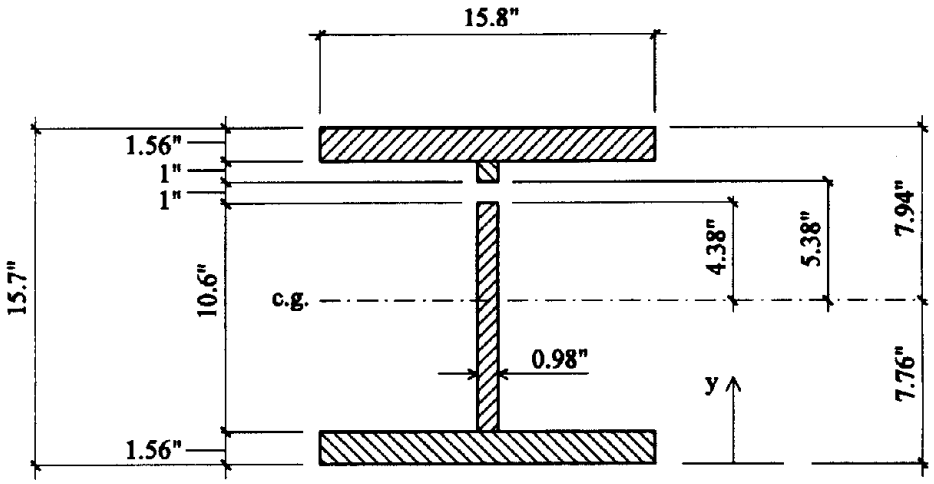

Note: parts numbered from top to bottom

part	area (in^2)	y_{cg} (in)	area y_{cg} (in^3)
1	24.7	14.9	368
2	0.98	13.7	13.4
3	10.4	6.86	71.3
4	24.7	0.78	19.3
sum	60.8	—	472

$c_{bottom} = 472 / 60.8 = 7.76$ in.

$c_{top} = 15.7 - 7.76 = 7.94$ in.

$I = I_1 + I_2 + I_3 + I_4$

where:

$I_1 = 15.8\,(1.56)^3 / 12 + 24.7\,(7.16)^2 = 1270\ in^4$

$I_2 = 0.98\,(1.0)^3 / 12 + 0.98\,(5.88)^2 = 34.0\ in^4$

$I_3 = 0.98\,(10.6)^3 / 12 + 10.4\,(0.92)^2 = 106\ in^4$

$I_4 = 15.8\,(1.56)^3 / 12 + 24.7\,(7.0)^2 = 1220\ in^4$

$I = 2630\ in^4$

B.3 Calculate Maximum Bending Stress at the Edge of "Relief" Hole Nearest the Extreme Fiber of the Column

$\sigma_b = M\,y / I = 12{,}000\,(5.38) / 2630 = 24.5$ ksi

Using a stress-concentration factor of 3.0*, the maximum tensile bending stress is:

$\sigma_{max} = 3.0\,(24.5) = 73.5$ ksi

73.5 ksi $>$ 73.0 ksi (tensile strength of column)

Therefore, fracture likely to occur.

*Note: This stress-concentration factor is that of a small circular hole in a flat bar under tension [Frocht, 1935].

Although this may be a conservative assumption for a bending member in the inelastic range, the factor was chosen to take into account additional stress concentration at the discontinuity existing between the web and flange of the column (fillet).

Maybe even more important, however, this is an area of high restraint, which prevents "necking down" of the material when stressed. For this reason, brittle fracture will occur prior to significant yielding. Moreover, suspect material in this region would compound the problem.

Table 1. Loading Sequence for Test Specimens

Load Step	Peak Displ.[1] (in)	Number of Cycles[1]	Displ. Rate (in/sec)	Data Points per Leg
1	0.1	2	0.05	5
2	0.25	3	0.10	5
3	0.5	3	0.10	8
4	0.75	3	0.10	10
5	1.0	3	0.10	10
6	2.0	3	0.10	12
7	3.0	3	0.10	12
8	4.0	2	0.10	16
9	5.0	2	0.20	20
10	6.0[2]	n (to failure)	0.20	24

[1]loading sequence follows the recommendations of the SAC Joint Venture memo titled "Test Protocol and Documentation Draft" (January 19, 1995)
[2]maximum stroke of actuator

Table 2. Mill Certificate Mechanical Properties for Beams and Columns

Specimen		Steel Producer	Member Size	ASTM Designation	F_y (ksi)	F_u (ksi)	Elong. (%)
PN1	Beam	ARBED[1]	W36x150	A-572 Gr 50[1]	62.6	74.7	22.5
	Column	Nucor-Yamato	W14x257	A-572 Gr 50	53.5	72.5	26.0
PN2	Beam	ARBED[1]	W36x150	A-572 Gr 50[1]	62.6	74.7	22.5
	Column	Nucor-Yamato	W14x257	A-572 Gr 50	53.5	72.5	26.0
PN3	Beam	Nucor-Yamato	W36x150	A-36	56.8	68.7	28.5
	Column	Nucor-Yamato	W14x257	A-572 Gr 50	53.5	72.5	26.0
NSF #1	Beam	British	W36x150	A-36	52.5	73.7	23.0
	Column	Nucor-Yamato	W14x211	A-572 Gr 50	54.0	73.0	27.0
NSF #6	Beam	N/A	W36x135	A-36	48.0	62.0	N/A
	Column	N/A	W14x233	A-572 Gr 50	52.0	78.0	N/A
	Tees	N/A	WT5x44	A-36	47.4	70.0	N/A
	Side Plates	N/A	1-1/4 in.	A-572 Gr 50	N/A	N/A	N/A

[1]all beam material requested was A-36, however, A-572 Grade 50 beams were received for Specimens PN1 and PN2

Table 3. Summary of Test Specimen Performance

Specimen	PN1	PN2	PN3	NSF #1	NSF #6
Δ_y (in)	0.99	0.95	1.02	1.06	0.98
Δ_u (in)	2.64	1.72	2.85	3.08	5.00
μ[1]	2.67	1.83	2.79	2.91	5.10
P_y (kip)	136	136	138	139	180
P_u[2] (kip)	225	172	163	236	150
P_{max}[3] (kip)	227	193	199	236	257
M_y[4] (kip-in)	18,300	18,300	17,800	18,700	24,200
M_u[4] (kip-in)	30,300	23,200	21,900	31,800	20,200
M_{max}[4] (kip-in)	30,600	25,900	26,700	31,800	34,600
k[5] (kip/in)	138	143	136	131	184
post-yield cycles	4 - 1/4	1 - 1/4	4 - 1/4	7 - 1/4	9 - 1/2
$\theta_{p,max}$[6] (%)	0.94	0.35	1.12	0.95	3.11[8,9]
$energy_d$[7] (kip-in)	1770	510	2530	3490	12,000[9]

[1]ductility factor = Δ_u / Δ_y
[2]strength of joint corresponding to ultimate ductility factor
[3]maximum strength of joint
[4]moment at column face = P x 134.5 inches
[5]elastic stiffness of joint
[6]maximum plastic rotation (prior to failure)
[7]energy dissipated (prior to failure)
[8]based on length of beam from actuator to column face (L = 134.5);
for length from actuator to end of reinforced beam section (L = 107), $\theta_{p,max}$ = 3.91 %
[9]prior to the "divot" failure, $\theta_{p,max}$ = 2.12 % and $energy_d$ = 9810 kip-in

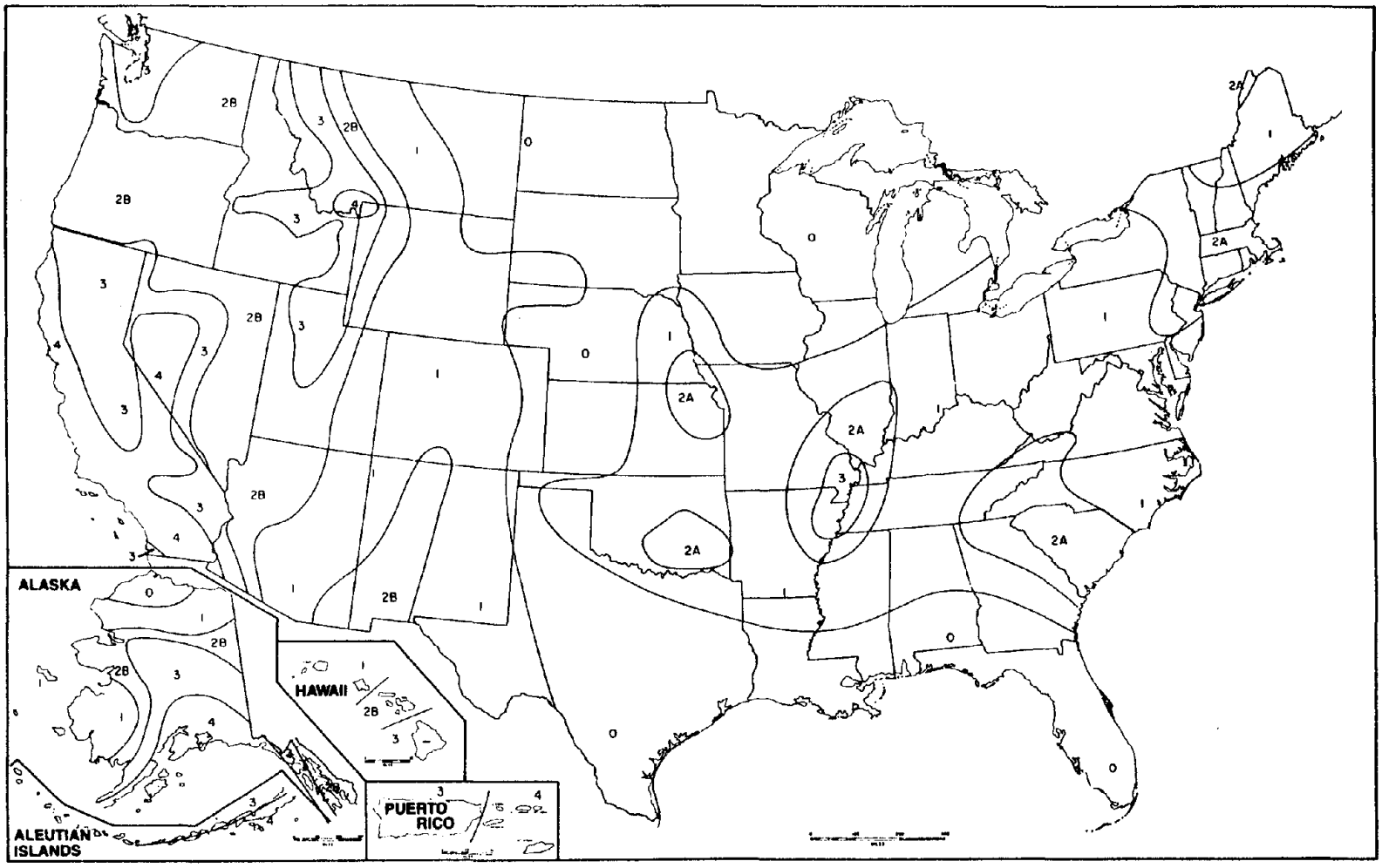

Figure 1-1. Seismic Zone Map of the United States.

(Source: International Conference of Building Officials, *Uniform Building Code*, Whittier, CA, 1994)

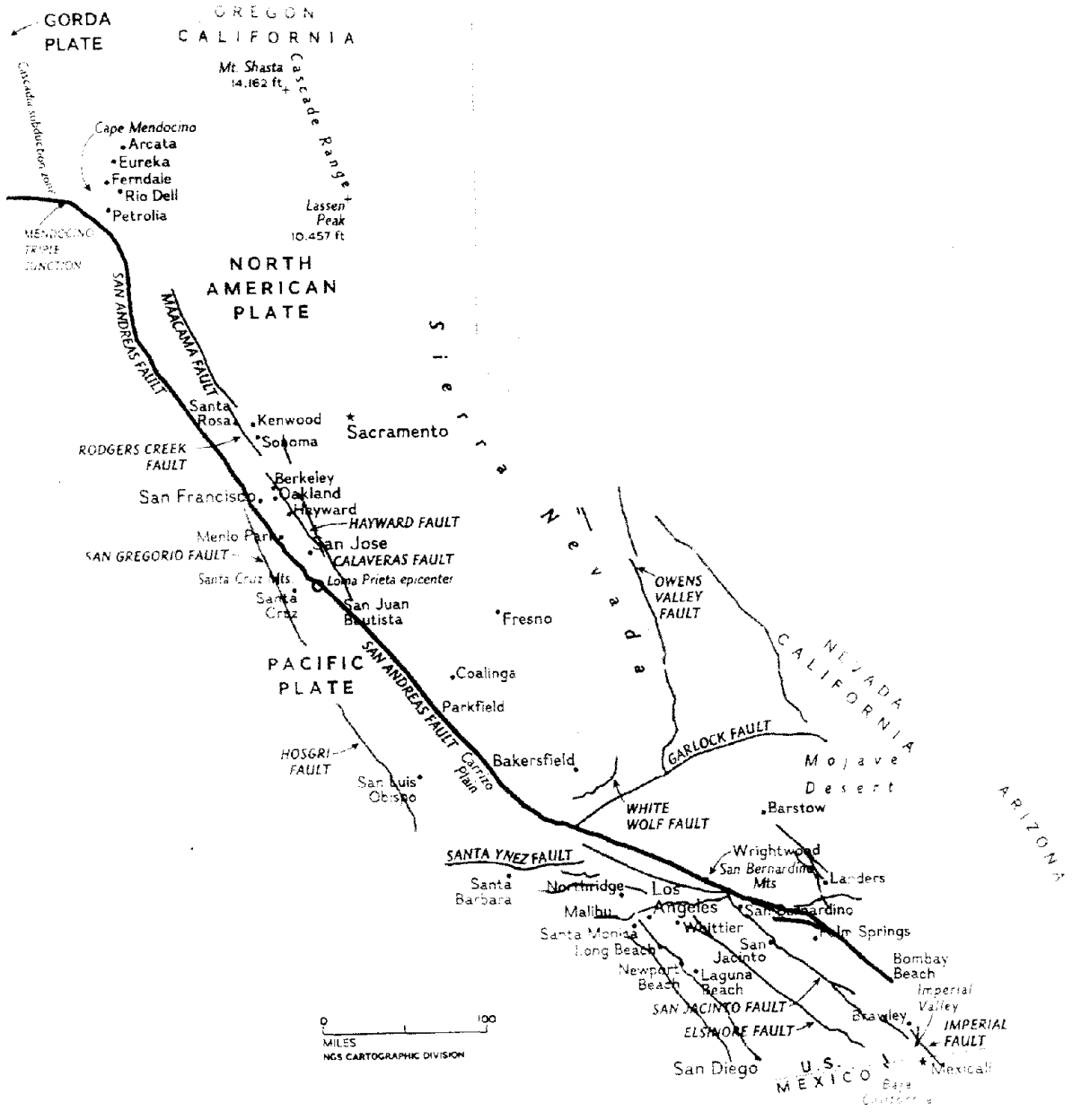

Figure 1-2. Major Faults Identified in California.

(Source: Rick Gore, "Living with California's Faults," *National Geographic*, April, 1995)

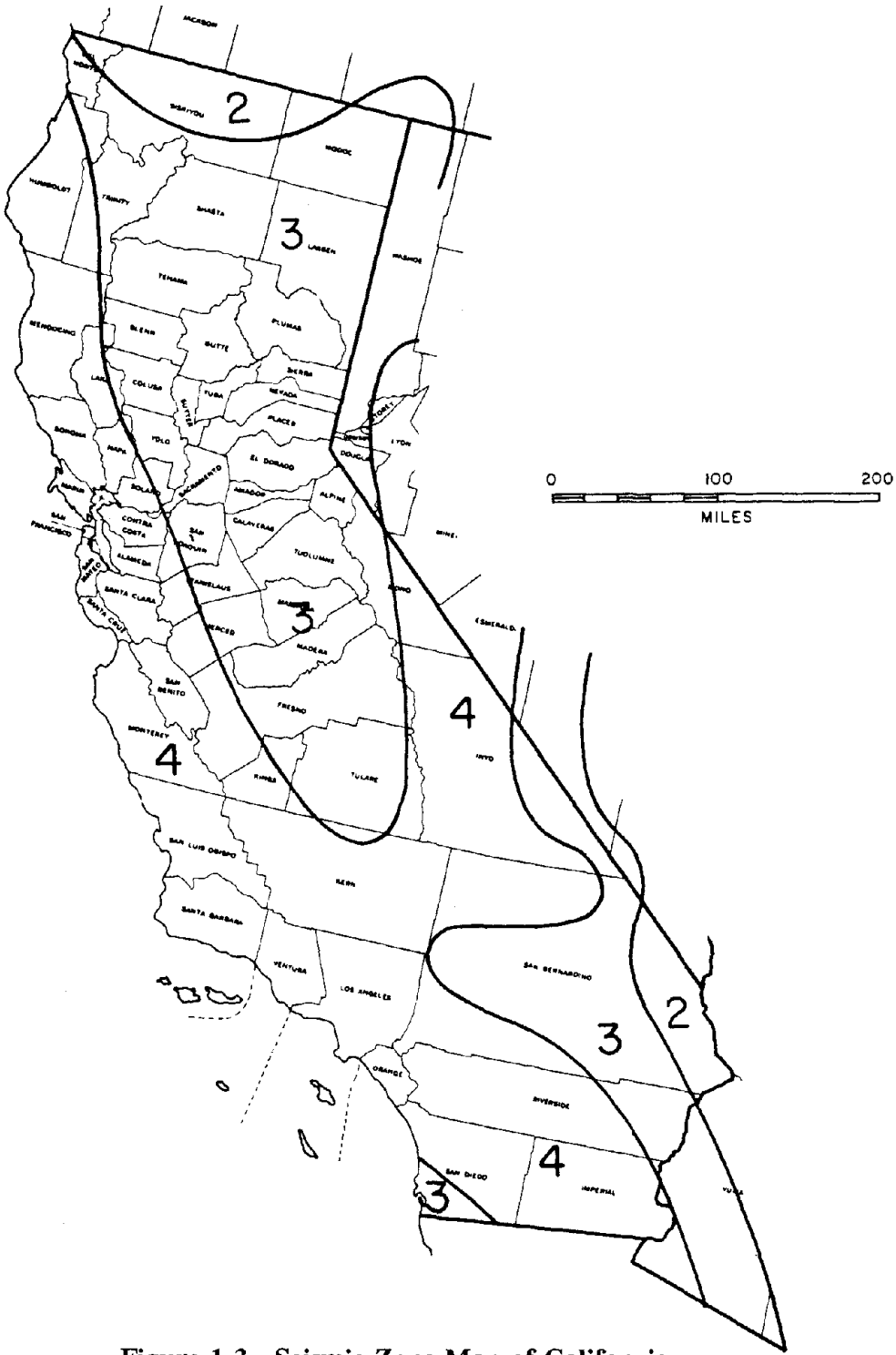

Figure 1-3. Seismic Zone Map of California.

(Source: SEAOC, *Recommended Lateral Force Requirements and Commentary*, Seismology Committee, San Francisco, 1990)

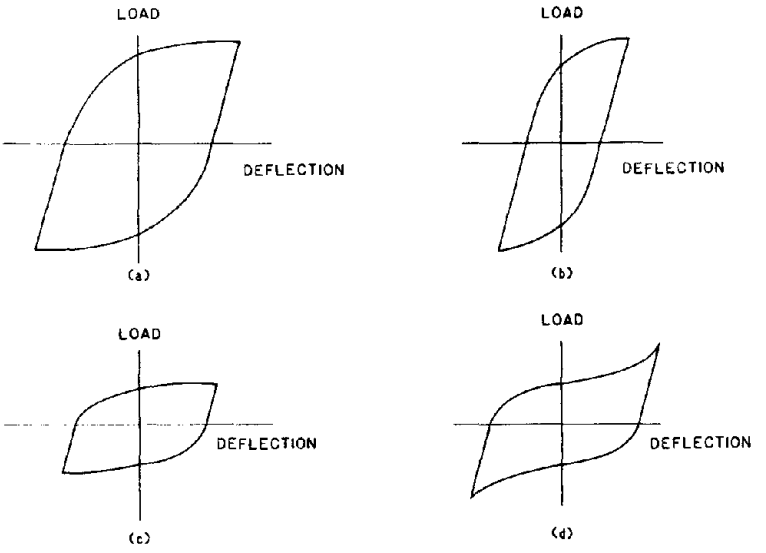

Figure 1-4. Hysteresis Loops of Seismic Moment Connections.

(Source: W. F. Chen and E. M. Lui, "Beam to Column Moment-Resisting Connections," *Steel Framed Structures, Stability and Strength*, edited by R. Narayanan, Essex, 1985)

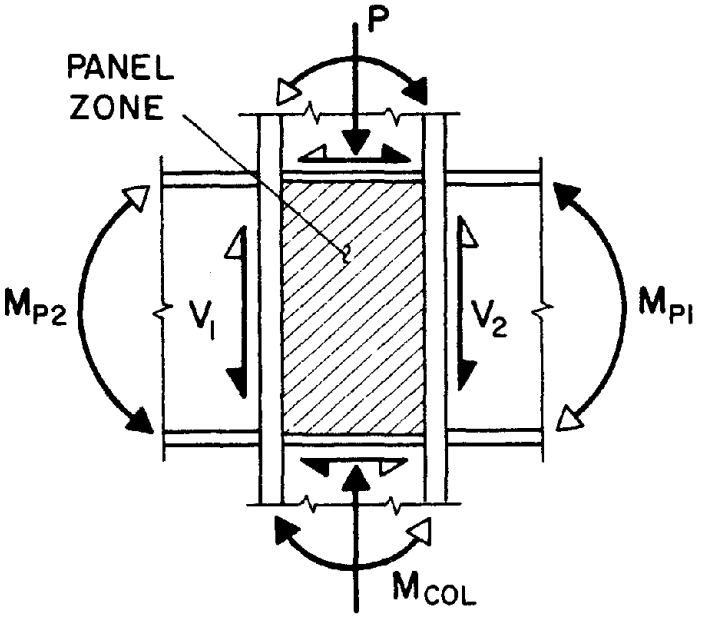

Figure 1-5. Free Body Diagram of a Moment-Resisting Connection.

(Source: Egor P. Popov, "Seismic Moment Connections for Moment-Resisting Steel Frames," *Report No. UCB/EERC-83/02*, Earthquake Engineering Research Center, University of California, Berkeley, 1983)

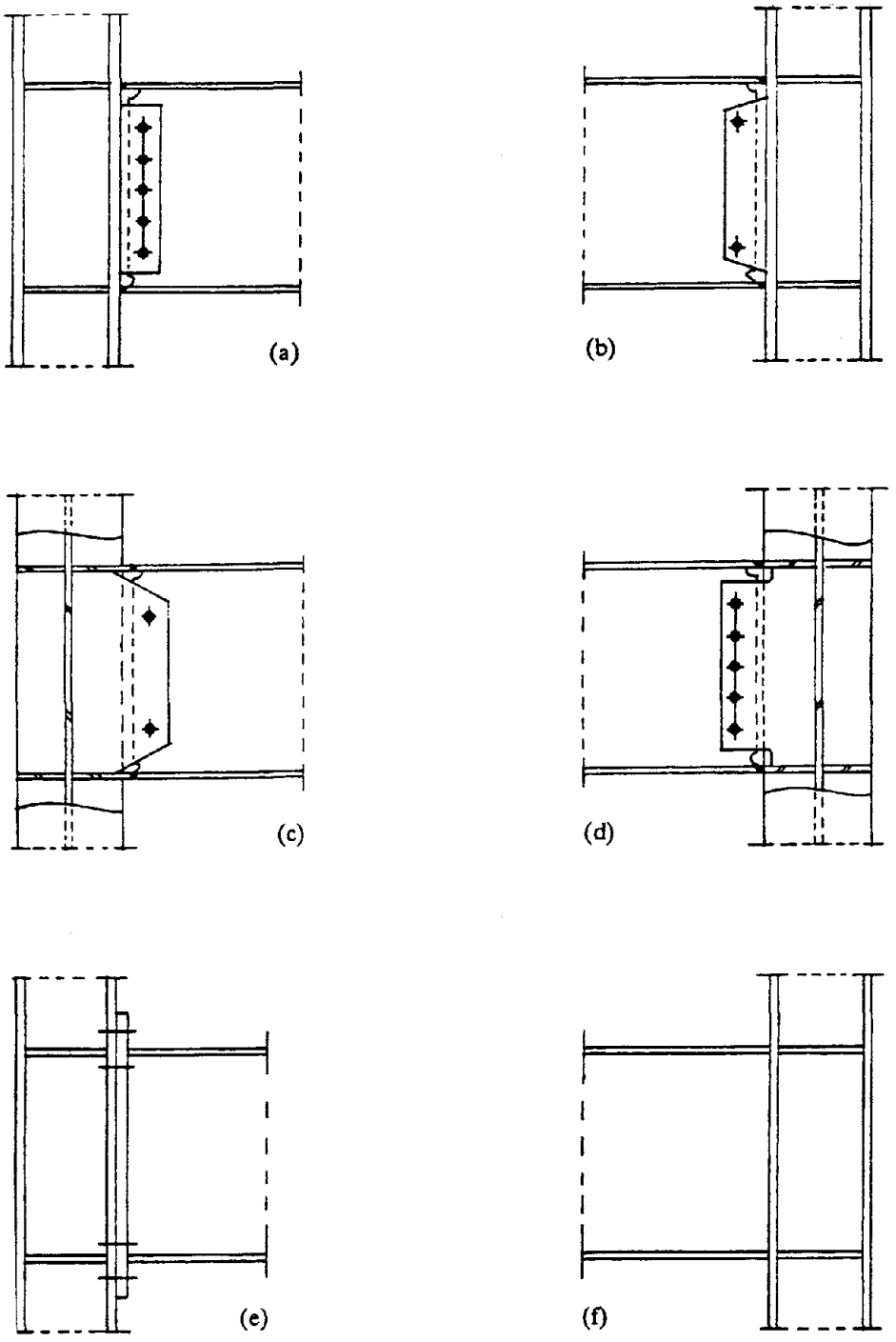

Figure 1-6. Typical Beam-to-Column Moment-Resisting Connections.

(Source: K. C. Tsai, "Steel Beam-Column Joints in Seismic Moment Resisting Frames," Dissertation, University of California, Berkeley, 1988)

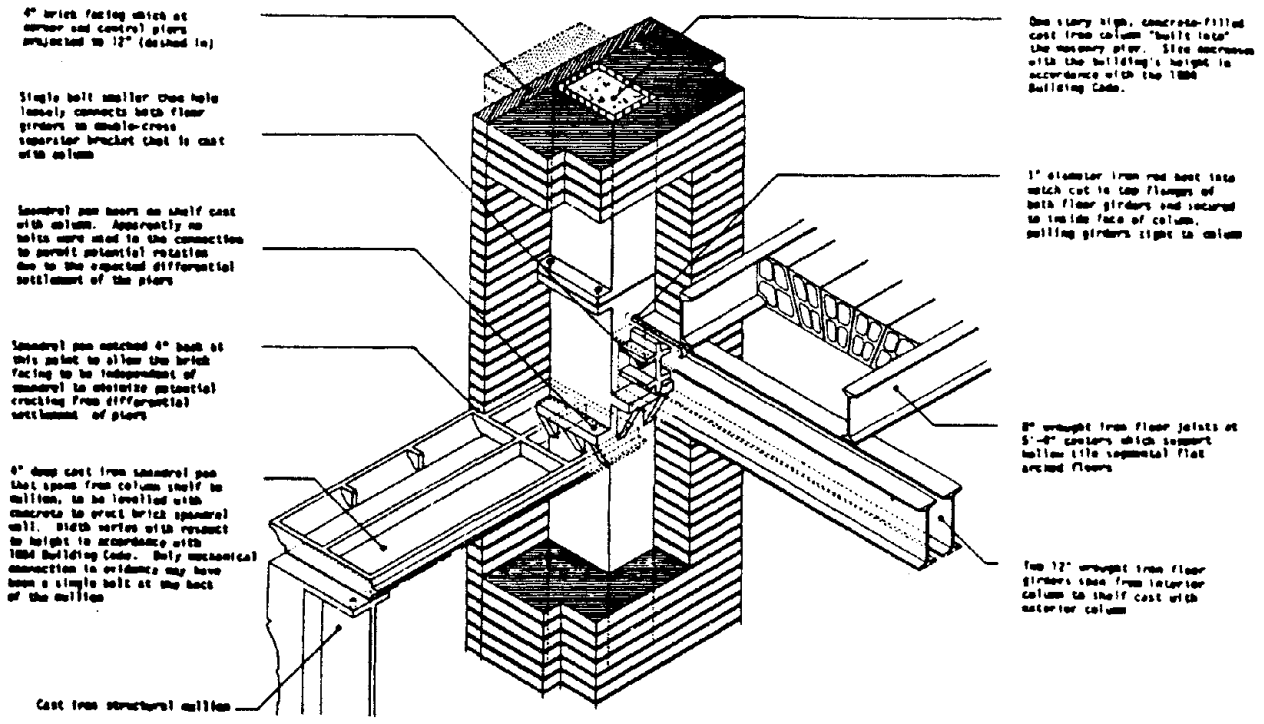

Figure 2-1. Beam-to-Column Connection of the Home Insurance Building (1885).

(Source: Stephen Tobriner, first draft of: *Fate of the Phoenix, A History of Safety and Reconstruction after Earthquakes and Fires in San Francisco 1849-1915*, University of California, Berkeley, 1995)

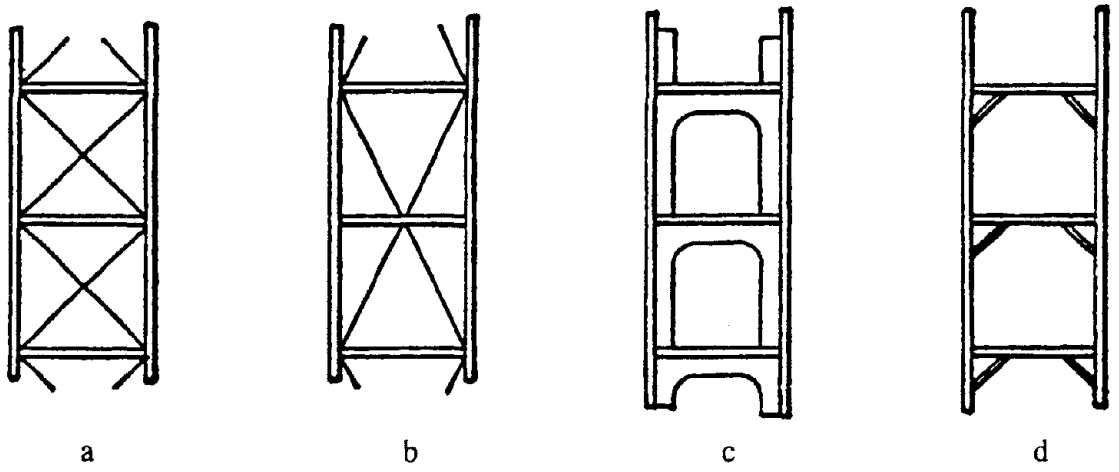

Figure 2-2. Freitag's Methods of Proper Bracing in Tall Buildings.

(Source: Joseph Kendall Freitag *Architectural Engineering with Special Reference to High Building Construction*, John Wile and Sons, New York, 1895)

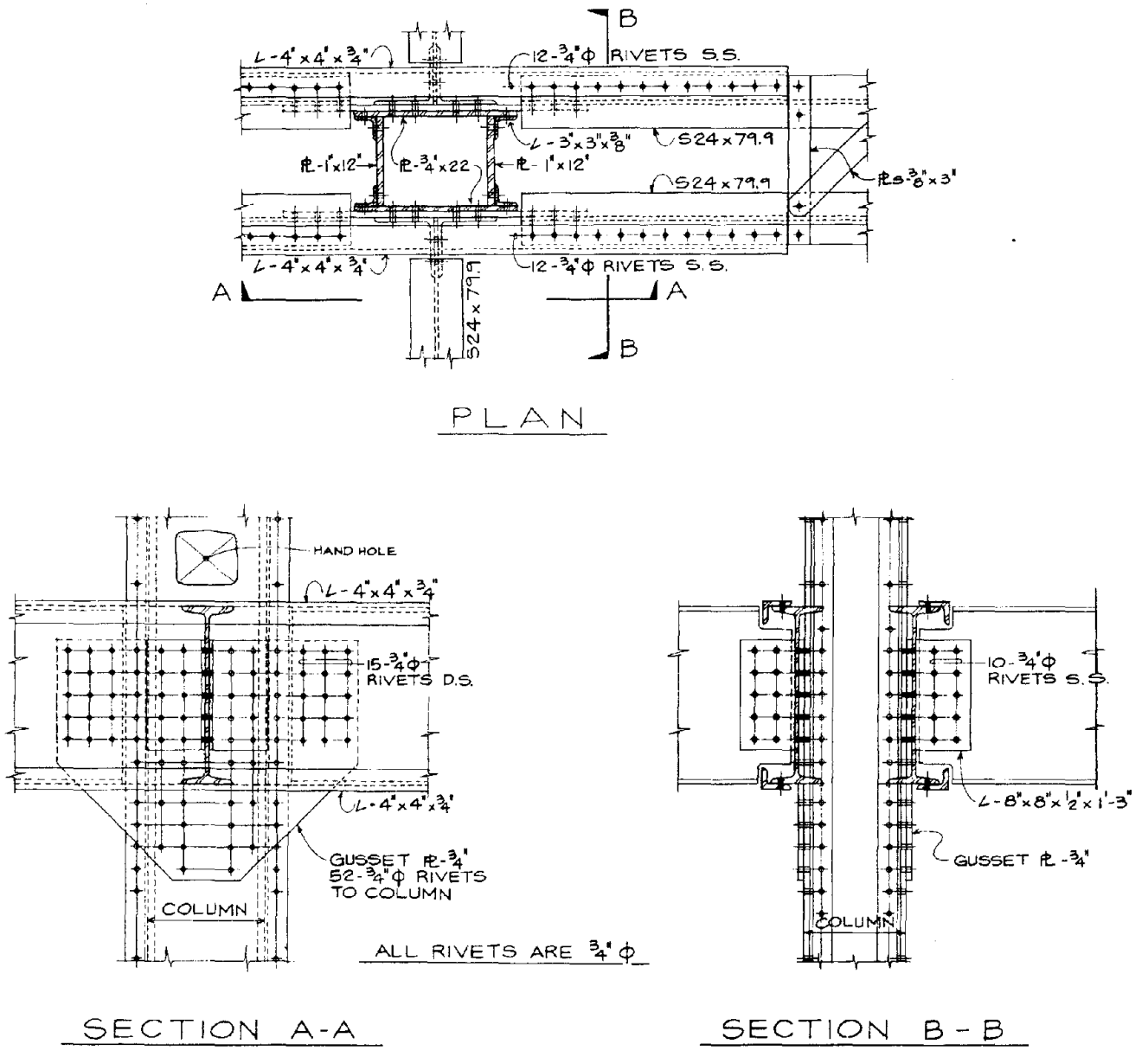

ESTIMATE OF WEIGHTS - LBS.		%
COLUMN SHAFT	2670	28
GIRDER	4000	41
BEAM	1600	16
DETAIL	1490	15
TOTAL	9760	100

EST. COST FACTOR = 2.00

Figure 2-3. A Typical Moment-Resisting Connection Prior to the 1920s.

(Source: F. Robert Preece and Alvaro L. Collin, "Structural Steel in the '90s," *Steel Tips*, Structural Steel Education Council, 1993)

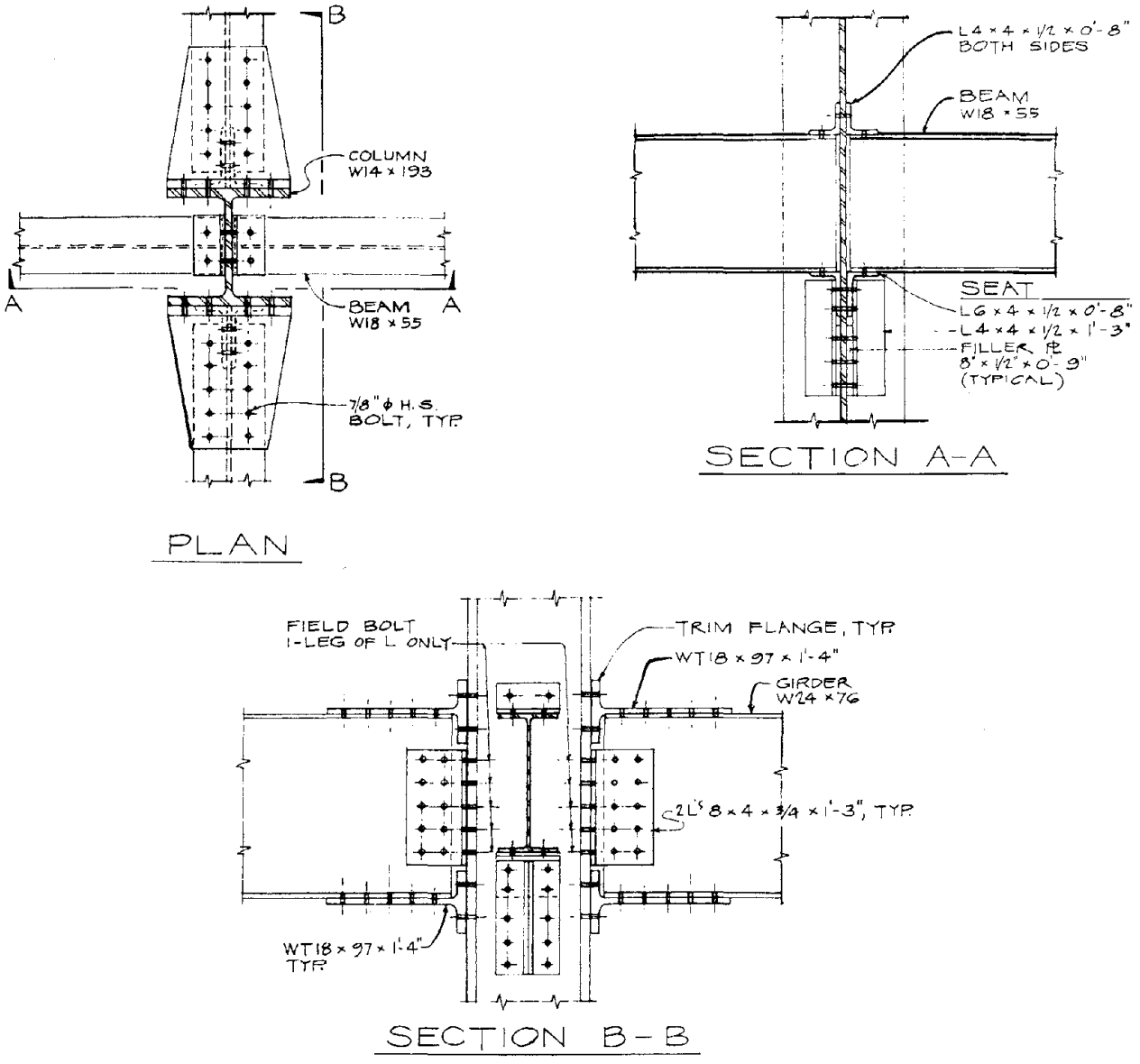

ESTIMATE OF WEIGHTS	LBS.	%
COLUMN SHAFT	2316	37
GIRDER	1900	30
BEAM	1100	18
DETAIL	914	15
TOTAL	6230	100

EST. COST FACTOR = 1.50

Figure 2-4. A Typical Riveted and Bolted Connection of Rolled Sections in the 1930s.

(Source: F. Robert Preece and Alvaro L. Collin, "Structural Steel in the '90s," *Steel Tips*, Structural Steel Education Council, 1993)

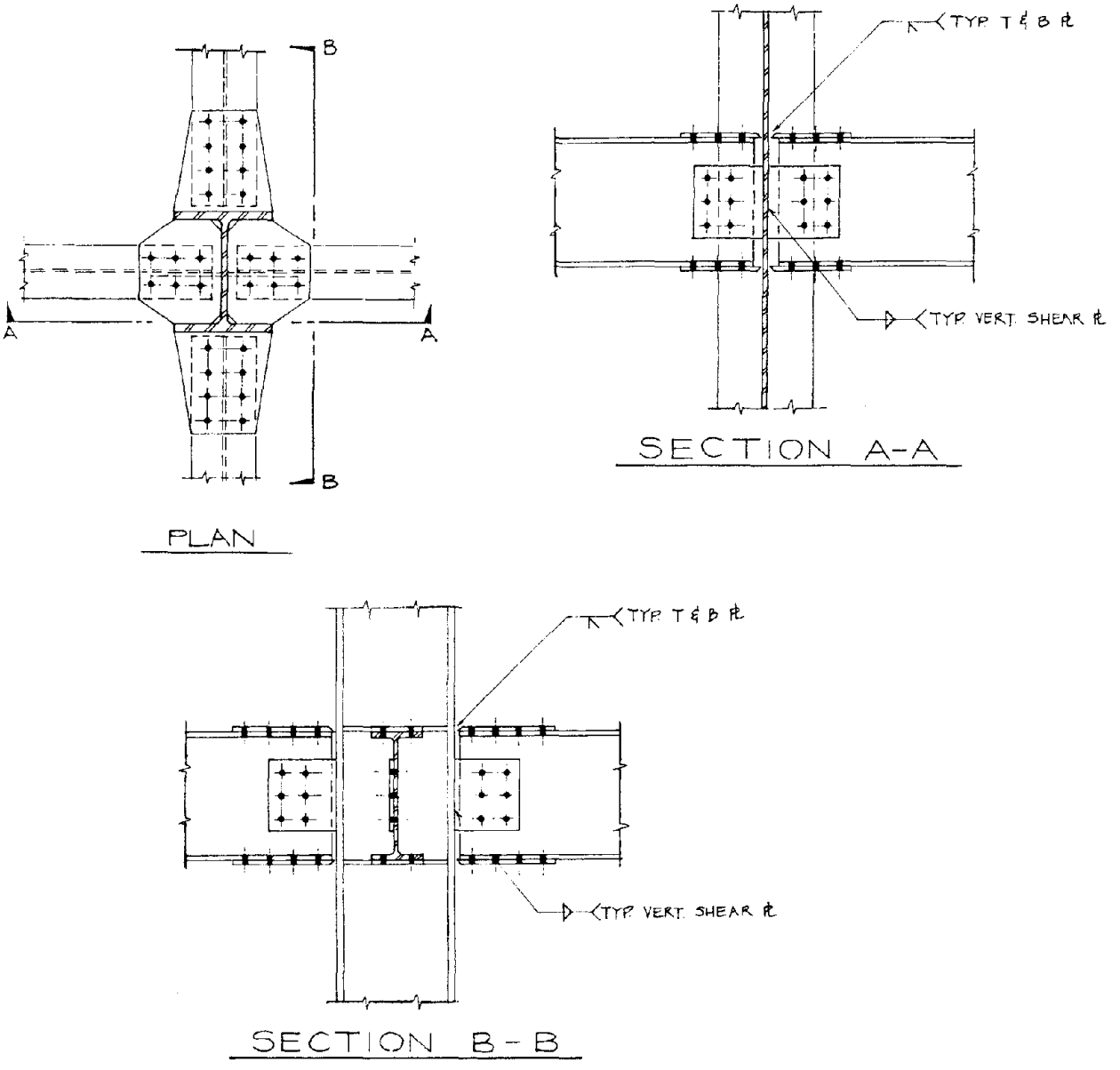

ESTIMATE OF WEIGHTS – LBS.		%
COLUMN SHAFT	2200	39
GIRDER	1700	30
BEAM	1000	18
DETAIL	750	13
TOTAL	5650	100

EST. COST FACTOR = 1.25

Figure 2-5. A Typical Shop Welded - Field Bolted Connection of the 1950s and 1960s.

(Source: F. Robert Preece and Alvaro L. Collin, "Structural Steel in the '90s," *Steel Tips*, Structural Steel Education Council, 1993)

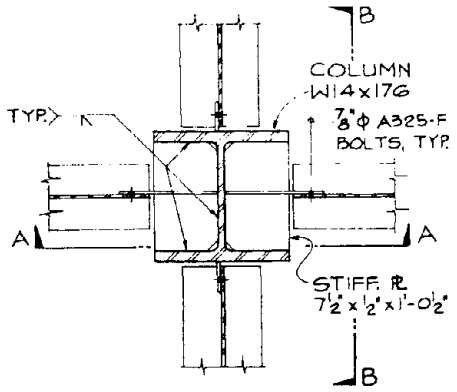

PLAN

ESTIMATE OF WEIGHTS - LBS.		%
COLUMN SHAFT	2112	42
GIRDER	1700	34
BEAM	1000	20
DETAIL	188	4
TOTAL	5000	100

EST. COST FACTOR = 1.00

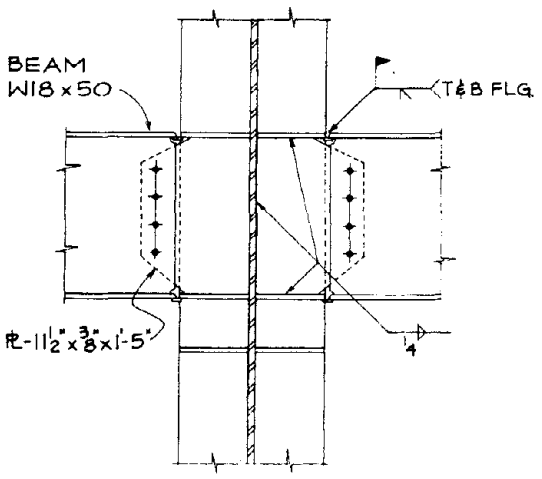

SECTION A-A

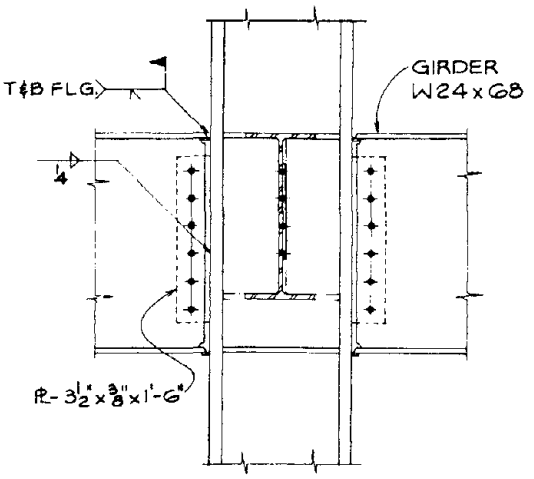

SECTION B-B

Figure 2-6. A Typical Welded Flange - Bolted Web Connection of the 1980s.

(Source: F. Robert Preece and Alvaro L. Collin, "Structural Steel in the '90s," *Steel Tips*, Structural Steel Education Council, 1993)

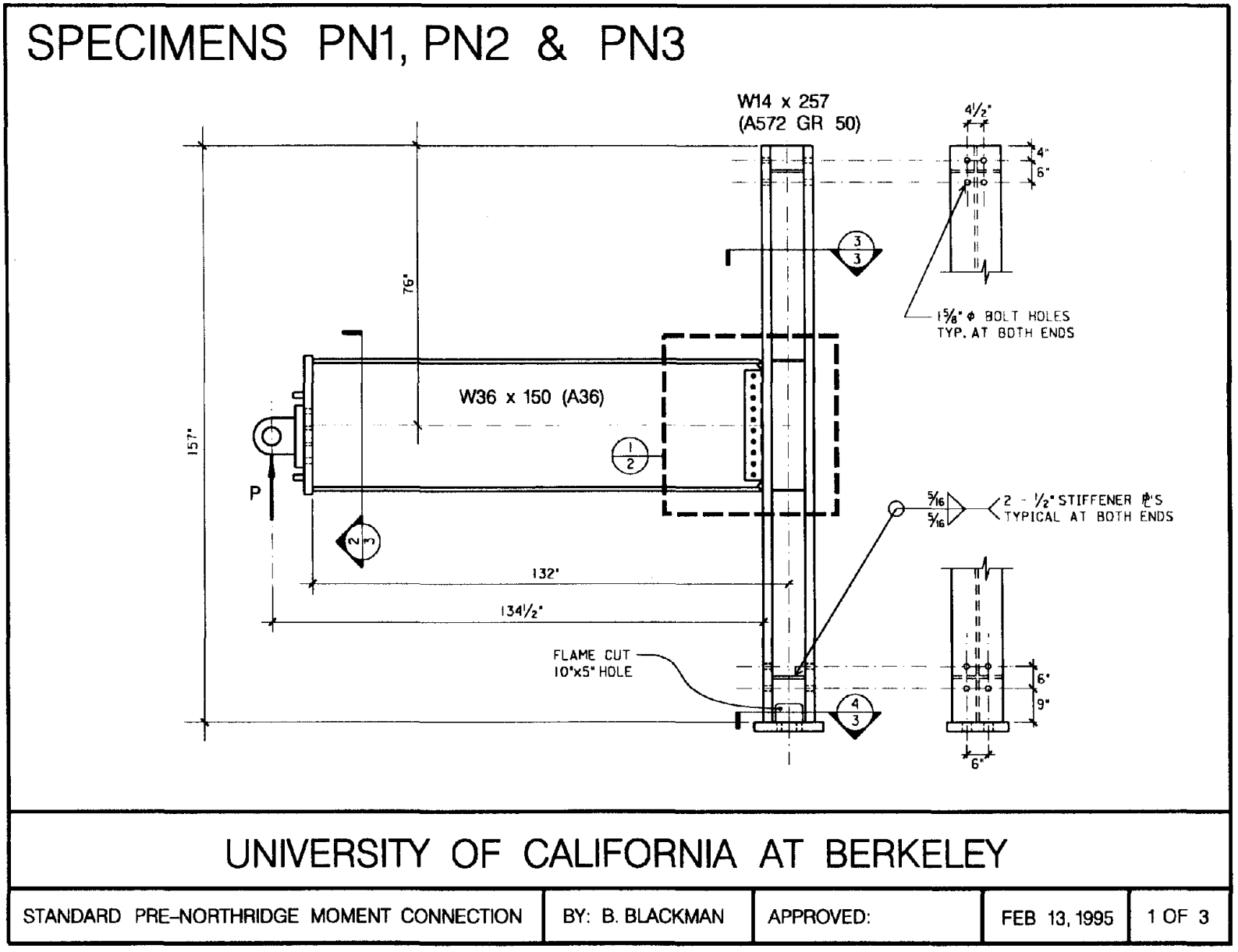

Figure 3-1. Standard Pre-Northridge Connection

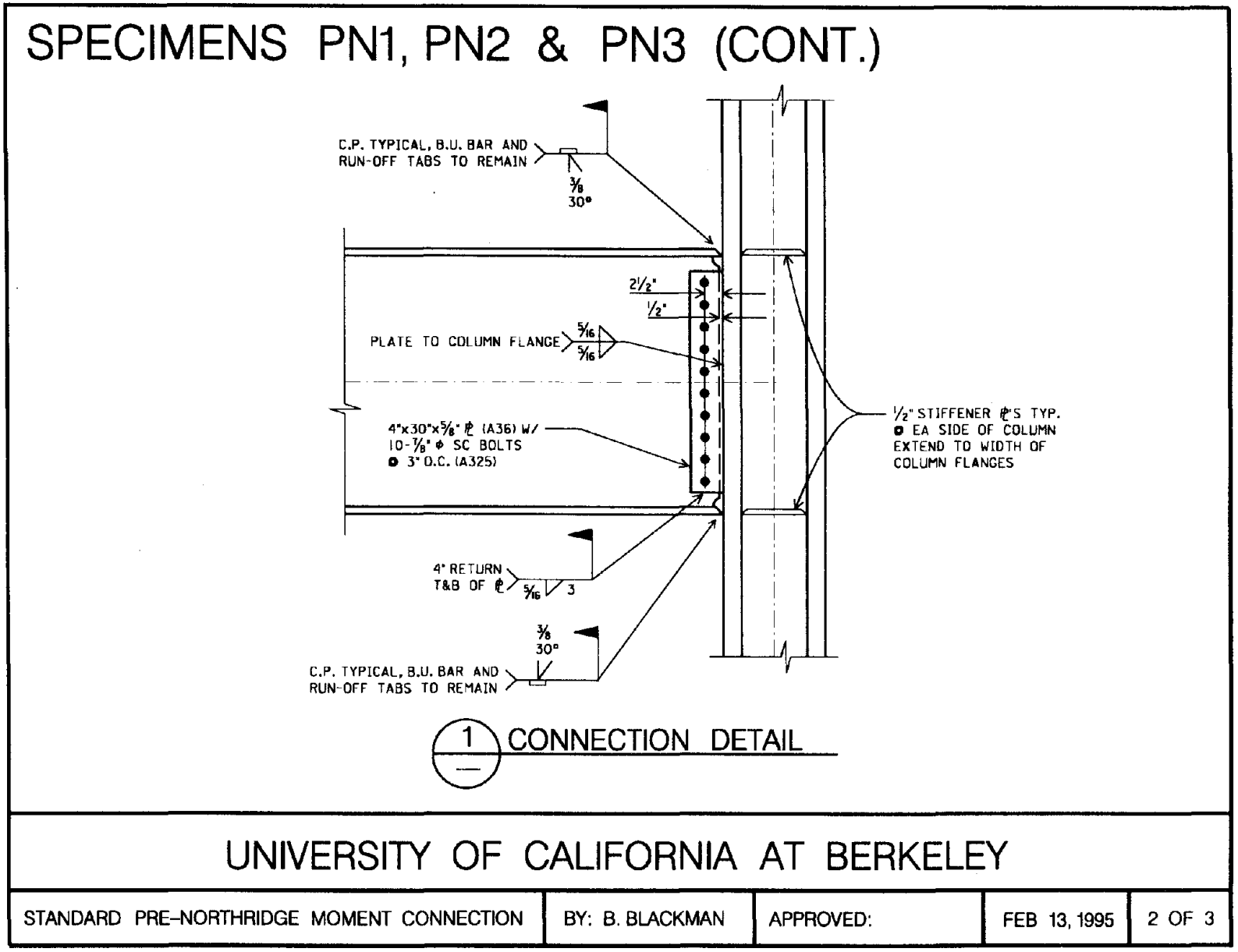

Figure 3-2. Standard Pre-Northridge Connection Detail

SPECIMENS PN1, PN2 & PN3 (CONT.)

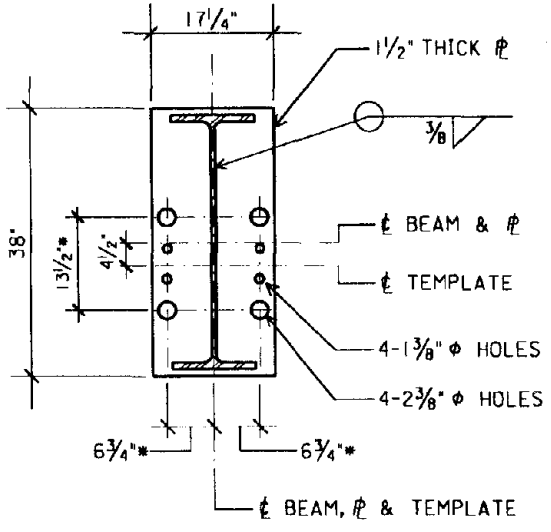

*NOTE: NOMINAL DIMENSIONS; USE TEMPLATE

2 DETAILED SECTION

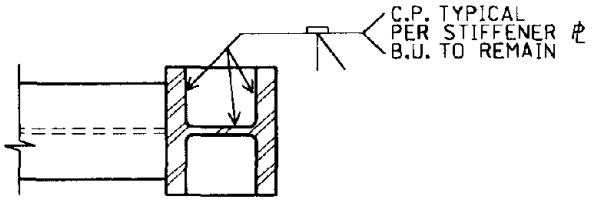

3 DETAILED SECTION

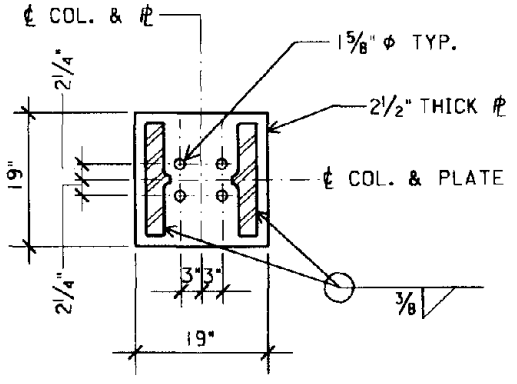

4 DETAILED SECTION

UNIVERSITY OF CALIFORNIA AT BERKELEY

STANDARD PRE-NORTHRIDGE MOMENT CONNECTION	BY: B. BLACKMAN	APPROVED:	FEB 13, 1995	3 OF 3

Figure 3-3. Detailed Sections for Standard Pre-Northridge Connection

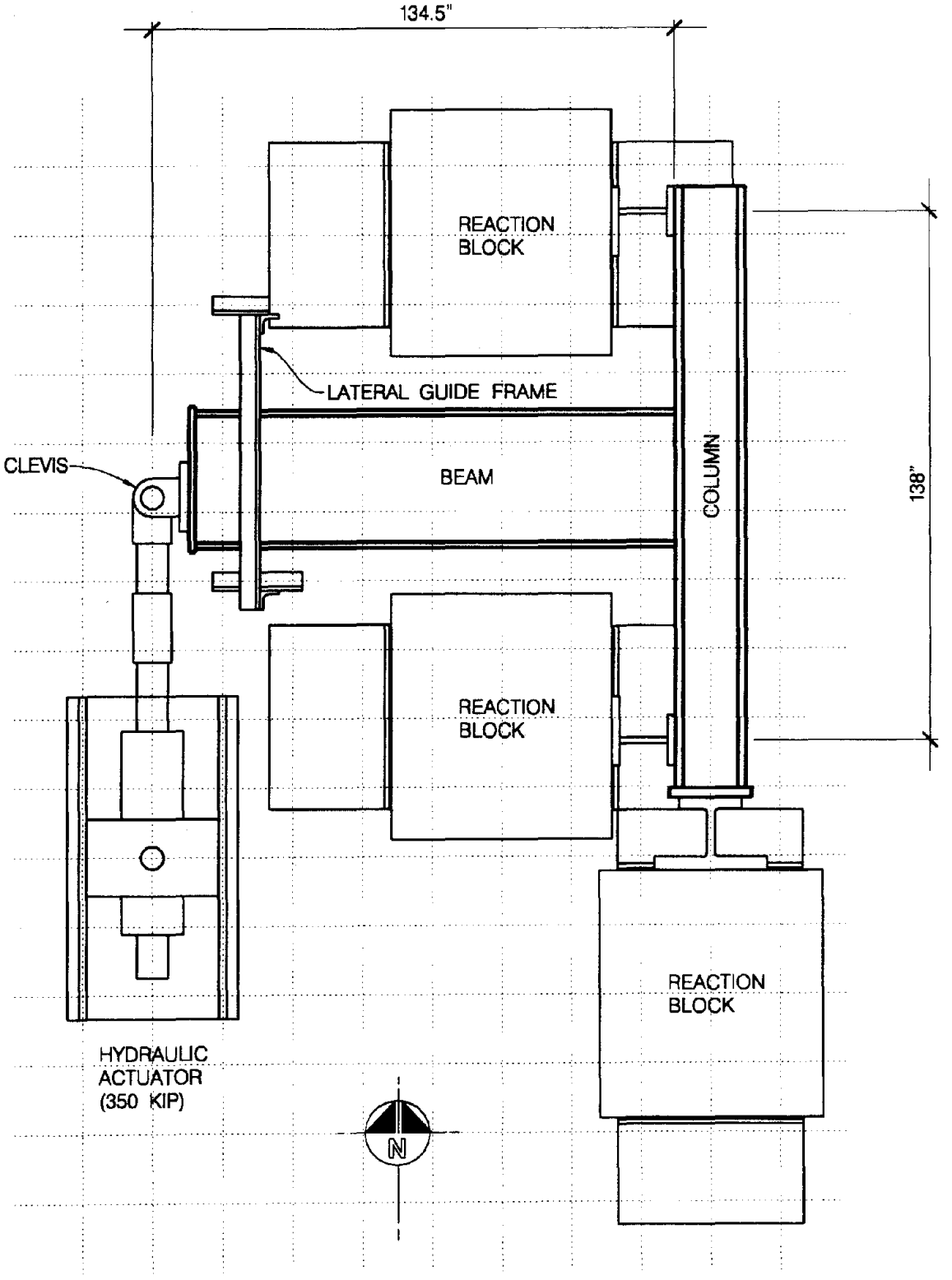

Figure 3-4. Plan of Test Setup

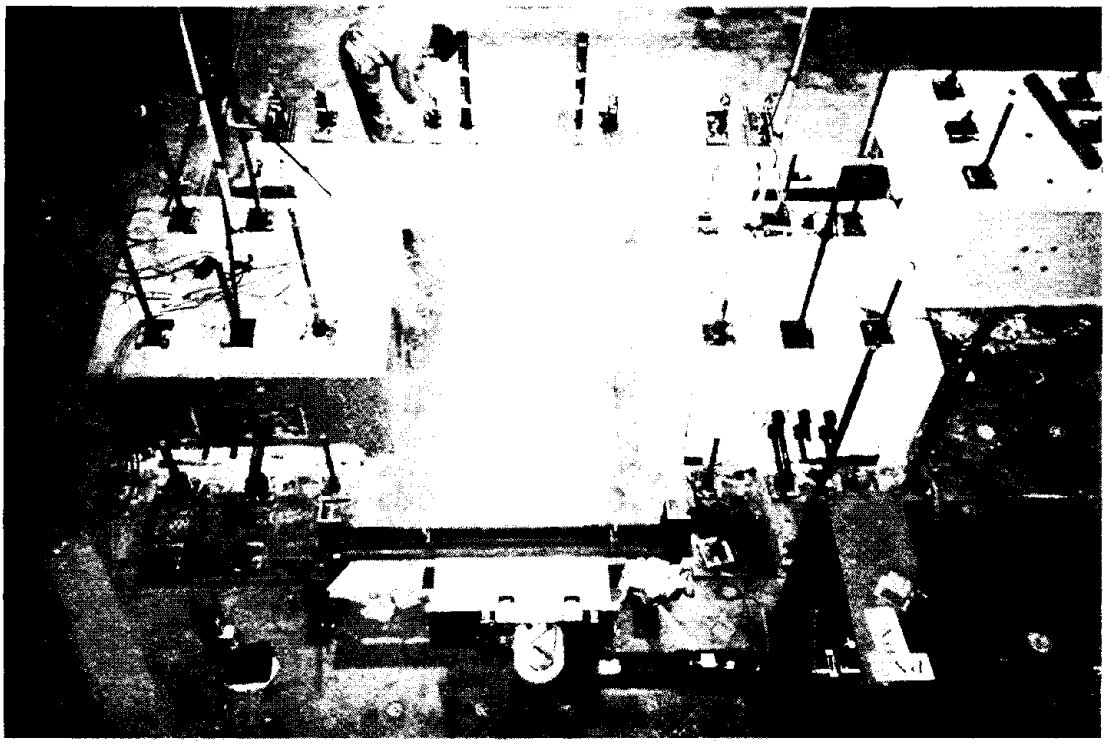

Figure 3-5. Test Setup at Davis Hall

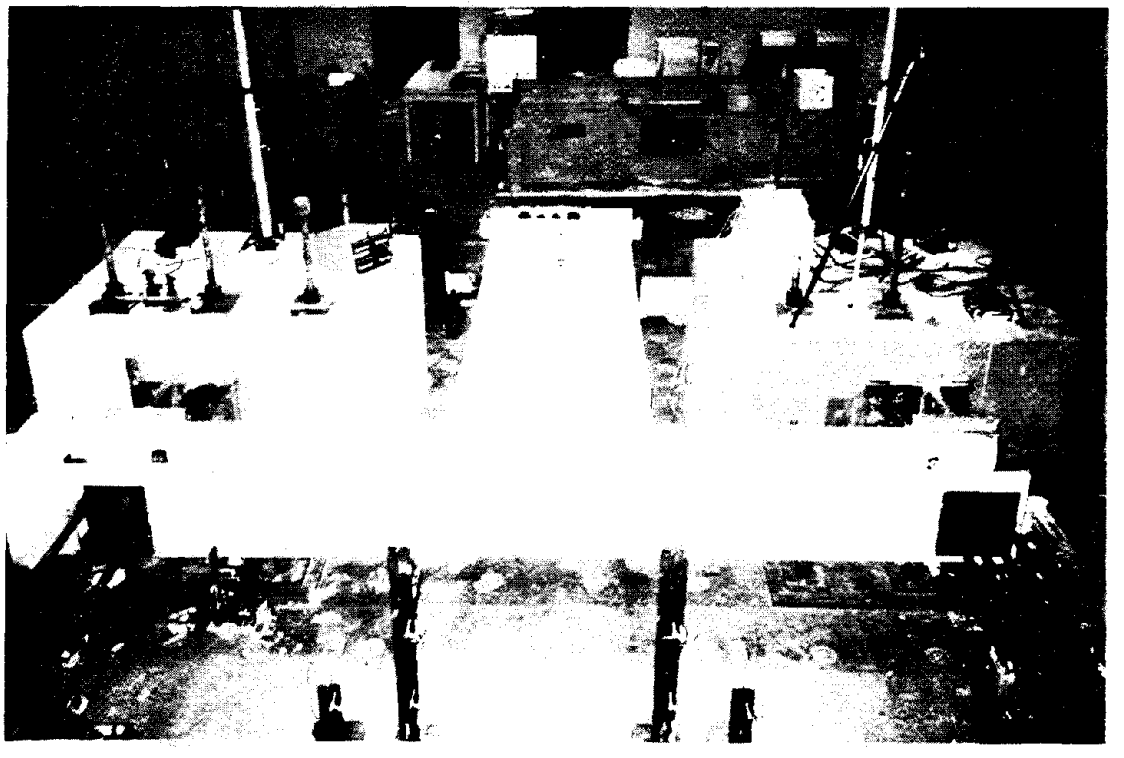

Figure 3-6. Test Setup at Davis Hall

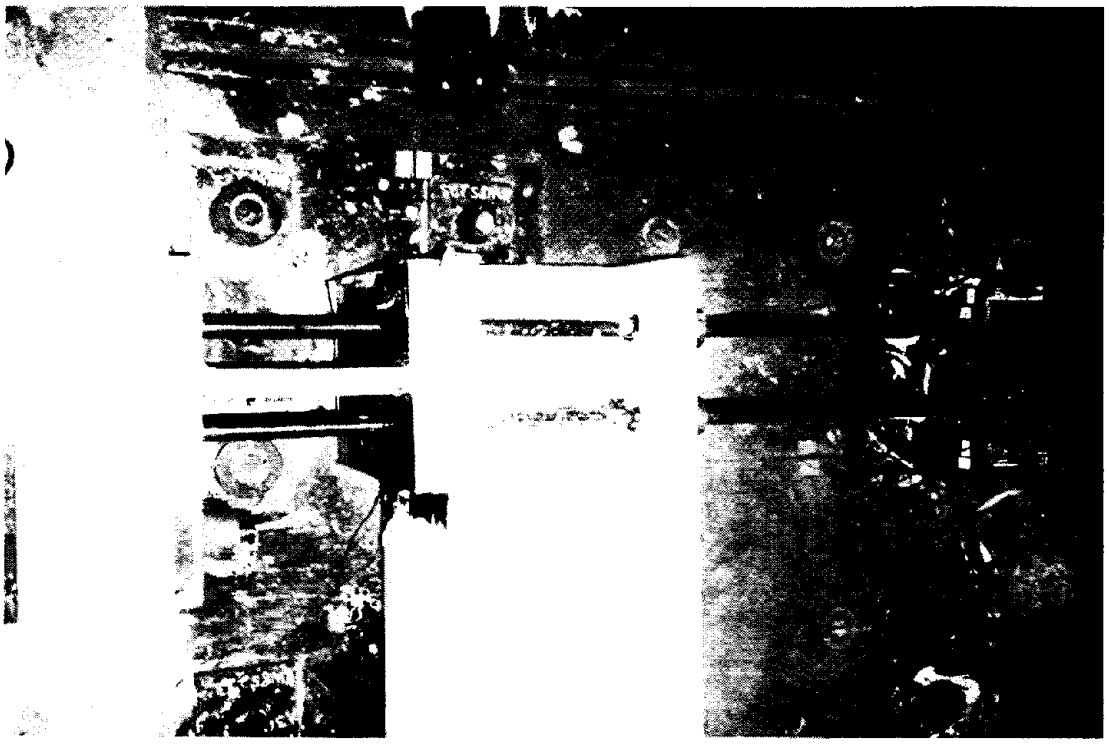

Figure 3-7. Built-Up Reaction Member and Stress Rods at Northwest Support

Figure 3-8. Built-Up Reaction Member and Stress Rods at Southwest Support

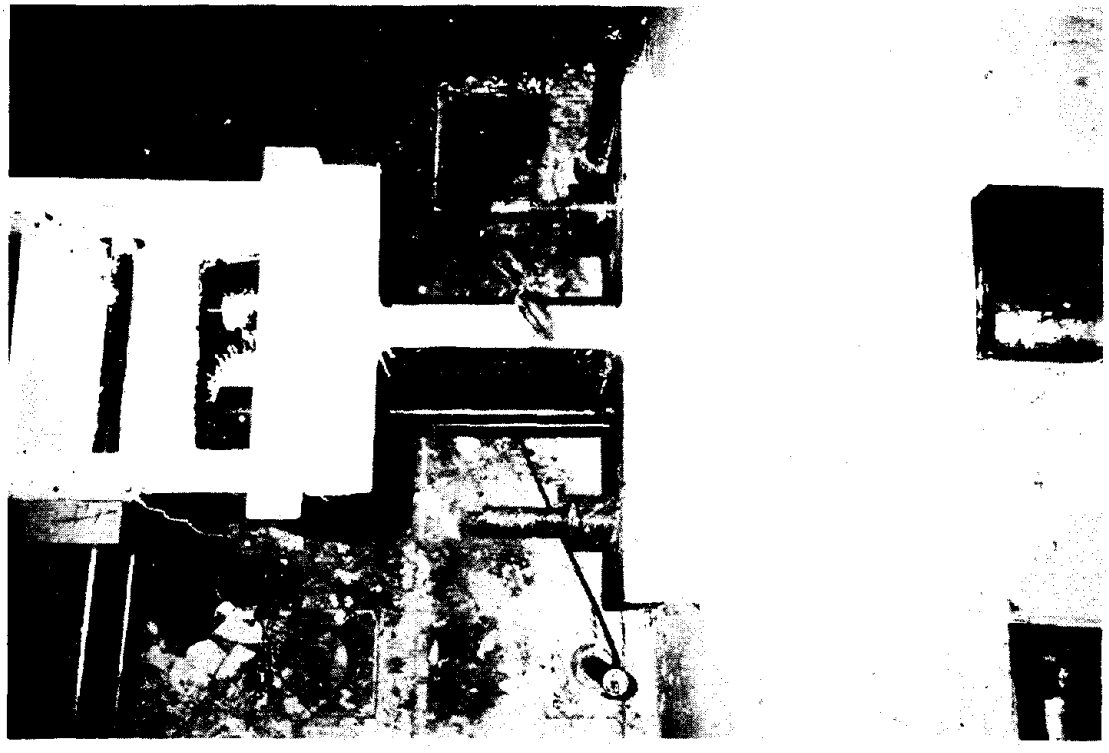

Figure 3-9. W14x455 Reaction Member with Stress Rods at South Support

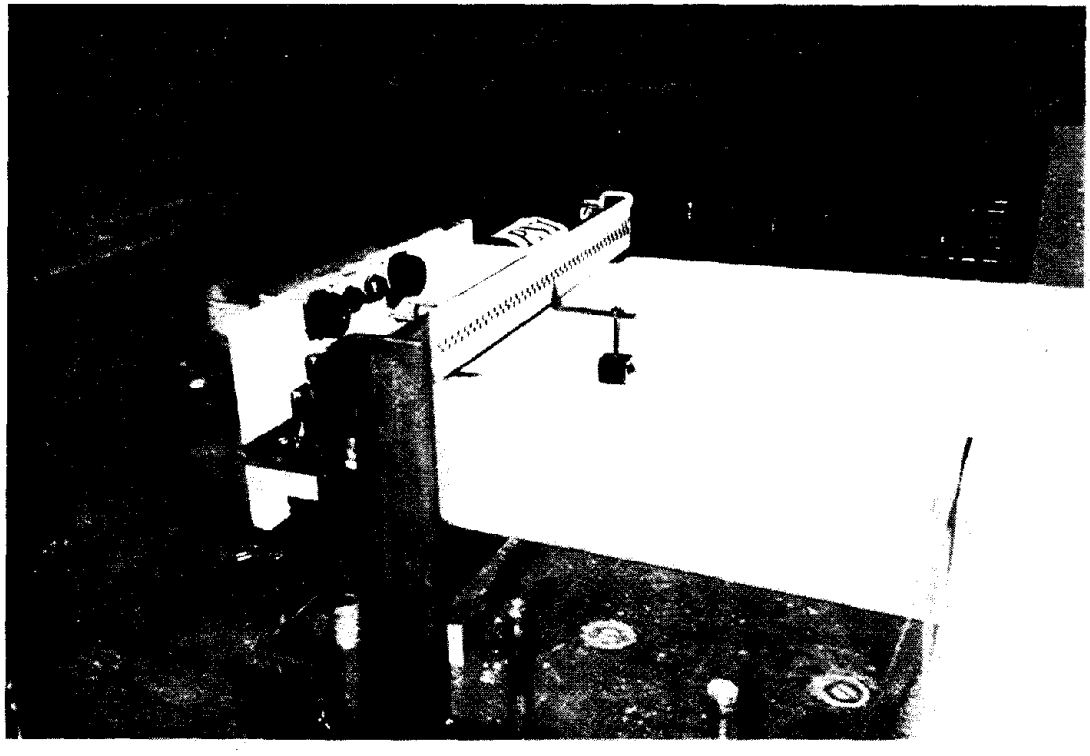

Figure 3-10. Lateral Guide Frame and Displacement Scale at End of Cantilevered Beam

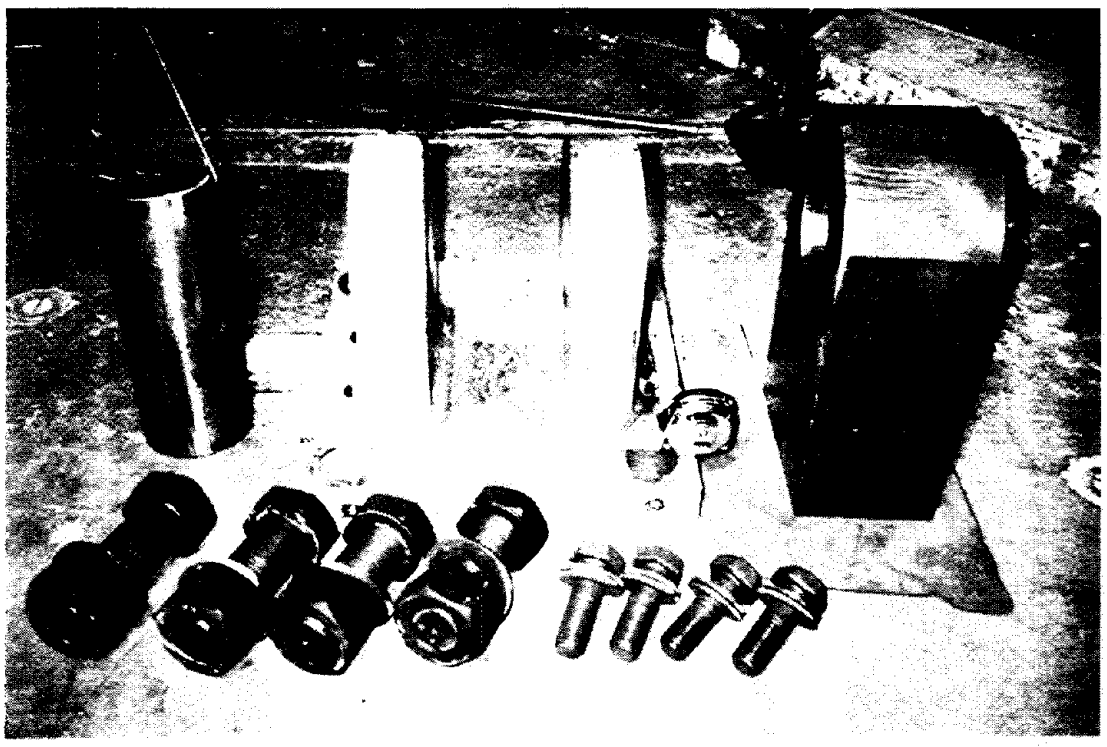

Figure 3-11. Clevis with Four - 1 1/4" ϕ Bolts, Four - 2 1/4" ϕ Bolts, and 5" ϕ Pin

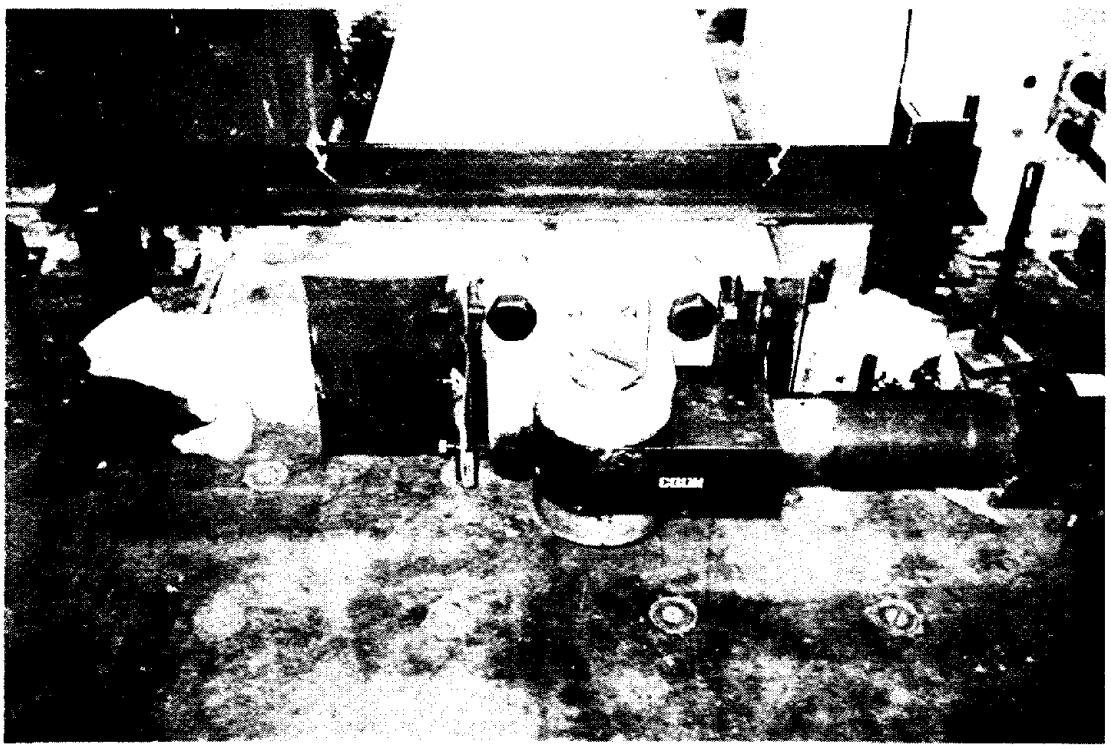

Figure 3-12. Clevis Attached to Beam End Plate

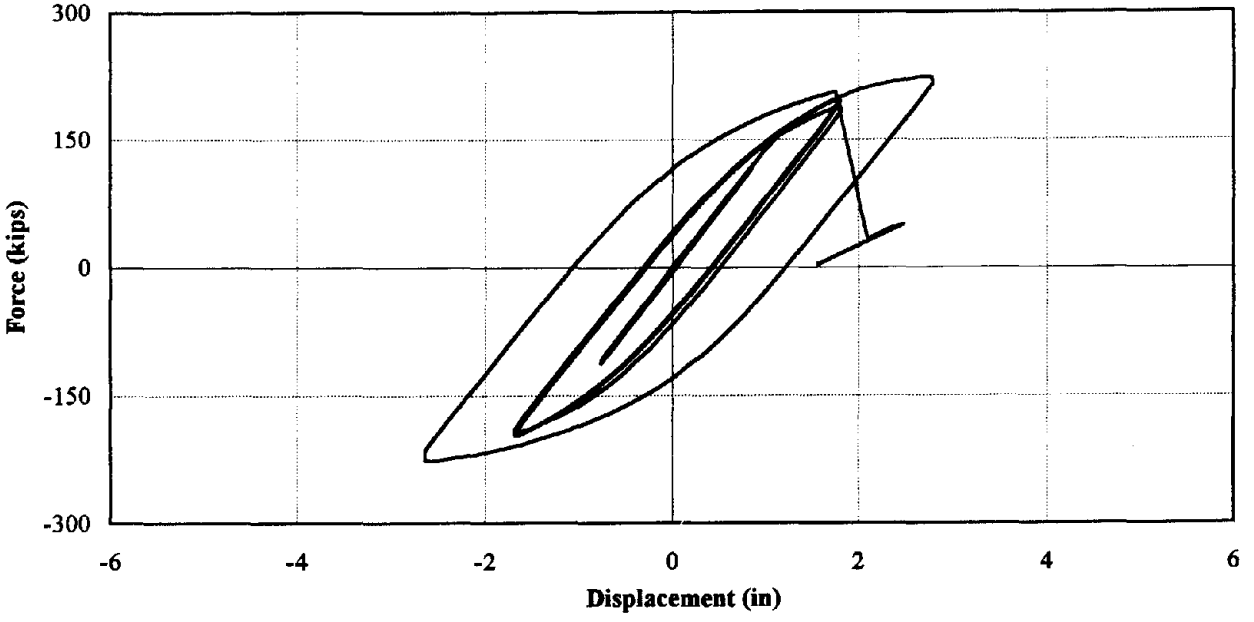

Figure 3-13. Specimen PN1 - Force vs. Displacement

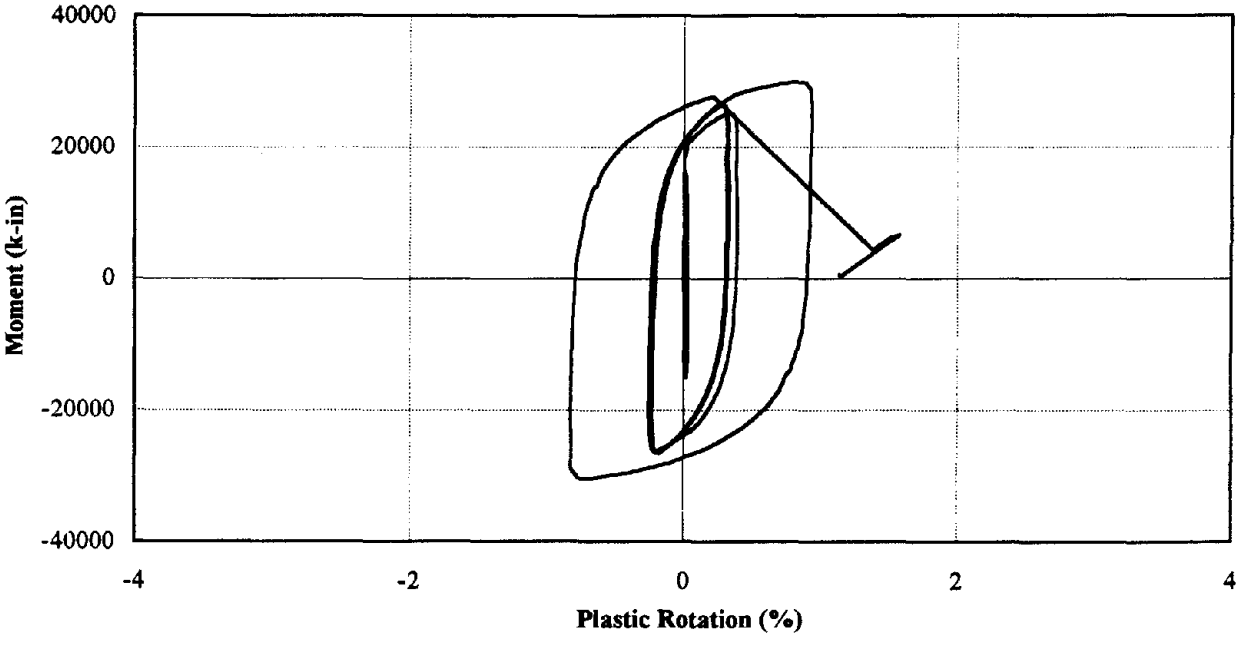

Figure 3-14. Specimen PN1 - Moment vs. Plastic Rotation

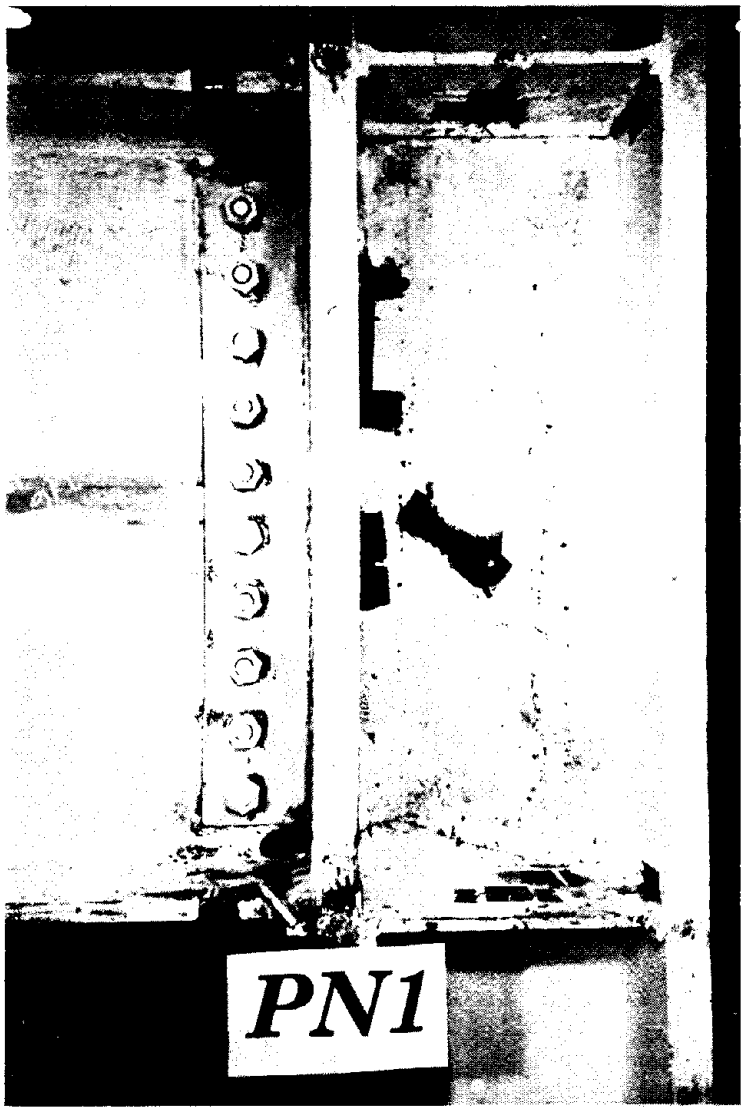

Figure 3-15. Specimen PN1 Joint after Test

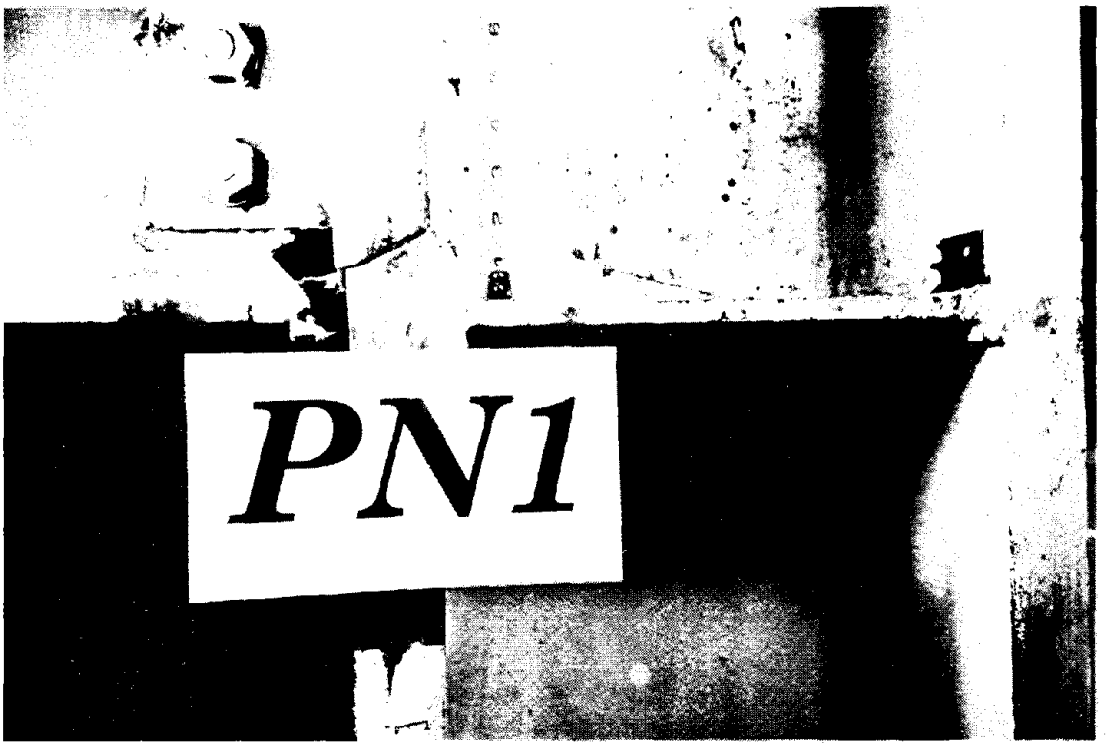

Figure 3-16. Failure of Column Flange at Bottom Groove Weld

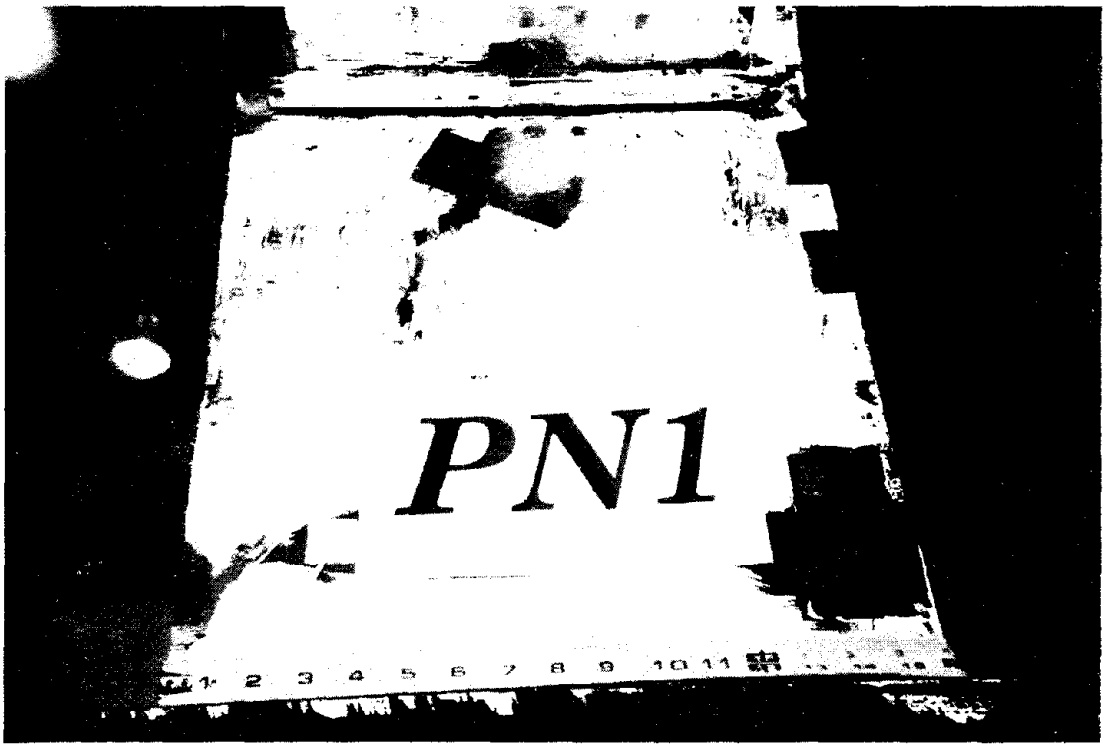

Figure 3-17. Separation Between Bottom Backup Bar and Column Flange

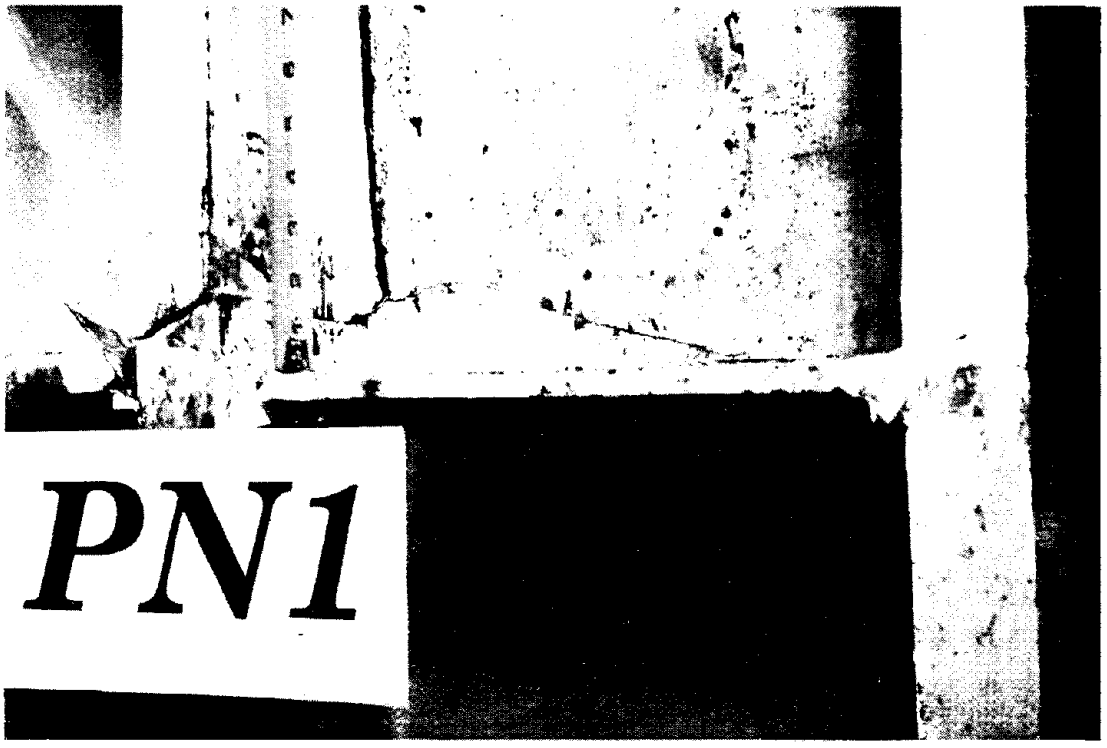

Figure 3-18. Cracks in Column Flange and Web

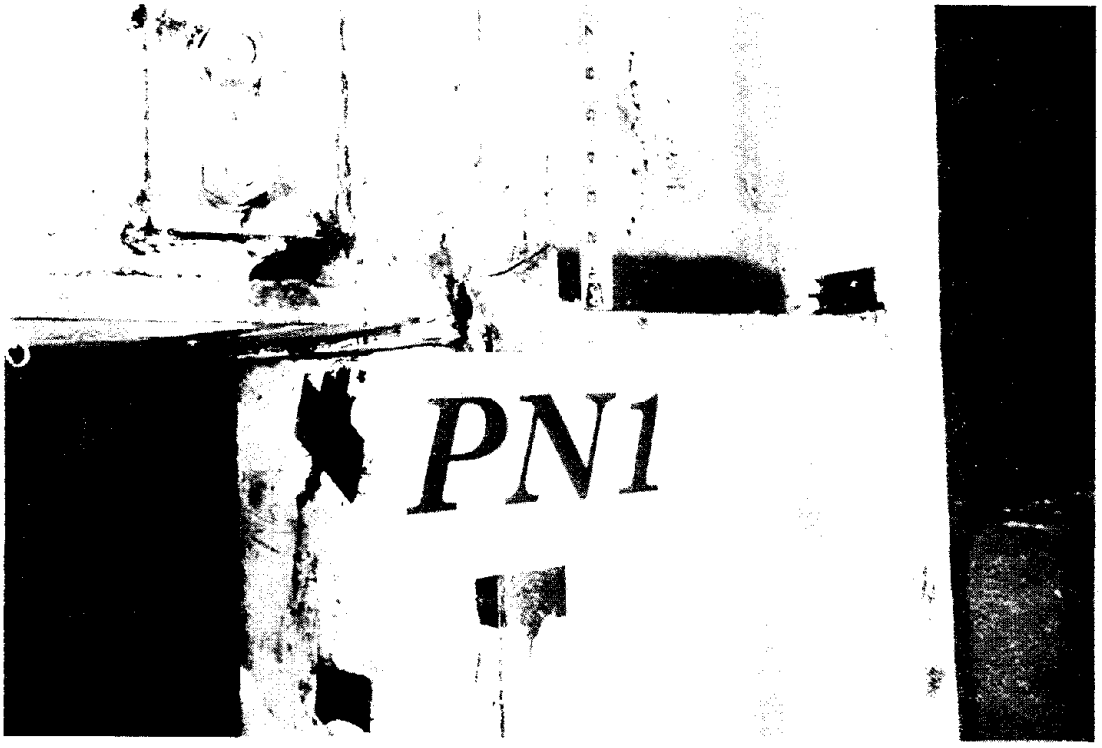

Figure 3-19. Crack in Column Flange

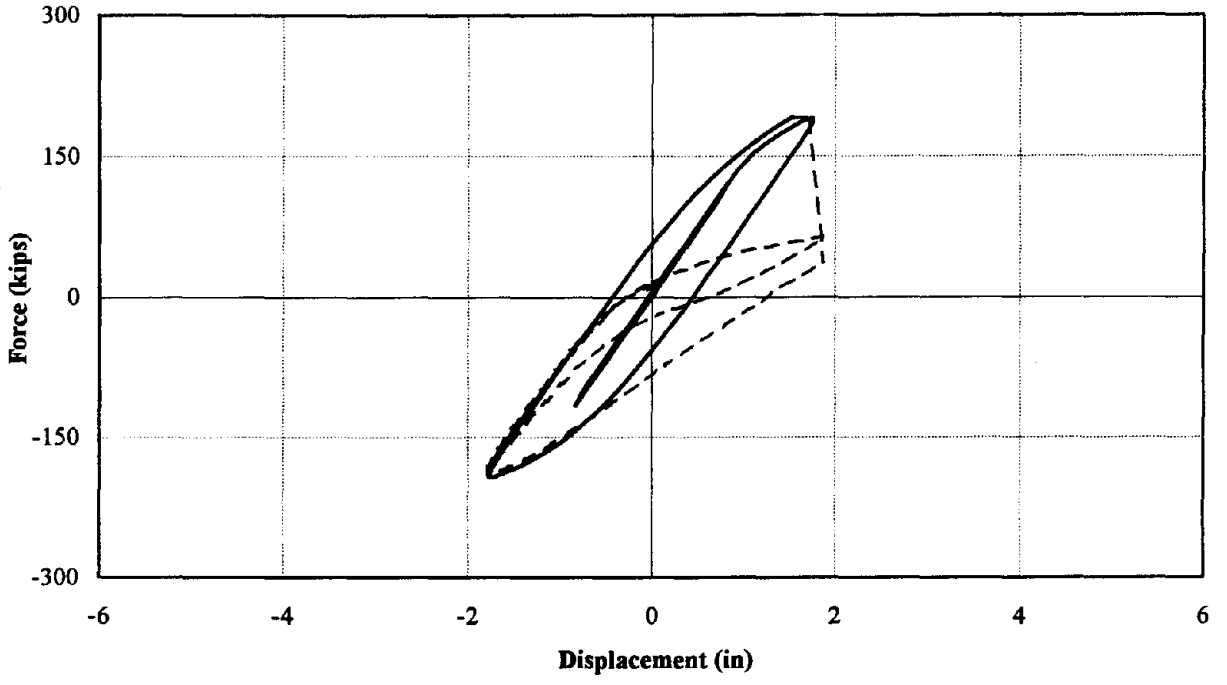

Figure 3-20. Specimen PN2 - Force vs. Displacement

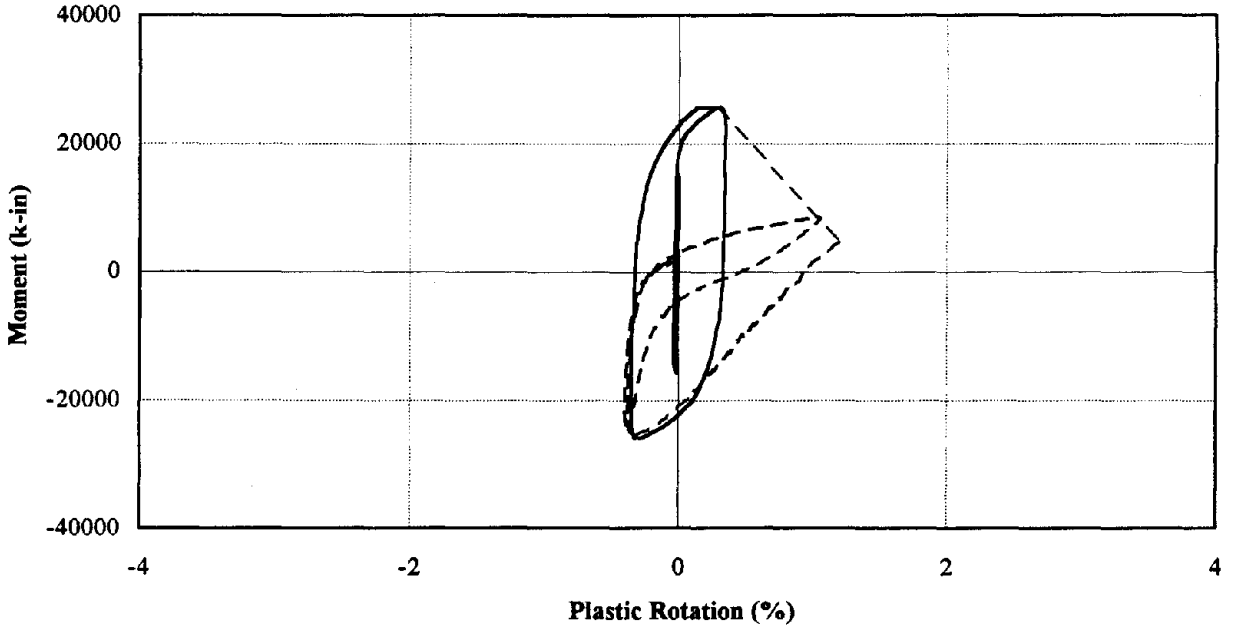

Figure 3-21. Specimen PN2 - Moment vs. Plastic Rotation

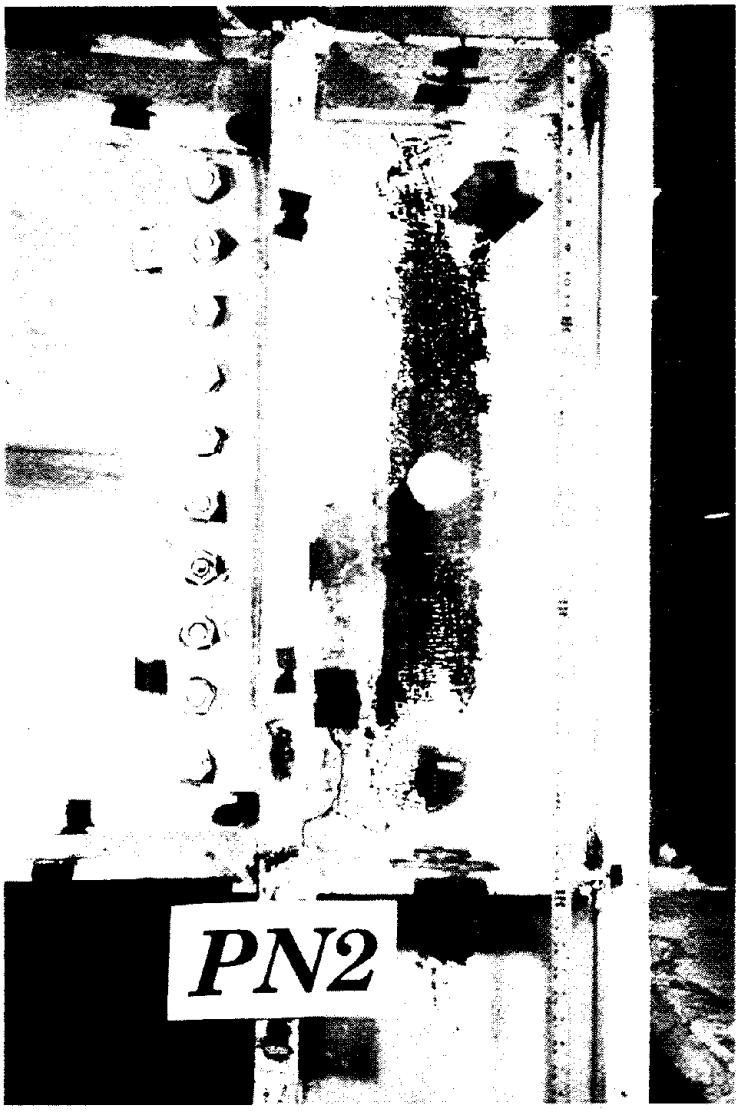

Figure 3-22. Specimen PN2 Joint after Test

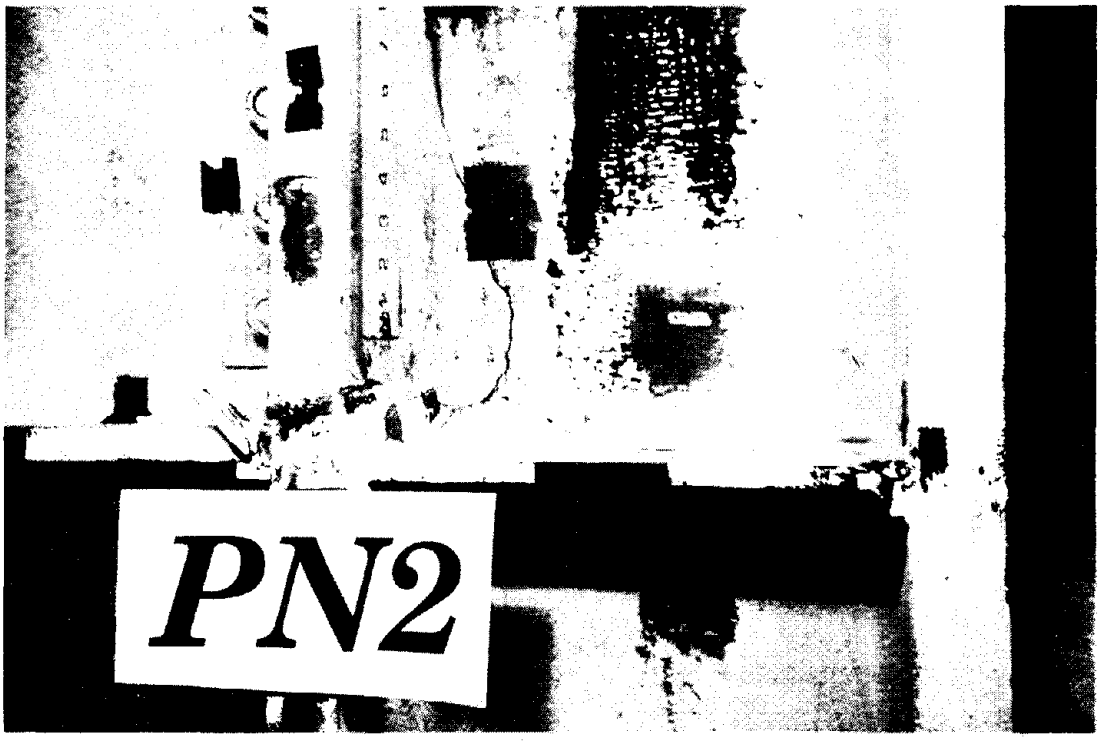

Figure 3-23. Cracks in Column Flange and Web Adjacent to Bottom Beam Flange

Figure 3-24. Separation Between Bottom Backup Bar and Column Flange

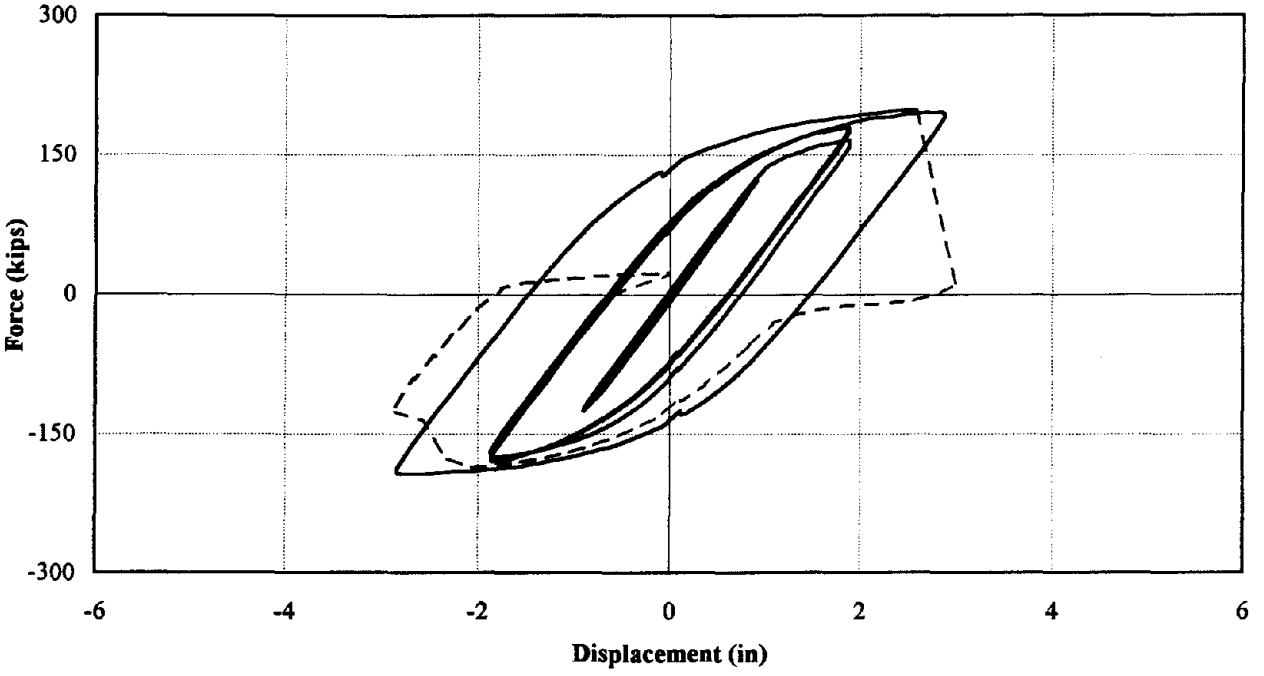

Figure 3-25. Specimen PN3 - Force vs. Displacement

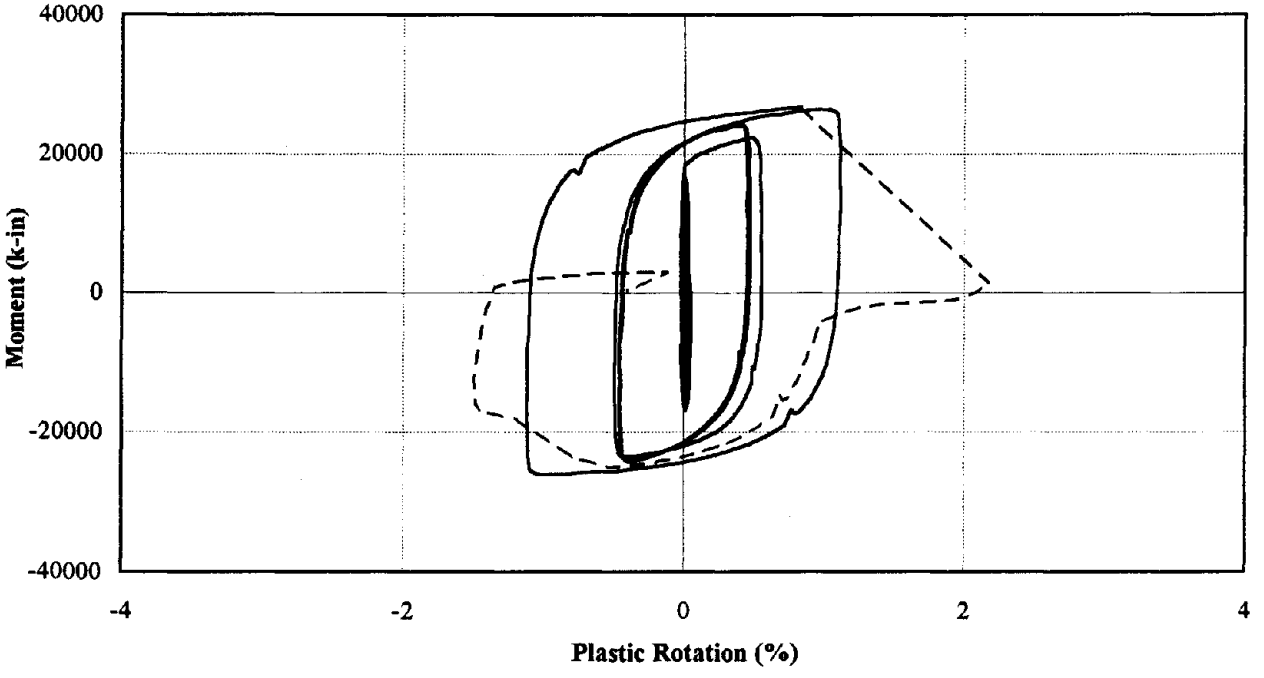

Figure 3-26. Specimen PN3 - Moment vs. Plastic Rotation

Figure 3-27. Specimen PN3 Joint after Test

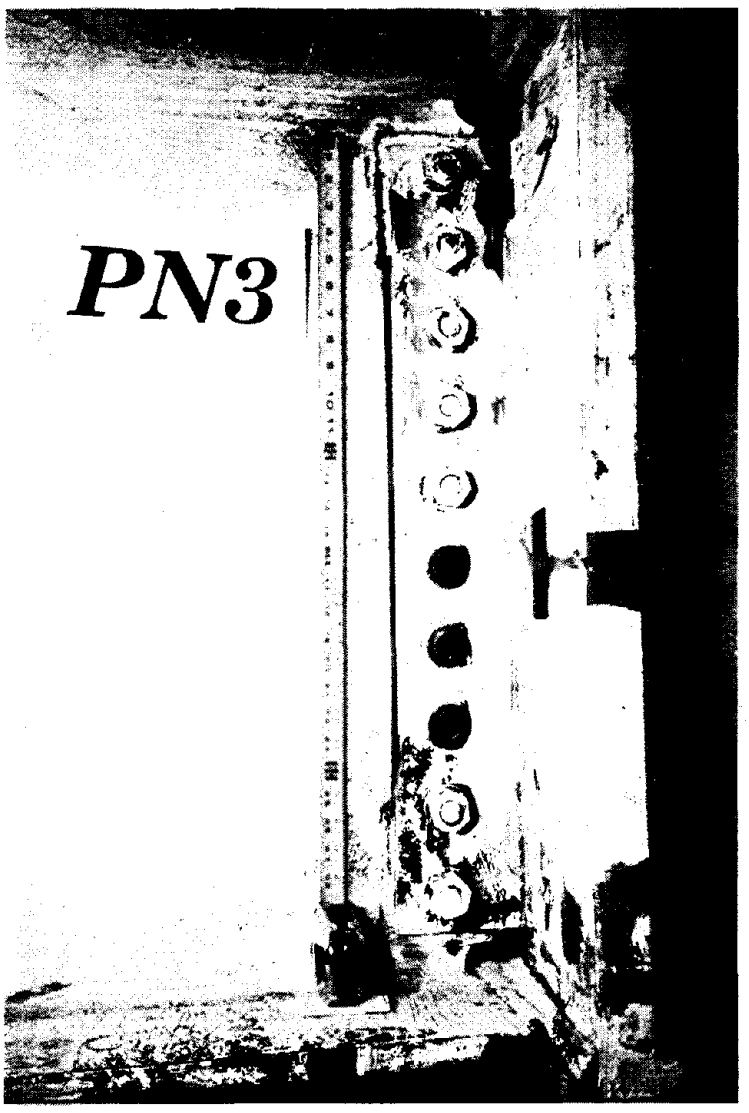

Figure 3-28. Damage to Shear Tab and Bottom Groove Weld

Figure 3-29. Tearing of Weld Return and Yielding at Top of Shear Tab

Figure 3-30. Brittle Failure of Shear Tab and Groove Weld at Bottom Flange

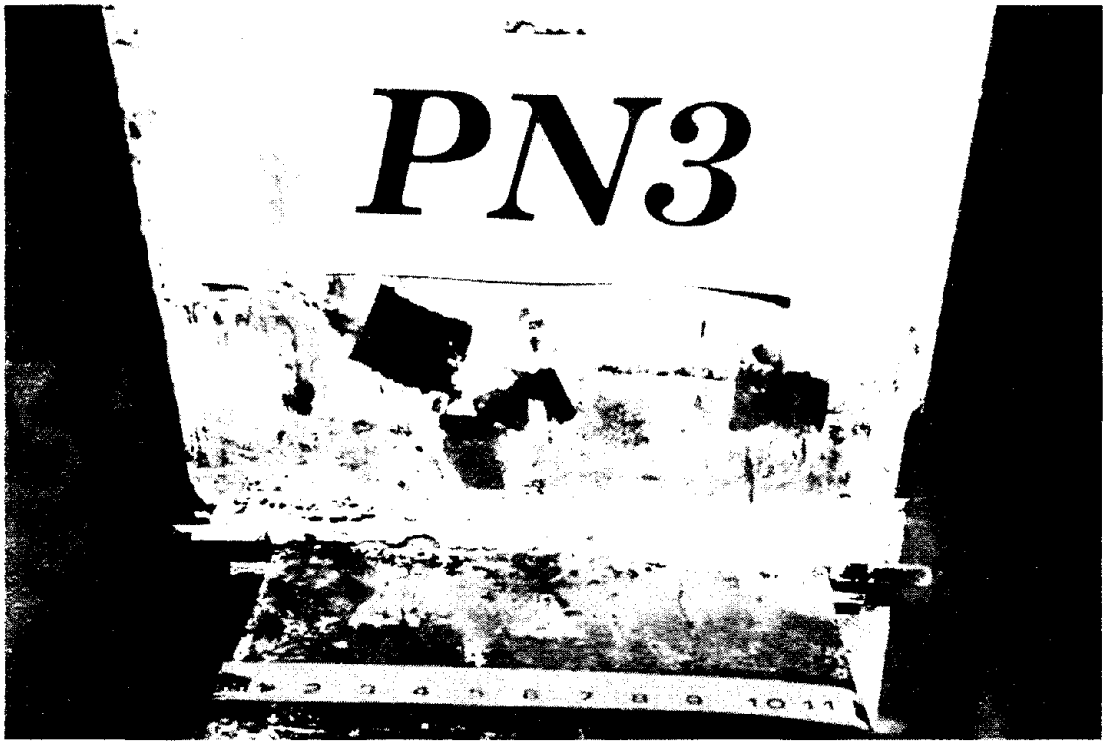

Figure 3-31. Gradual Tearing of Top Beam Flange Adjacent to Groove Weld

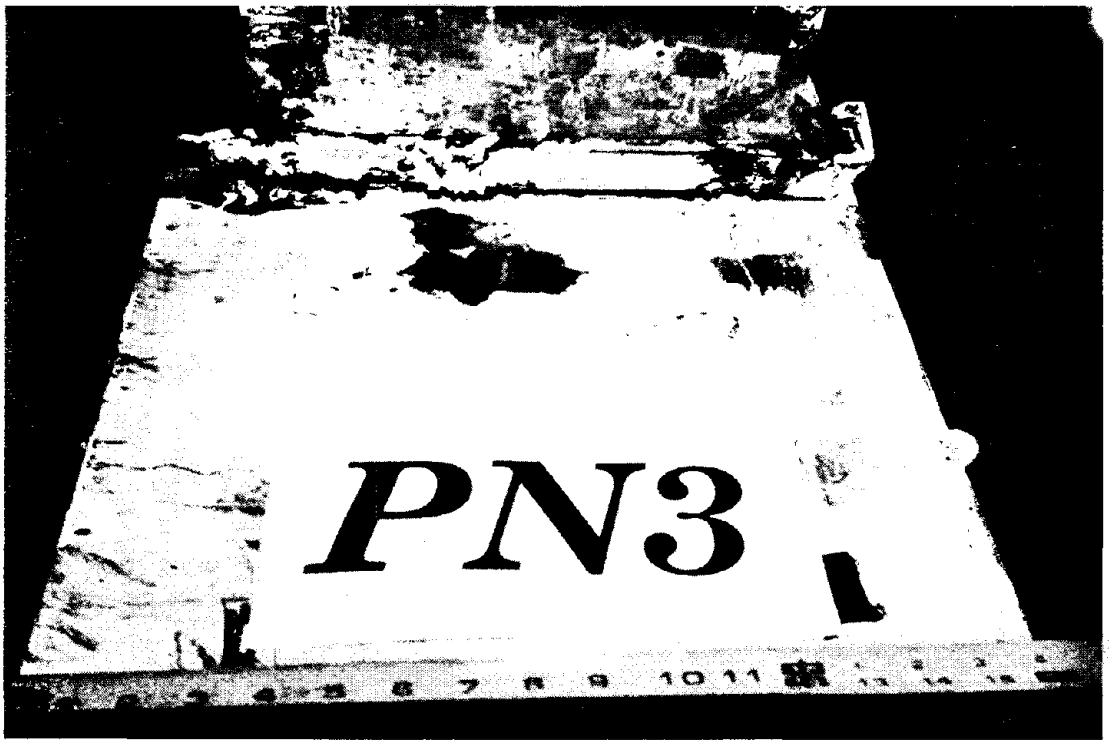

Figure 3-32. Separation Between Bottom Backup Bar and Column Flange

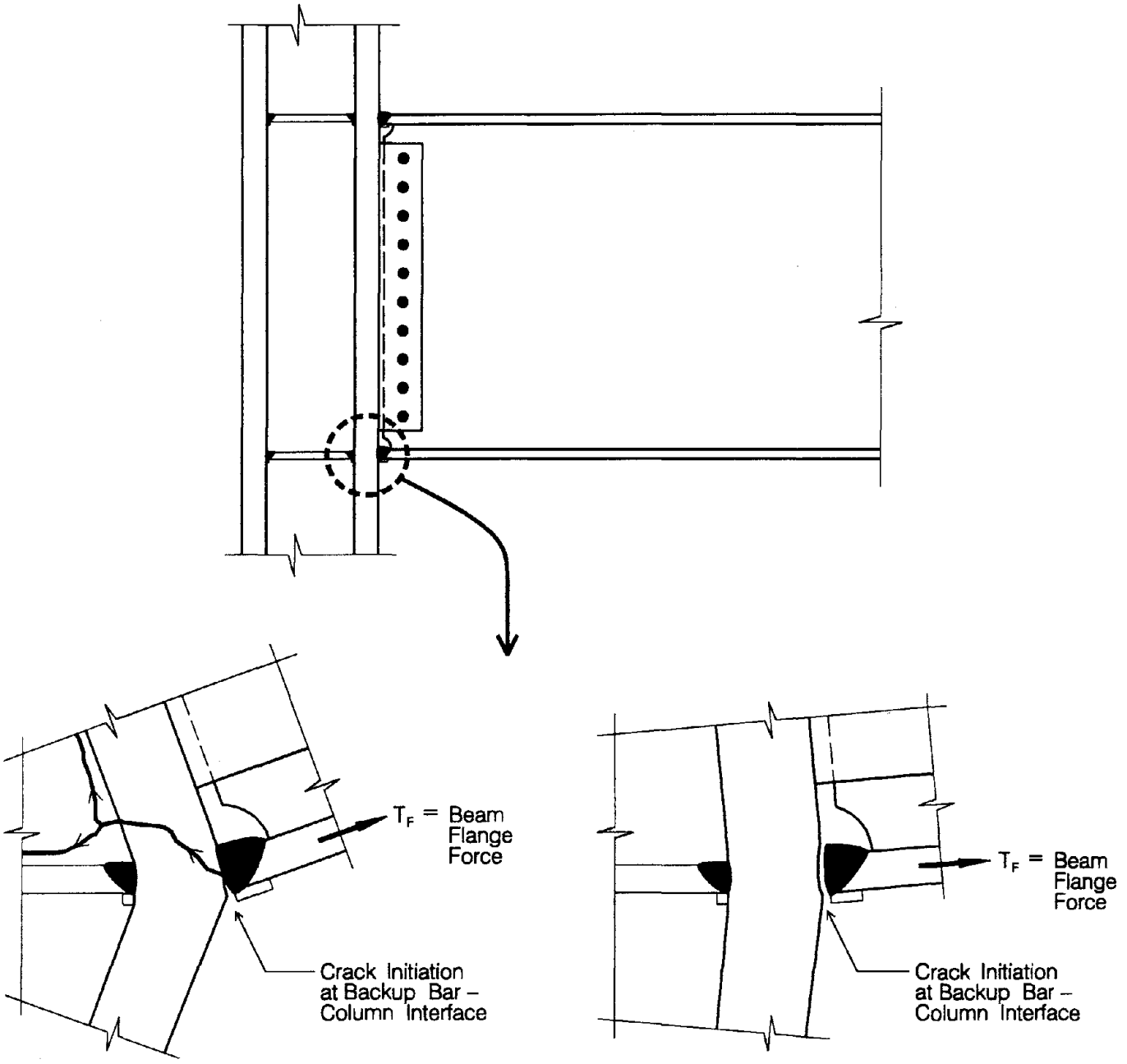

Figure 3-33a. Specimens PN1 and PN2 Crack Propagation.

Figure 3-33b. Specimen PN3 Crack Propagation.

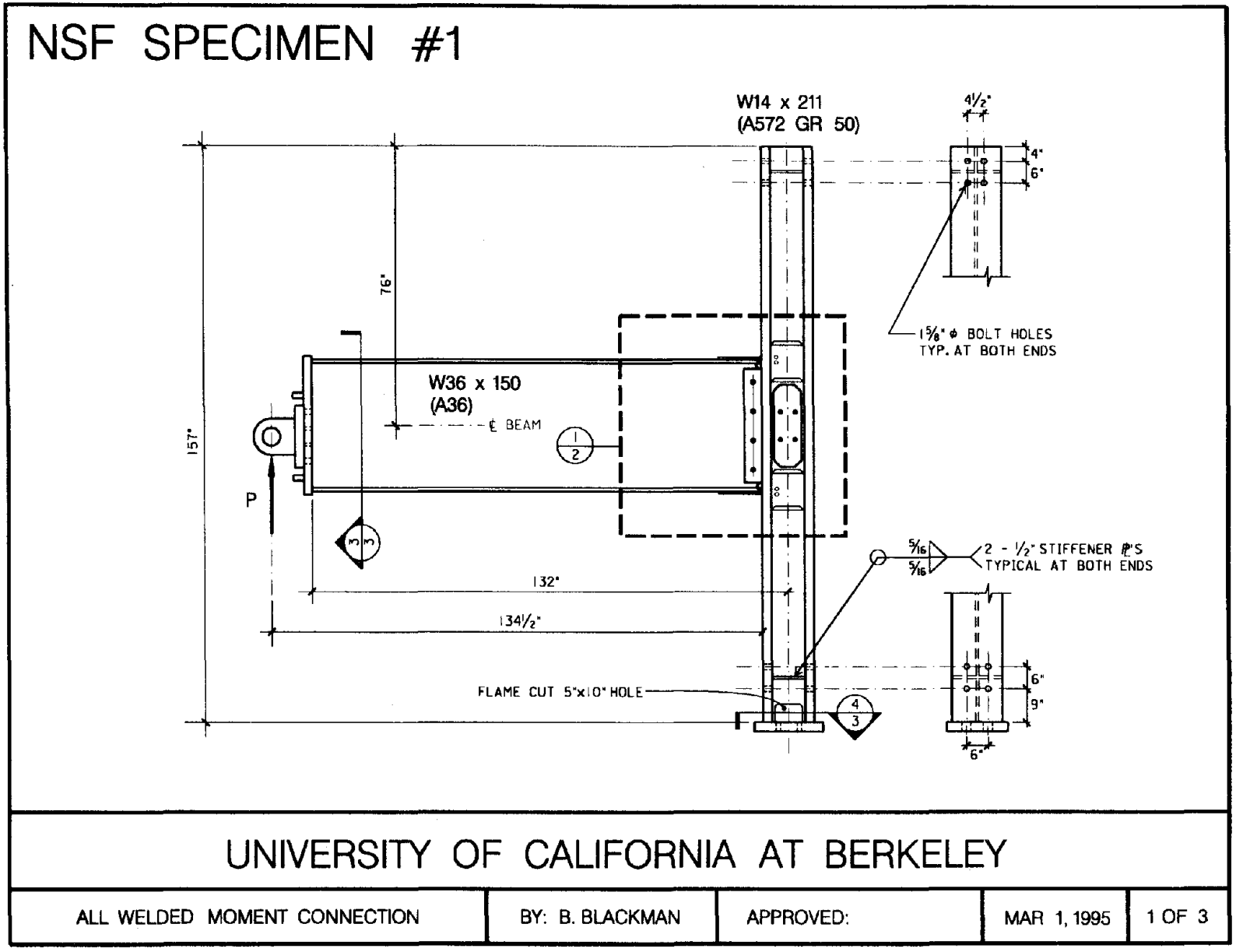

Figure 4-1. All-Welded Connection with Separated "Continuity" Plate Configuration

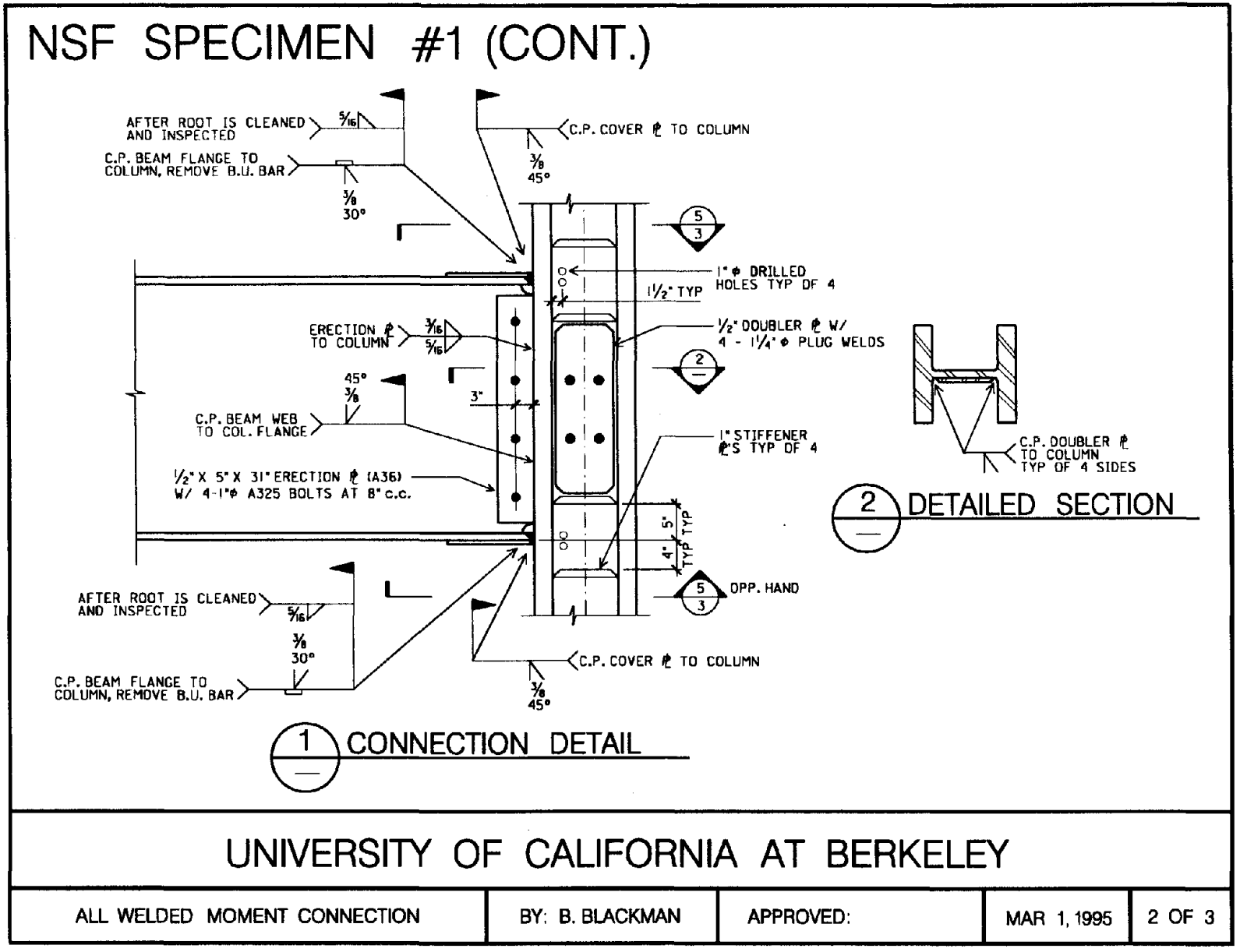

Figure 4-2. All-Welded Connection Details

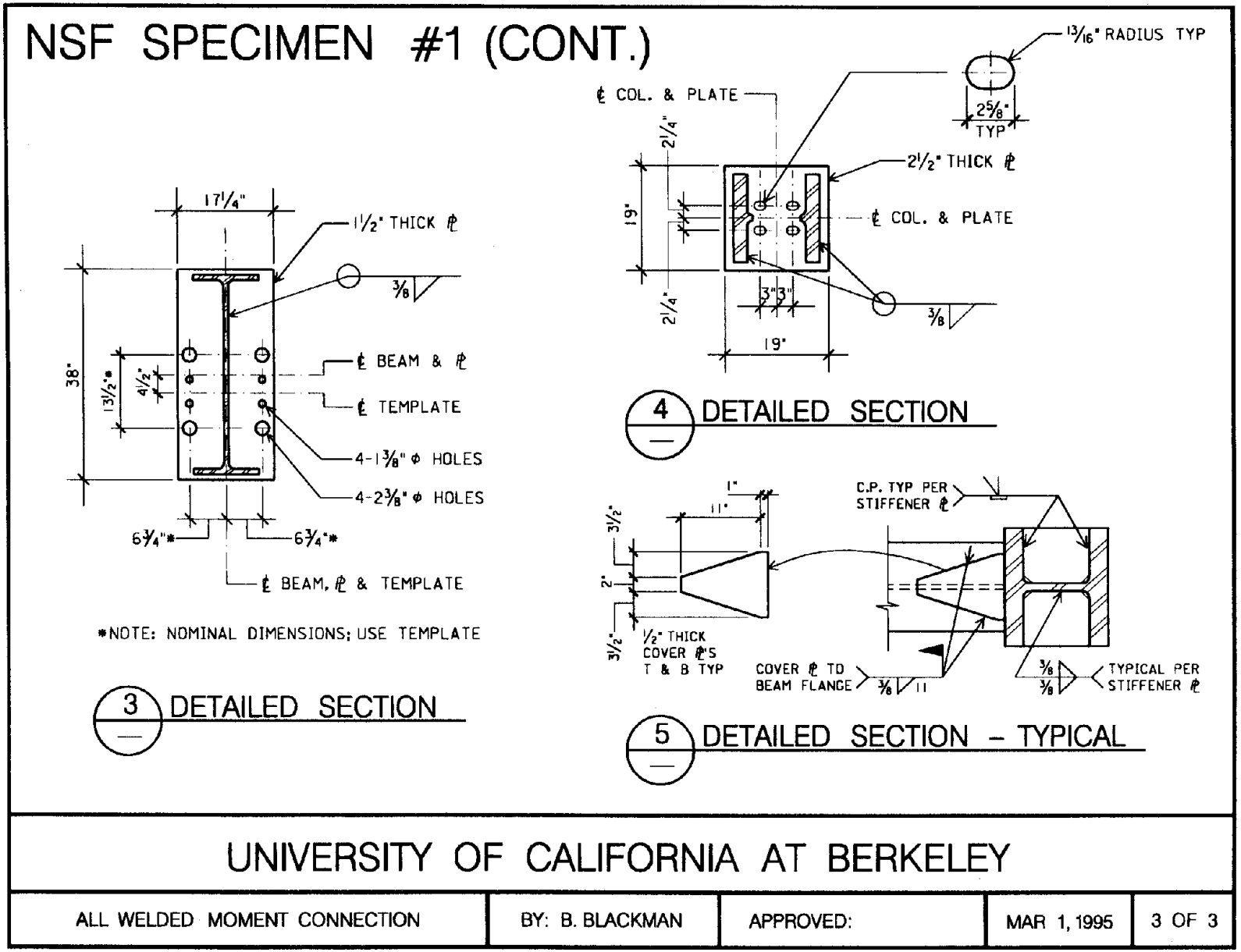

Figure 4-3. Detailed Sections for All-Welded Connection

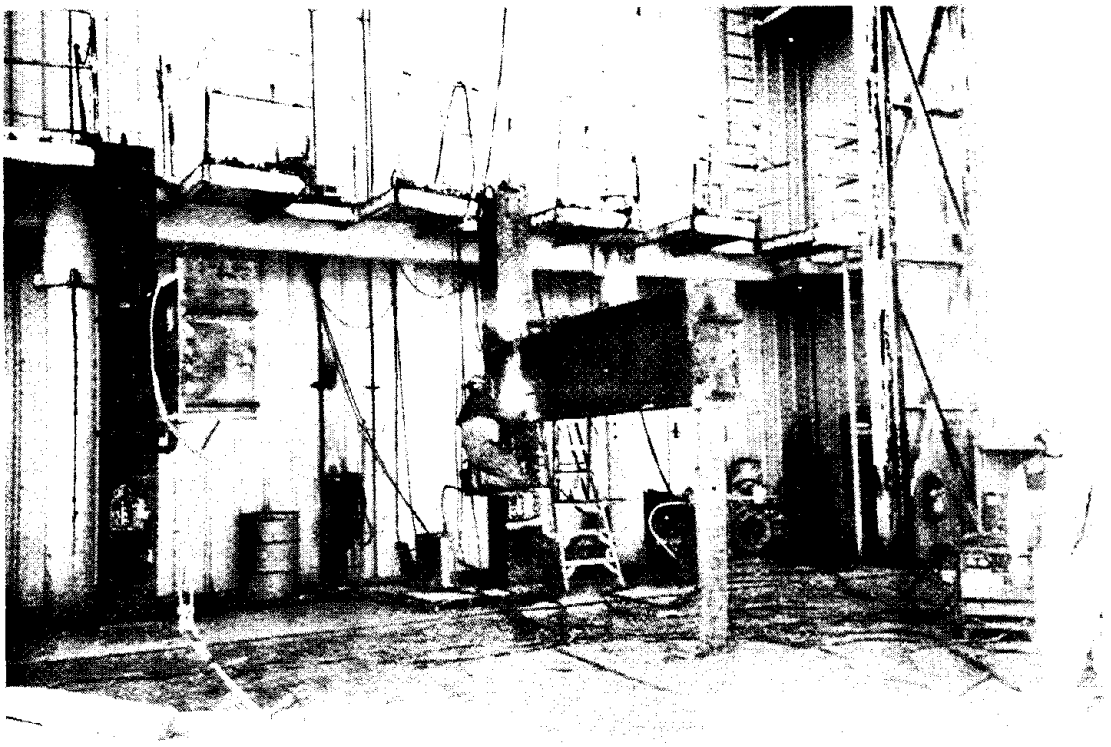

Figure 4-4. Fabrication of NSF Specimen #1 Simulating Field Conditions

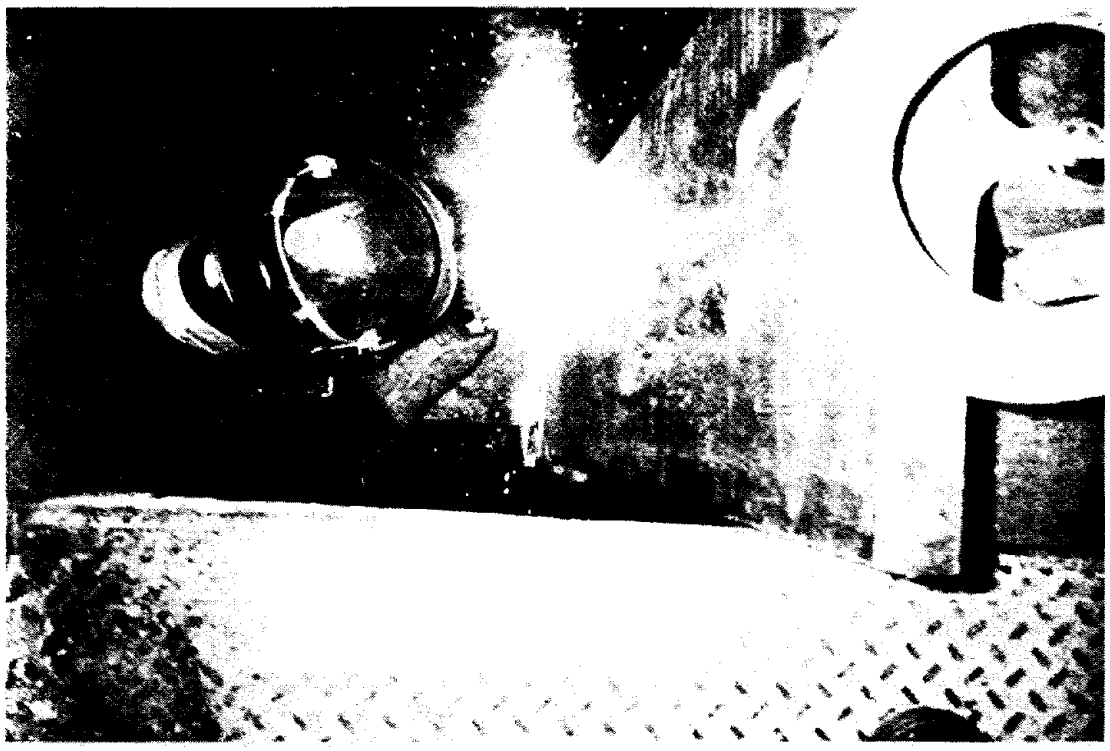

Figure 4-5. Root Pass of Top Beam Flange-to-Column Weld

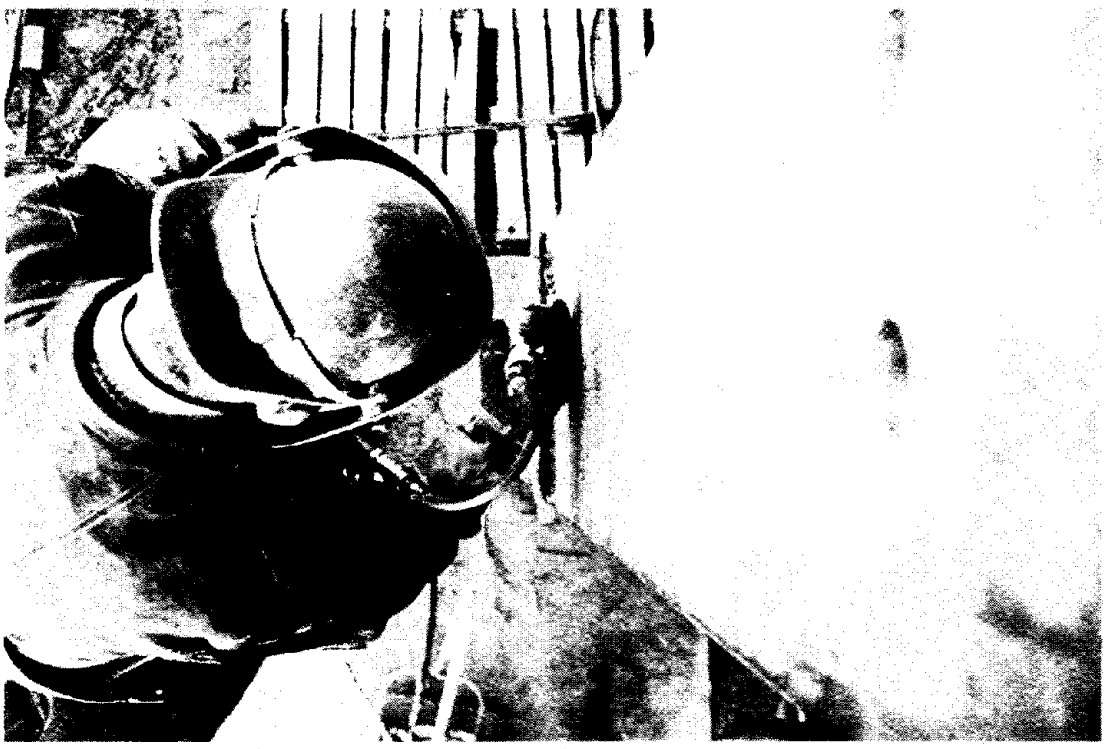

Figure 4-6. Peening the Top Beam Flange-to-Column Weld

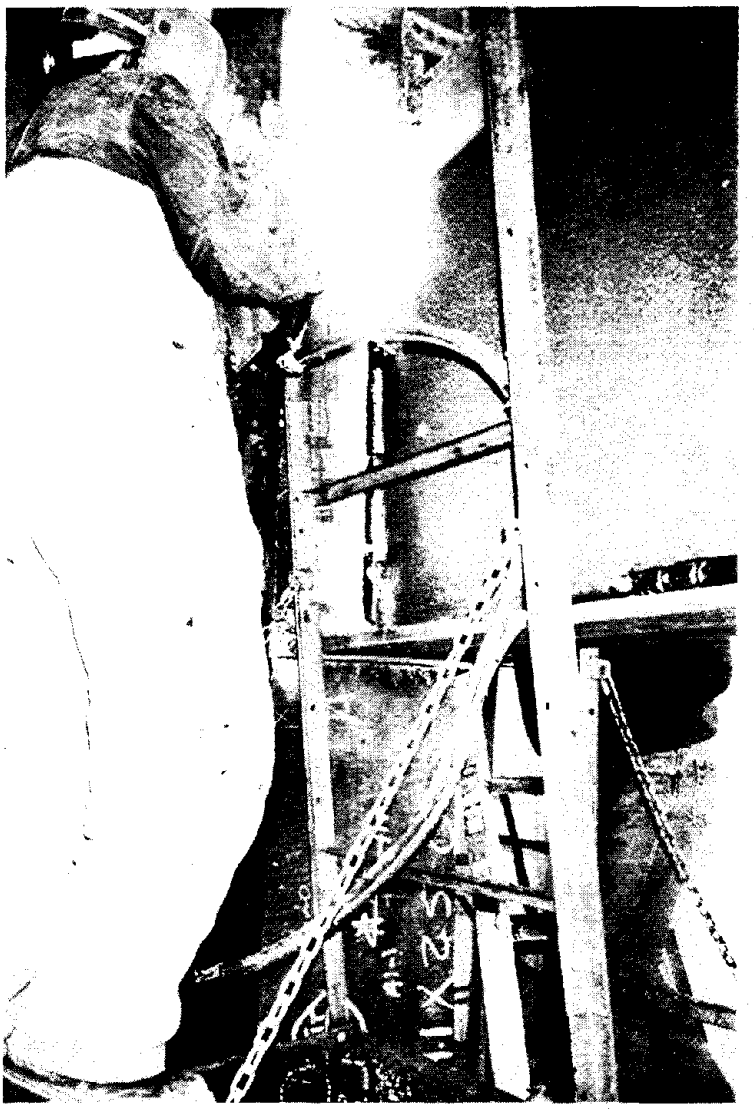

Figure 4-7. Beam Web-to-Column Weld in the Vertical Position

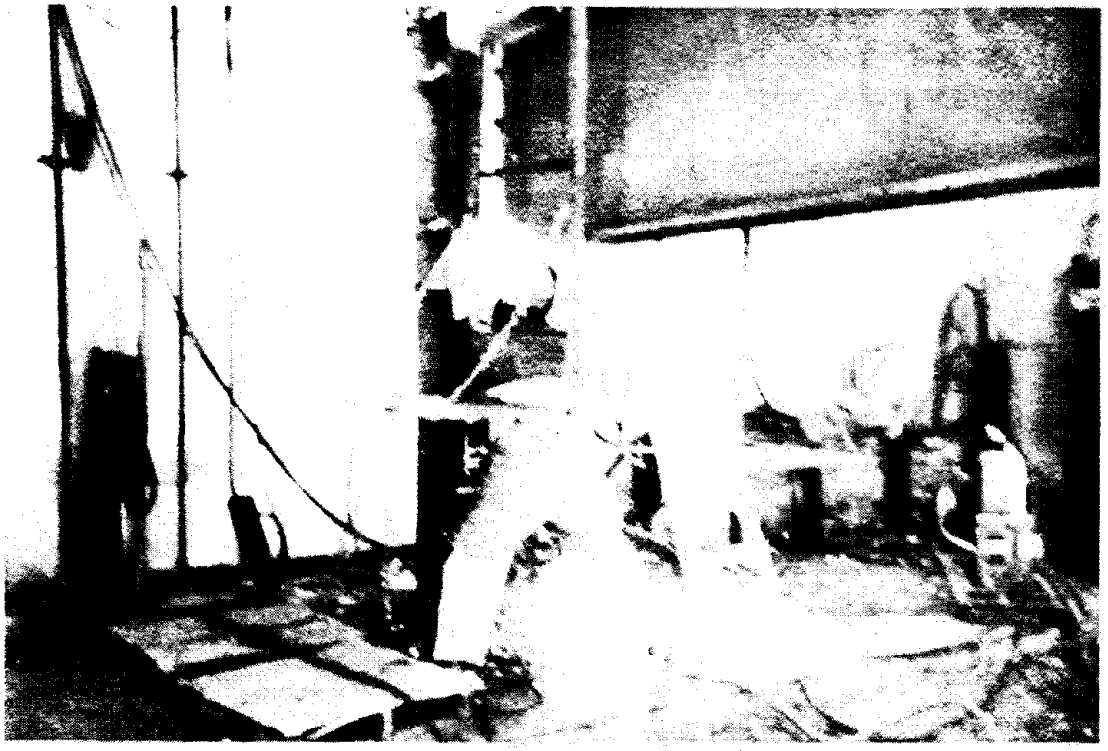

Figure 4-8. Removal of Bottom Backup Bar with Air Carbon Arc

Figure 4-9. Visual Inspection of Bottom Beam Flange Weld after Backup Bar Removal

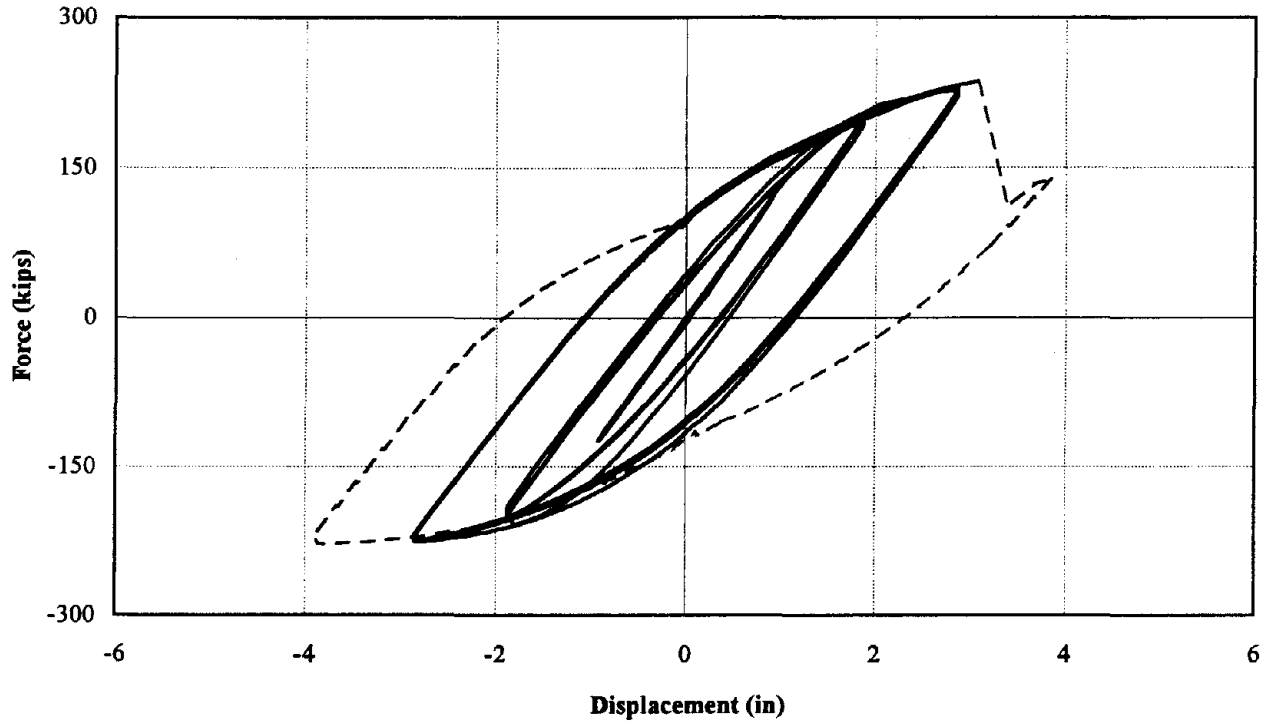

Figure 4-10. NSF #1 - Force vs. Displacement

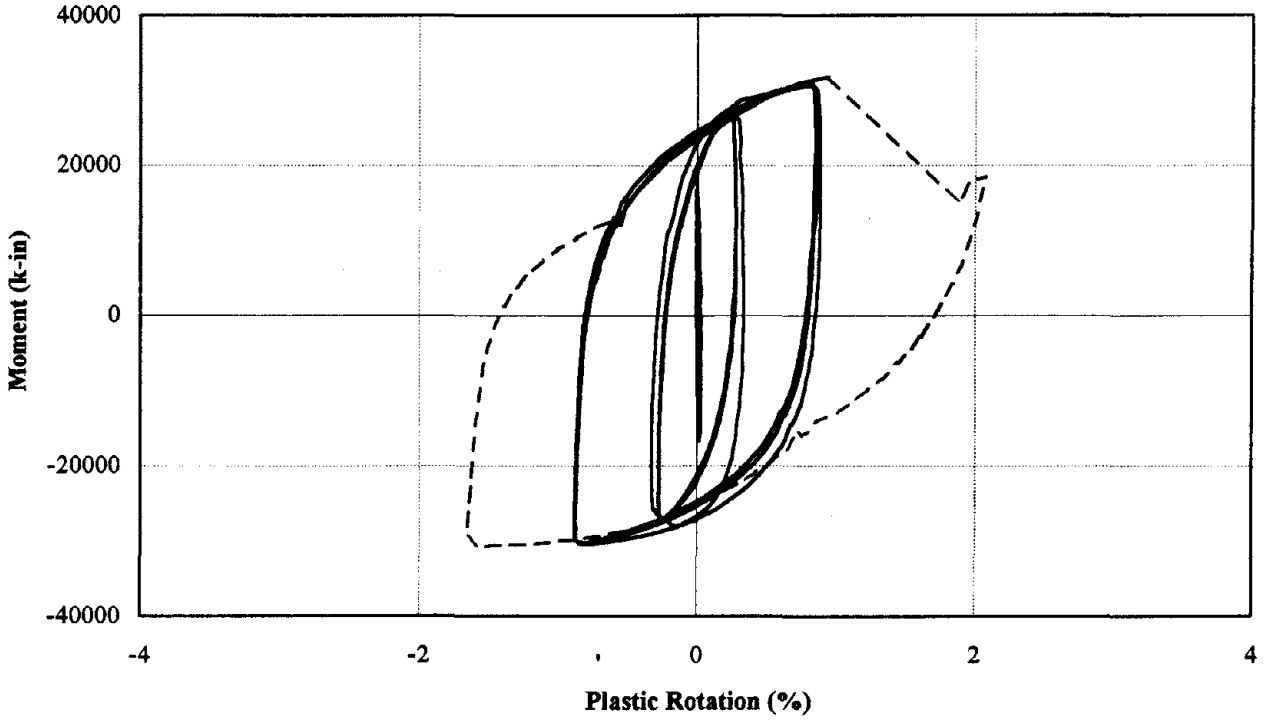

Figure 4-11. NSF #1 - Moment vs. Plastic Rotation

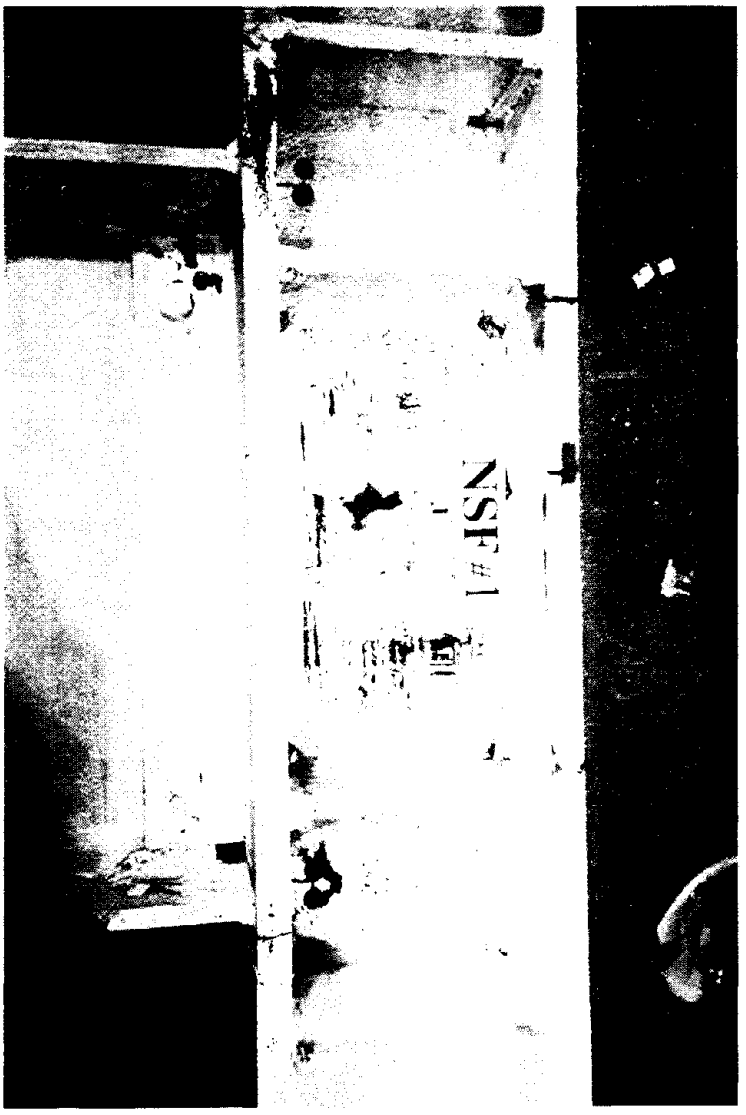

Figure 4-12. NSF Specimen #1 Joint after Test

Figure 4-13. Crack in Column K-Region Adjacent to Top Beam Flange @ Displ. = -1.80 in. and Force = -209.5 kips

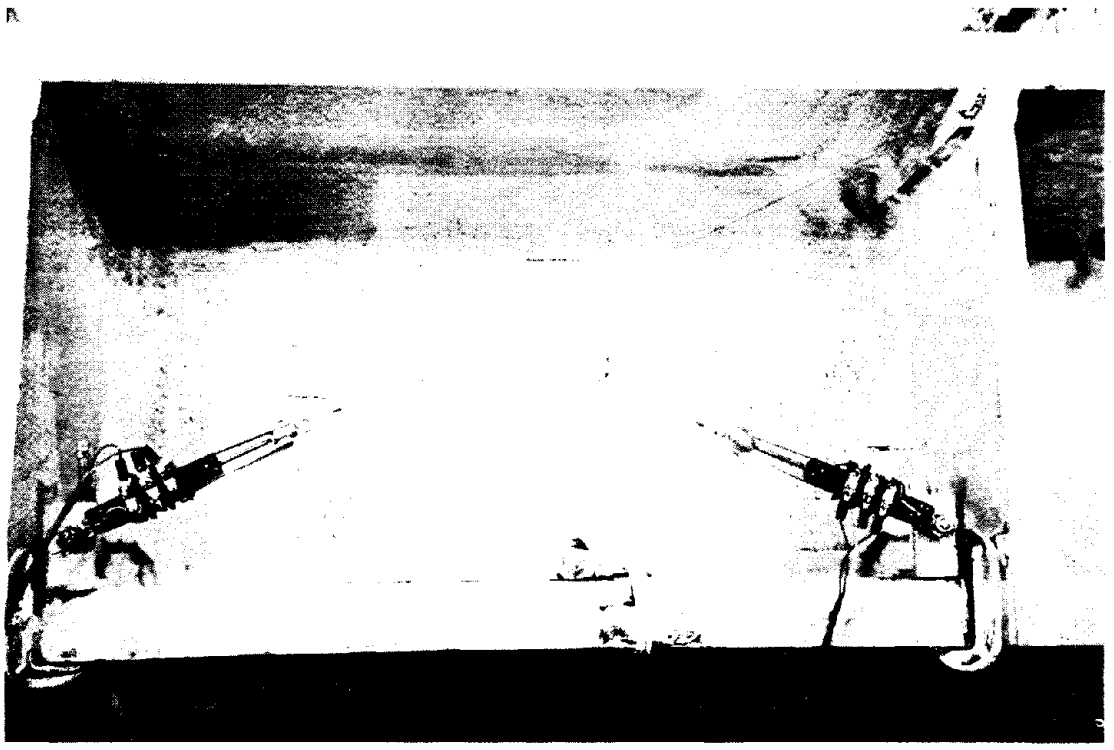

Figure 4-14. Whitewash Spalling of Doubler Plate During Third 2-in. Displacement Cycle

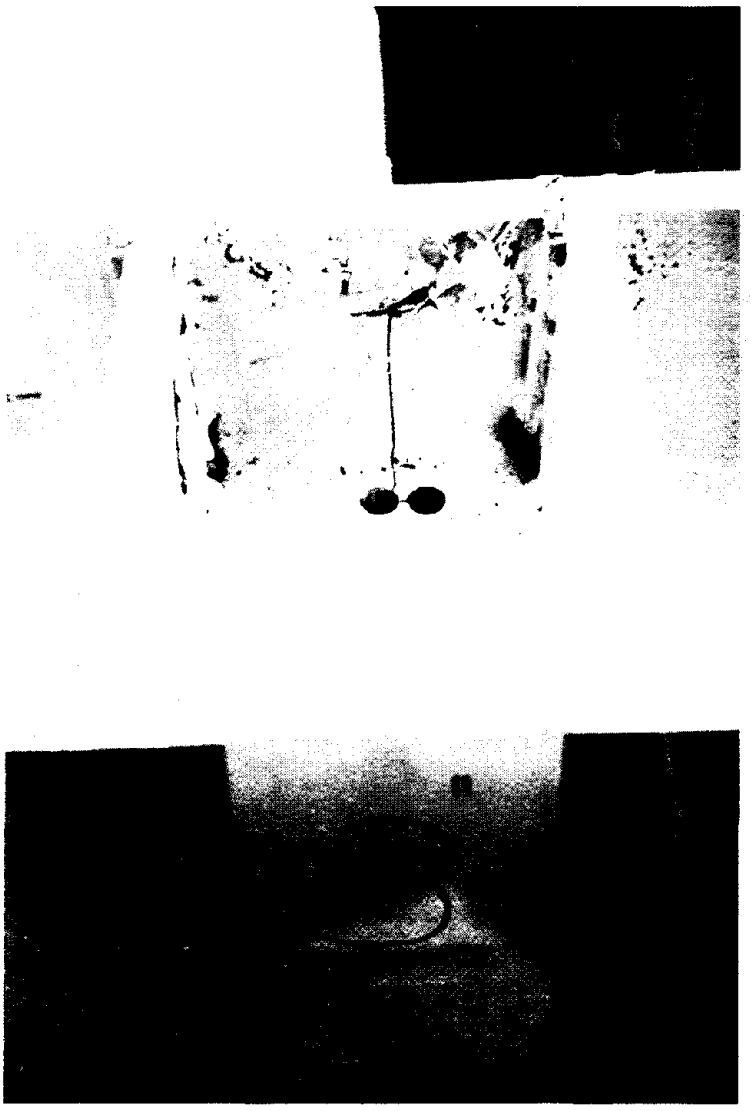

Figure 4-15. Propagation of Column Crack Adjacent to Top Beam Flange During 3-in. Displacement, Cycle 1

Figure 4-16. Failure of Column Flange Adjacent to Bottom Beam Flange @ Displ. = 3.08 in. and Force = 236.3 kips

Figure 4-17. Crack in Column Flange Adjacent to Bottom Beam Flange (Note: crack propagated under cover plate near column centerline)

Figure 4-18. Propagation of Column Crack into the Top Beam Flange and Cover Plate-to-Column Weld Area During 4-in. Displacement, Cycle 1

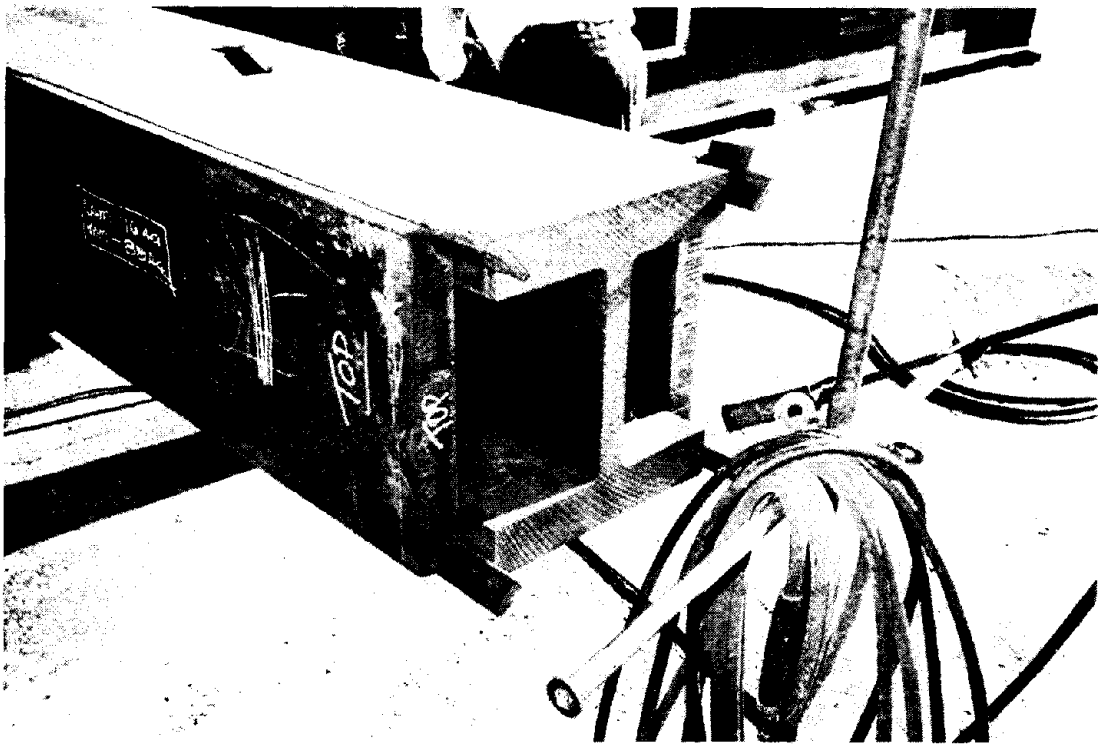

Figure 4-19. Plated Box-Column Typical of Modern Steel Construction

Figure 4-20. Typical Internal Continuity Plate for Box-Columns

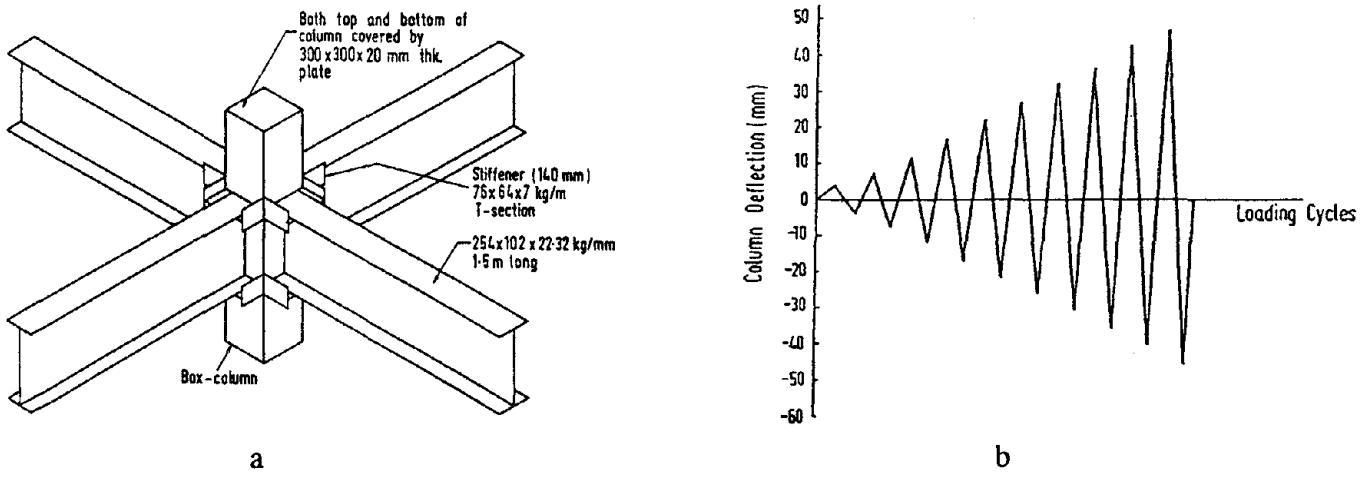

Figure 4-21. Configuration and Loading Sequence of I-Beam to Box-Column Specimens Recently Tested at the University of Singapore

Source: N. E. Shanmugam and L. C. Ting, "Welded Interior I-Beam to Box-Column Connections," *ASCE Journal of Structural Engineering*, vol. 121, no. 5, May 1995.

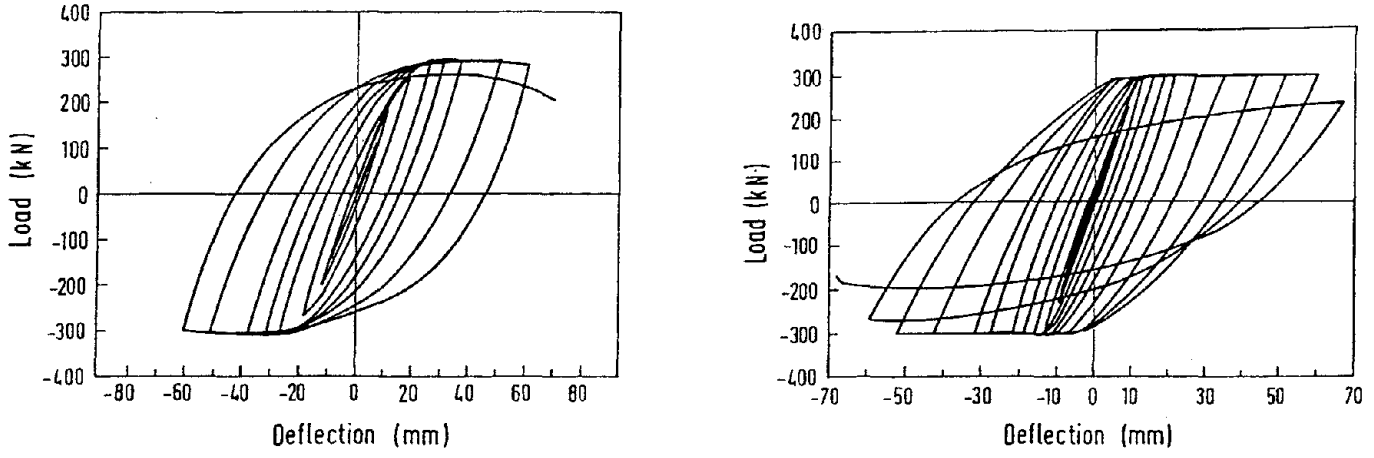

Figure 4-22. Hysteretic Loops for Two I-Beam to Box-Column Connections Stiffened by External Tees and Tested at the University of Singapore

Source: N. E. Shanmugam and L. C. Ting, "Welded Interior I-Beam to Box-Column Connections," *ASCE Journal of Structural Engineering*, vol. 121, no. 5, May 1995.

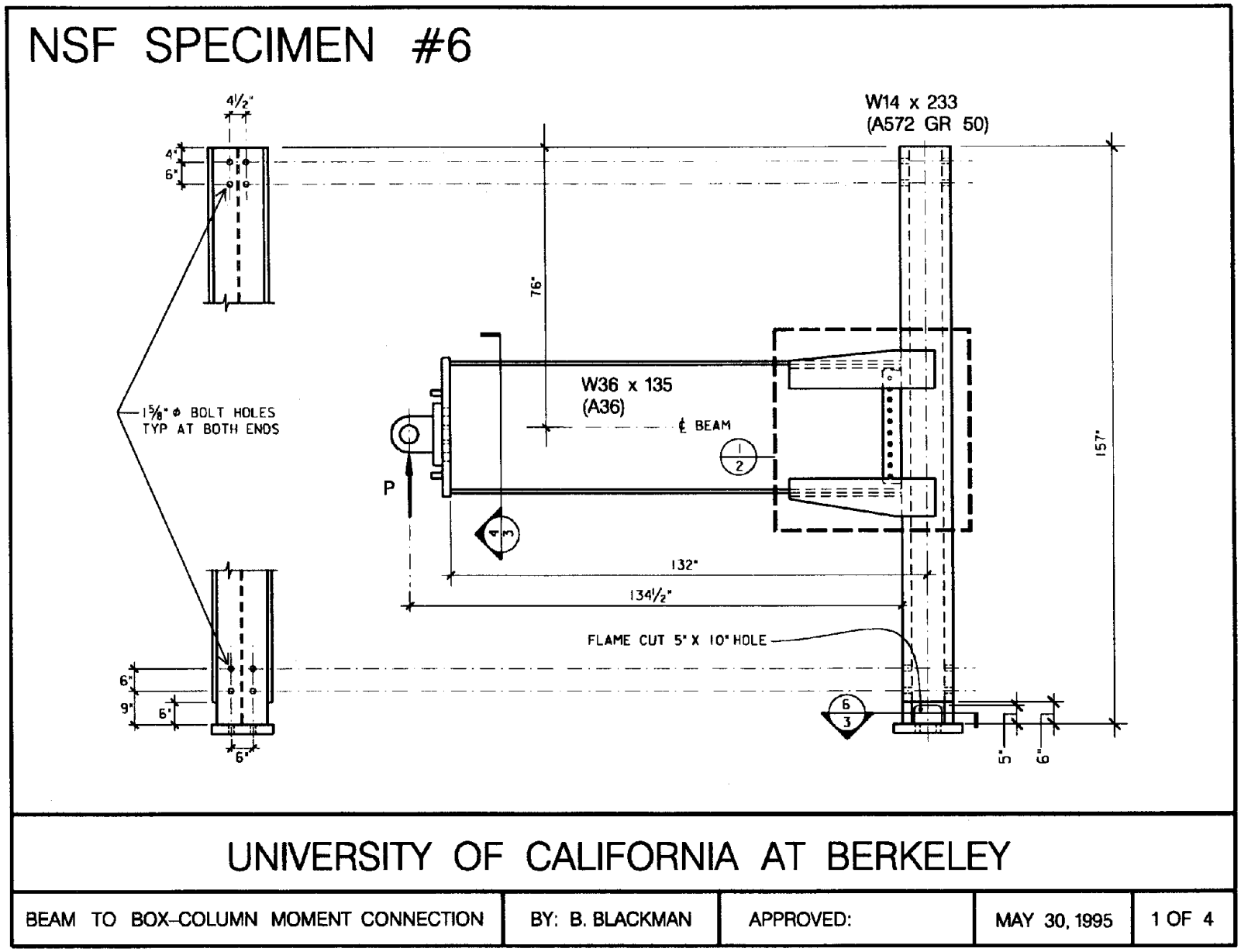

Figure 4-23. Beam-to-Box Column Connection with External Tee Stiffeners

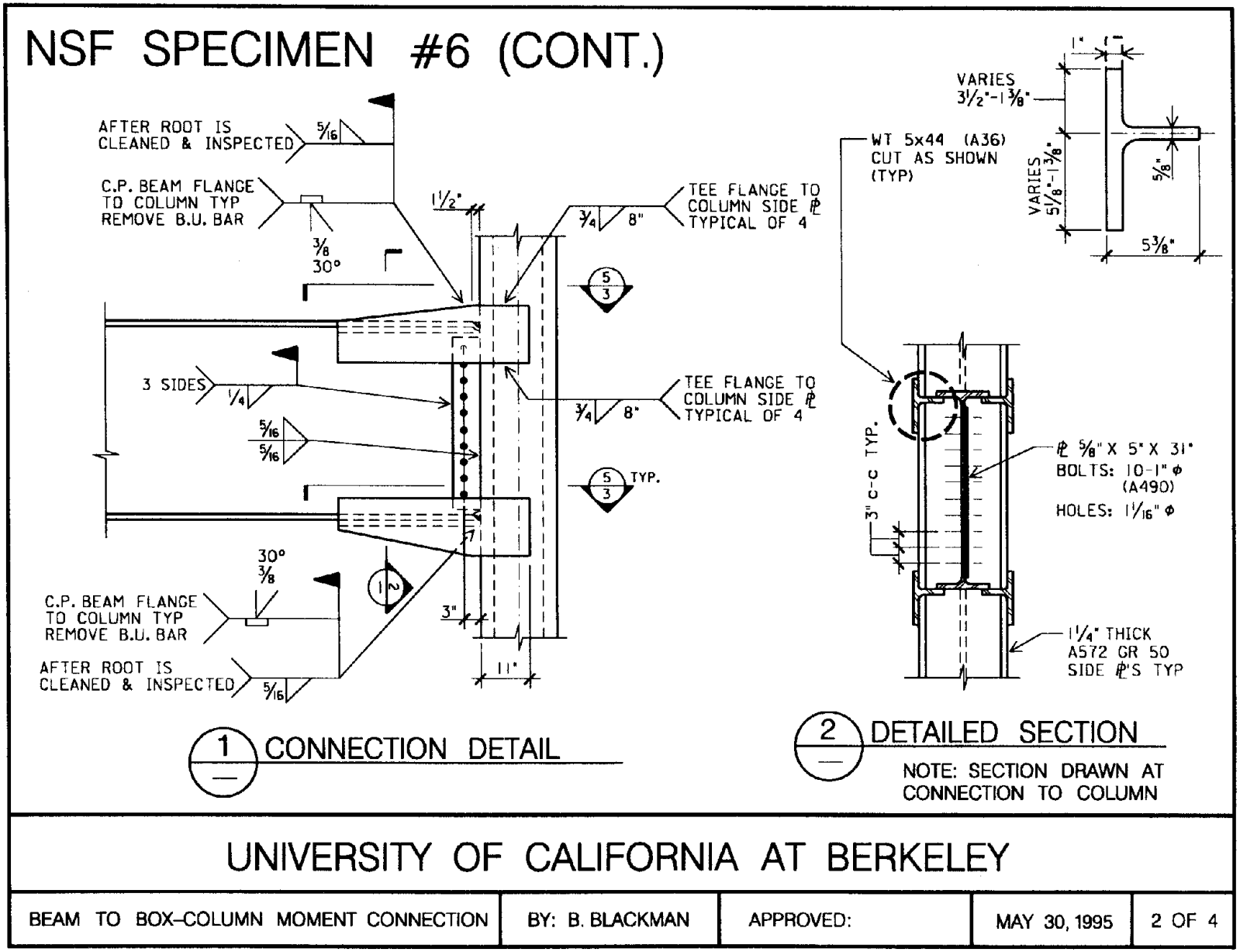

UNIVERSITY OF CALIFORNIA AT BERKELEY				
BEAM TO BOX-COLUMN MOMENT CONNECTION	BY: B. BLACKMAN	APPROVED:	MAY 30, 1995	2 OF 4

Figure 4-24. Beam-to-Box Column Connection Details

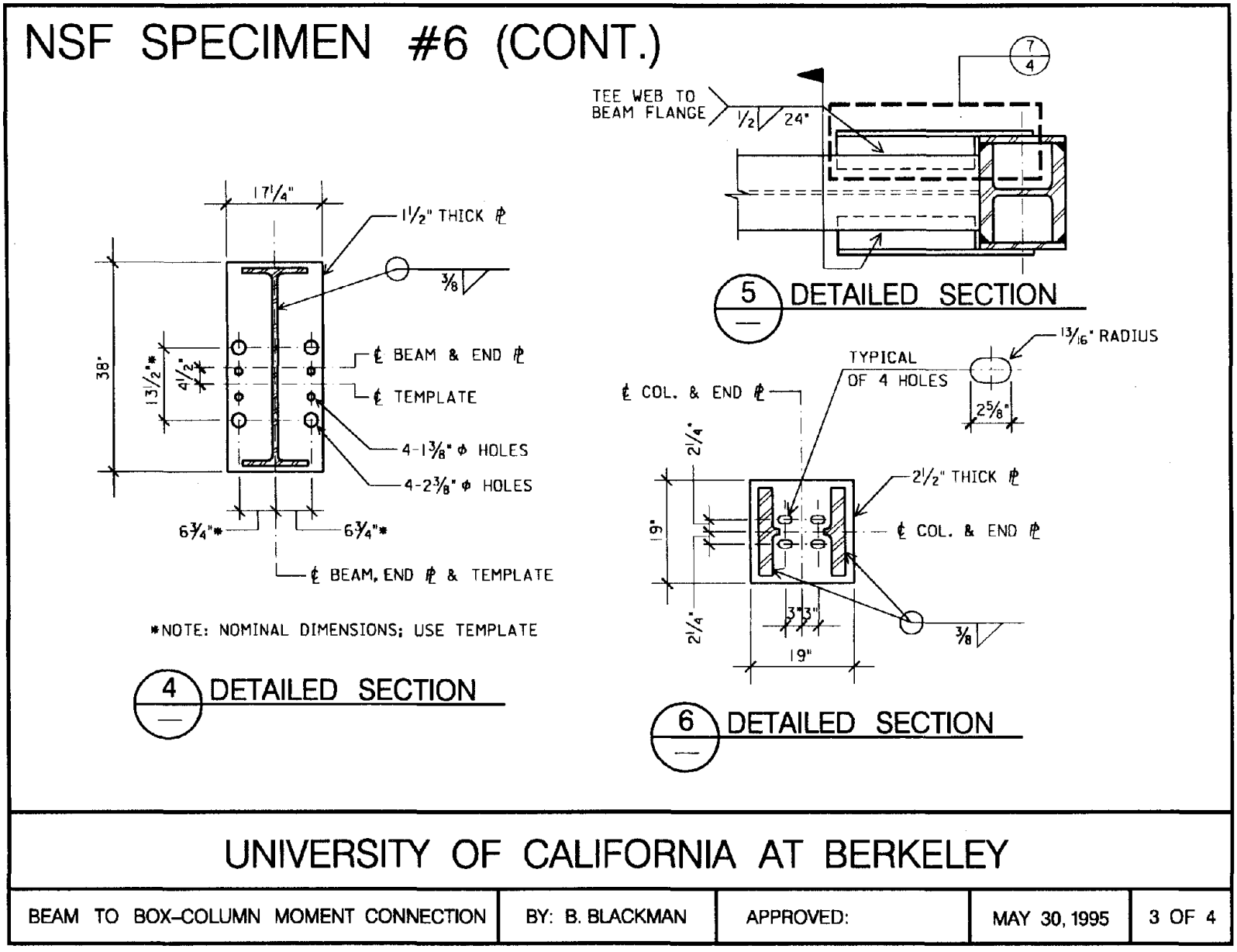

Figure 4-25. Beam-to-Box Column Detailed Sections

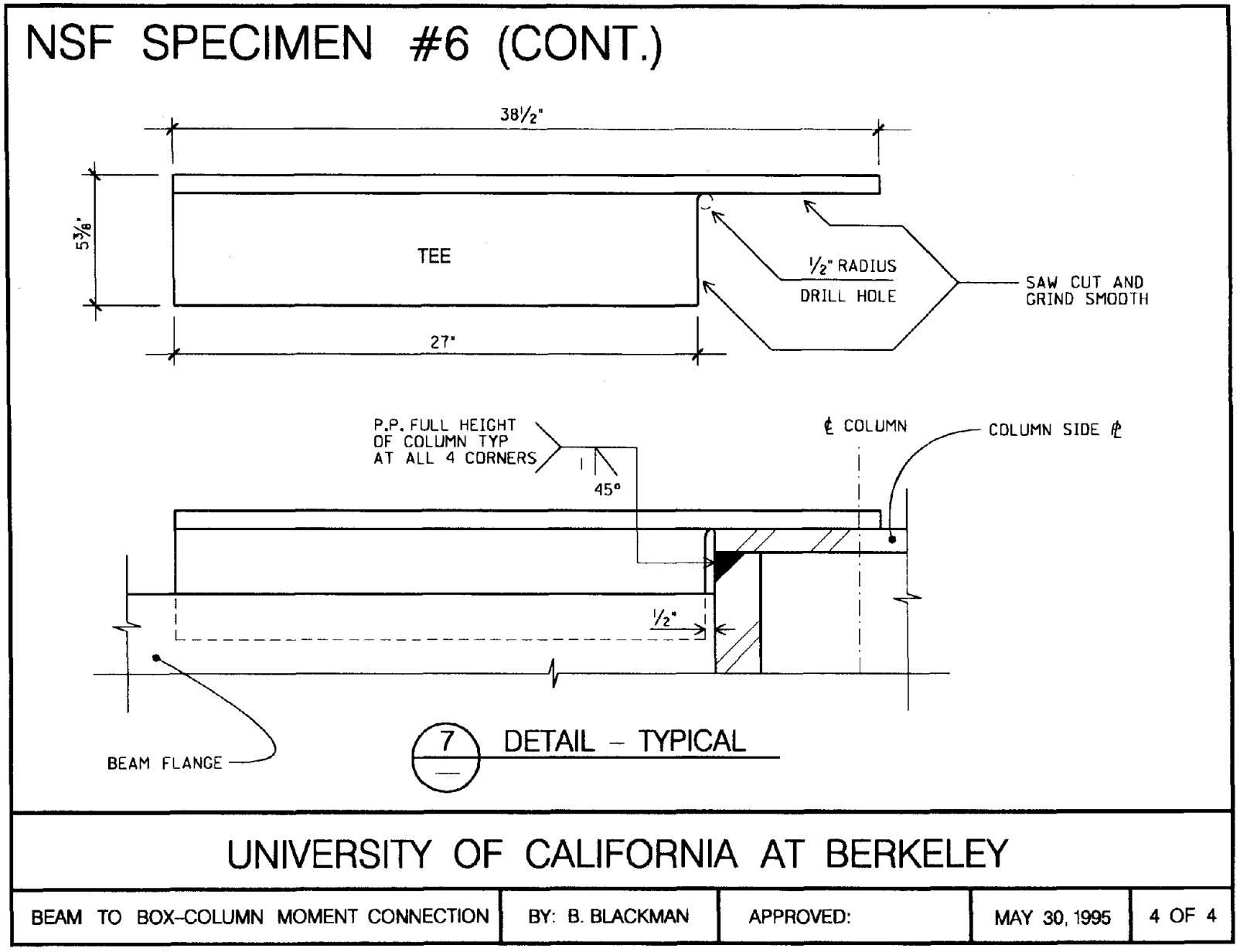

Figure 4-26. Beam-to-Box Column Tee and Weld Details

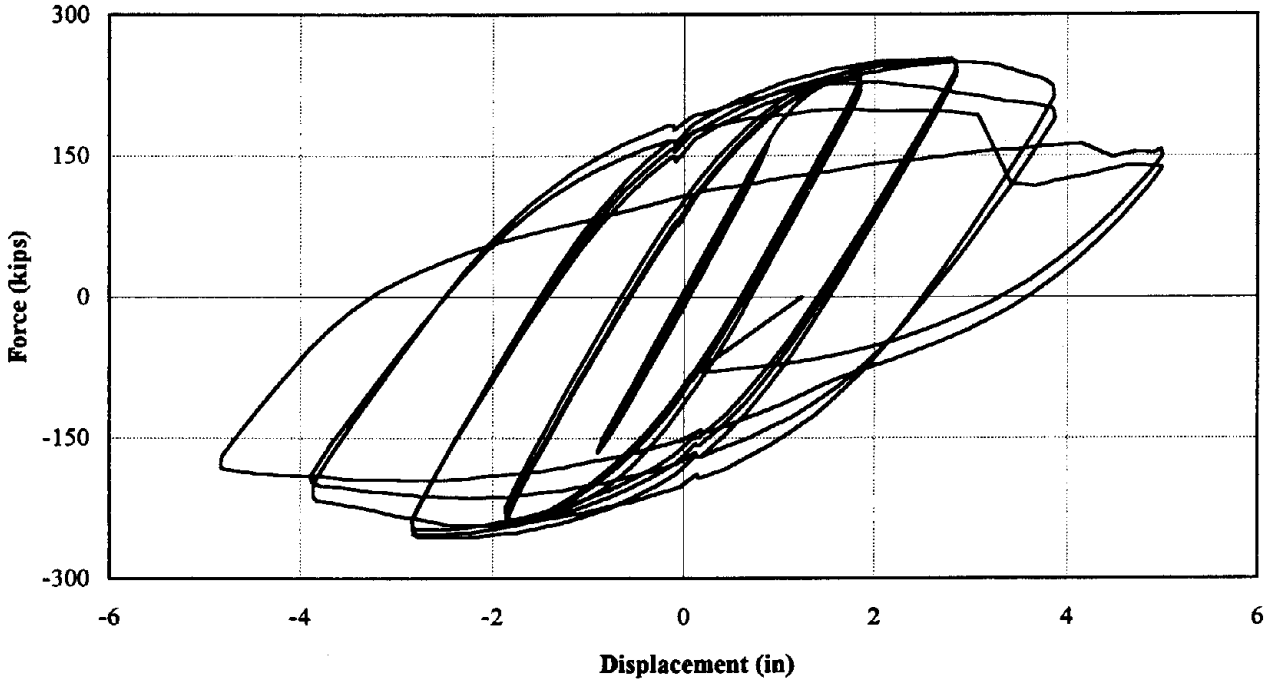

Figure 4-27. NSF #6 - Force vs. Displacement

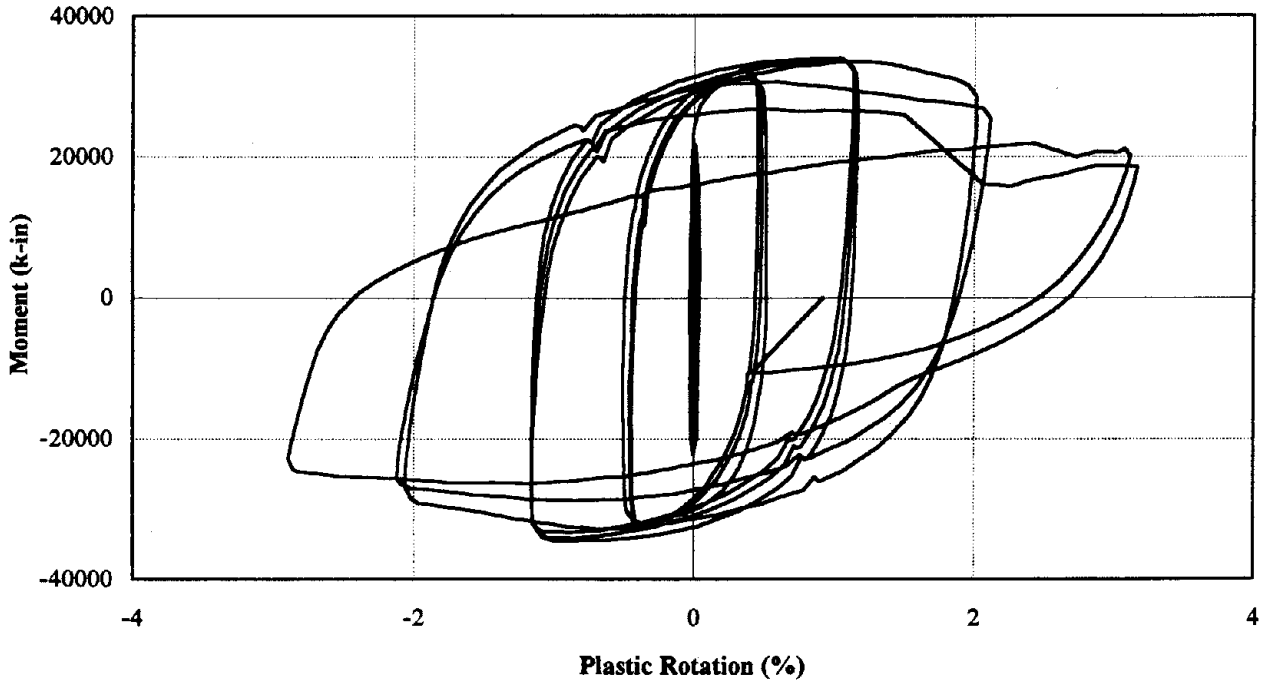

Figure 4-28. NSF #6 - Moment vs. Plastic Rotation

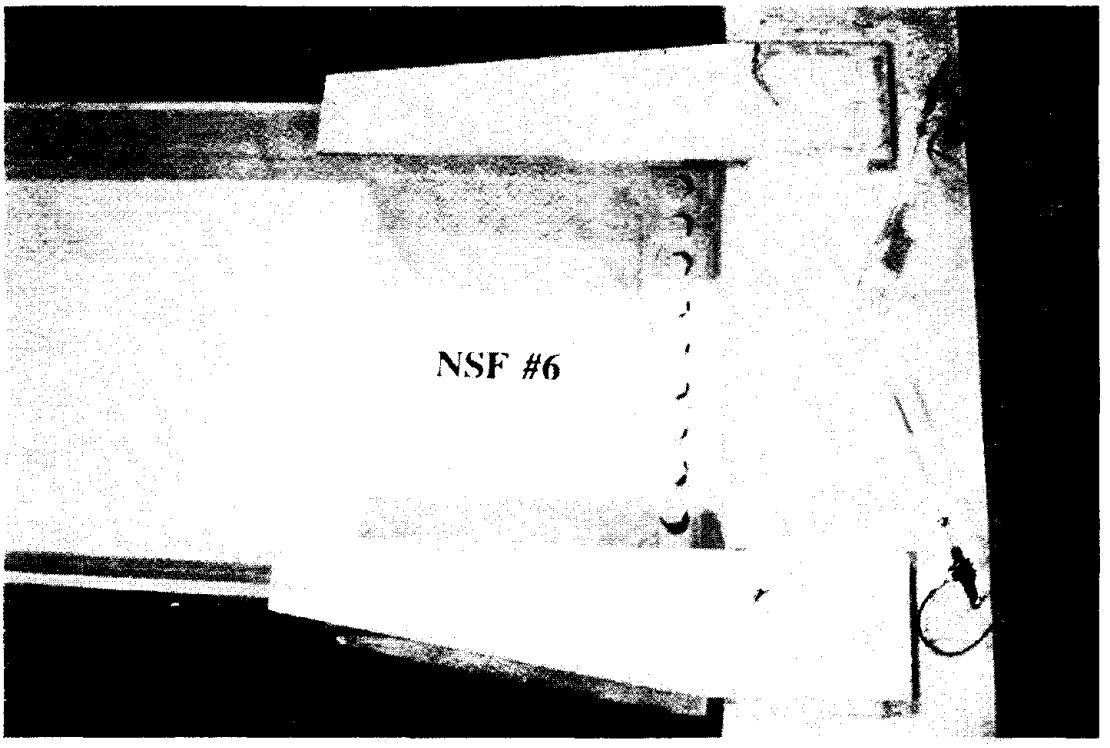

Figure 4-29. NSF Specimen #6 Joint prior to Test

Figure 4-30. NSF Specimen #6 Joint after Test

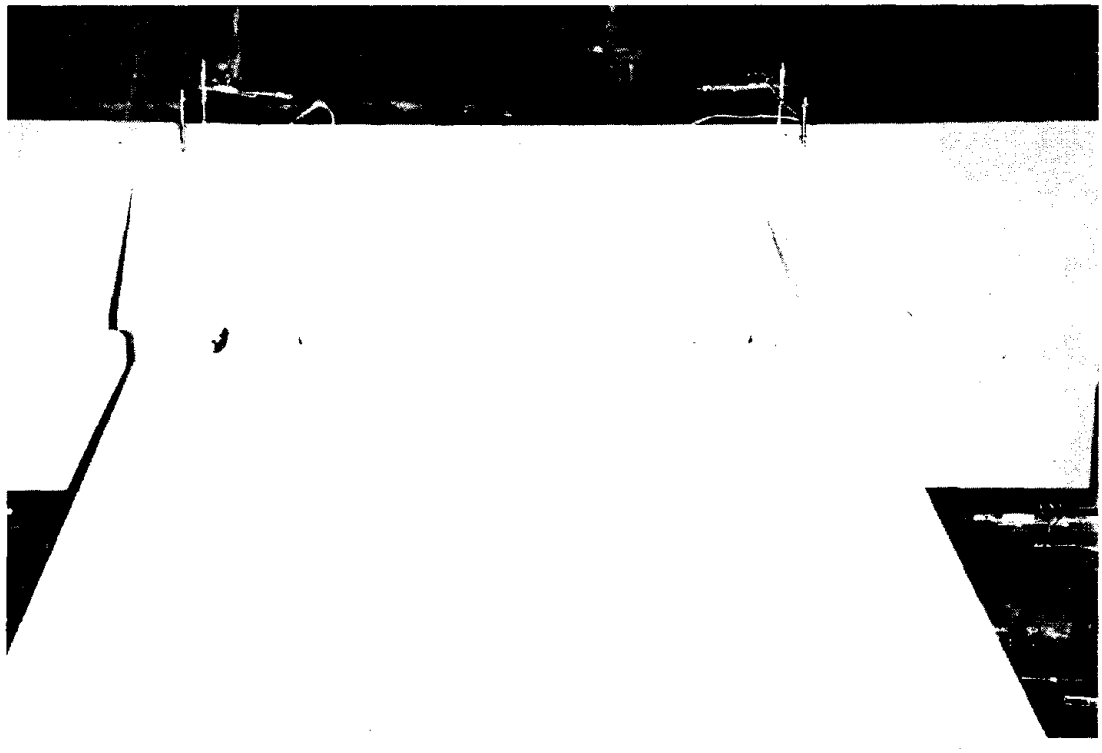

Figure 4-31. View of Joint from Actuator prior to Test

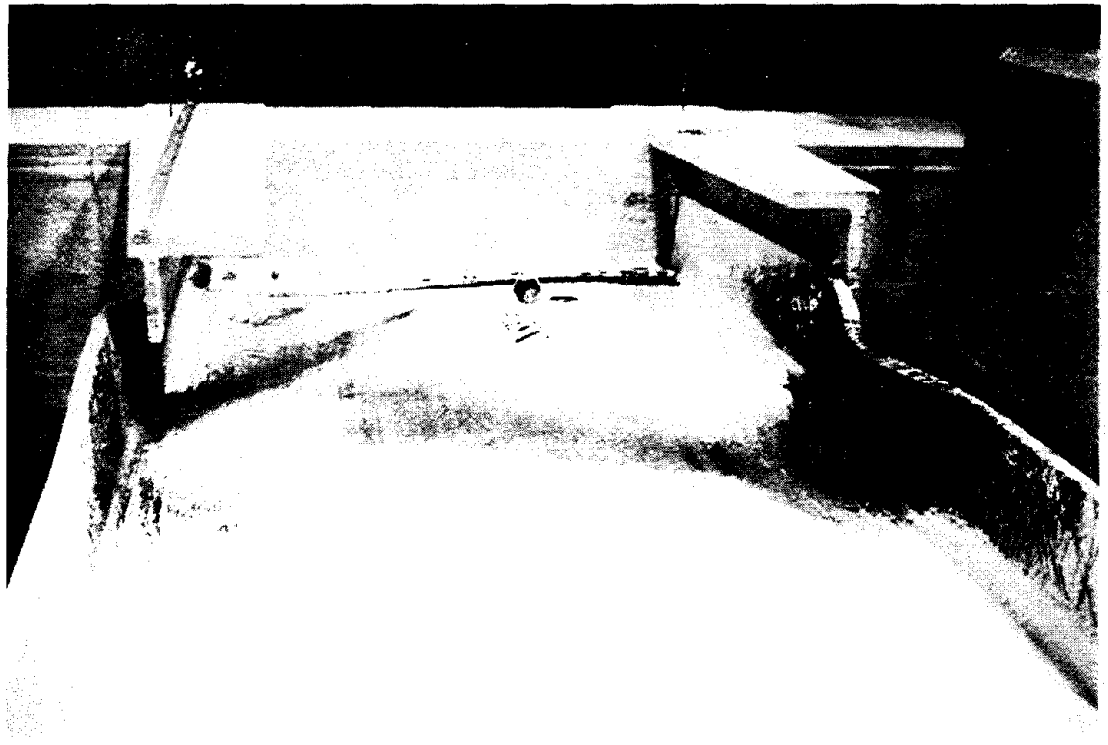

Figure 4-32. View of Joint from Actuator after Test

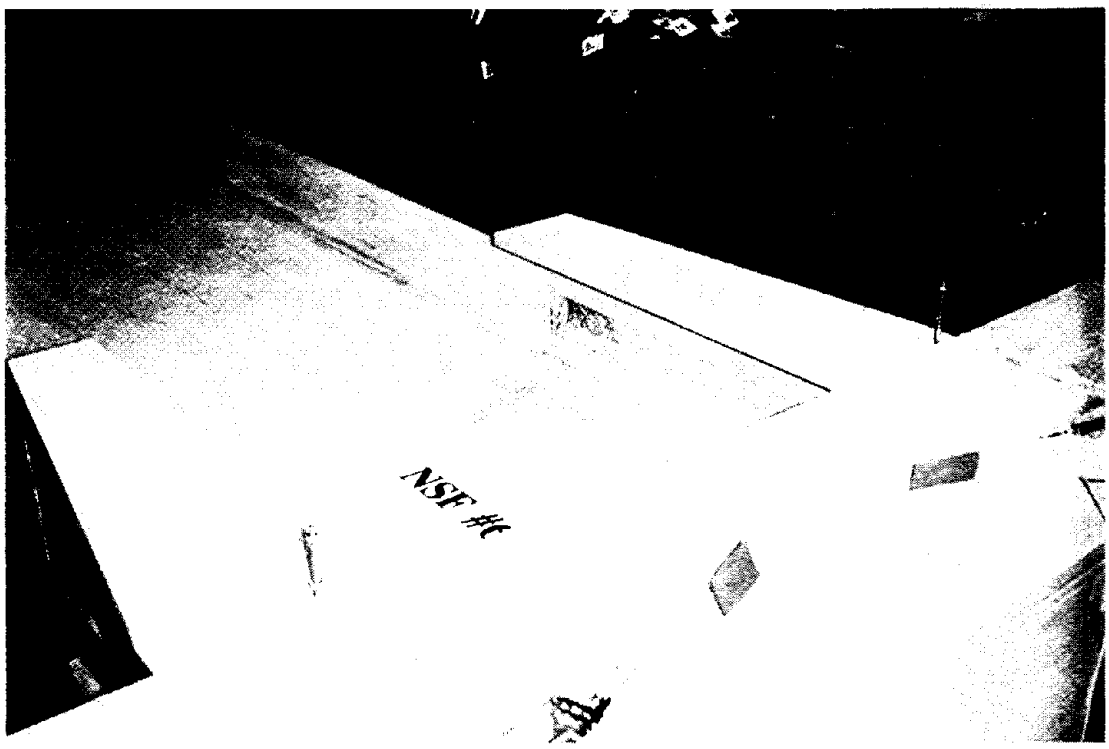

Figure 4-33. First Sign of Yielding in Beam Web Adjacent to Top Beam Flange at 2-in. Displacement, Cycle 1

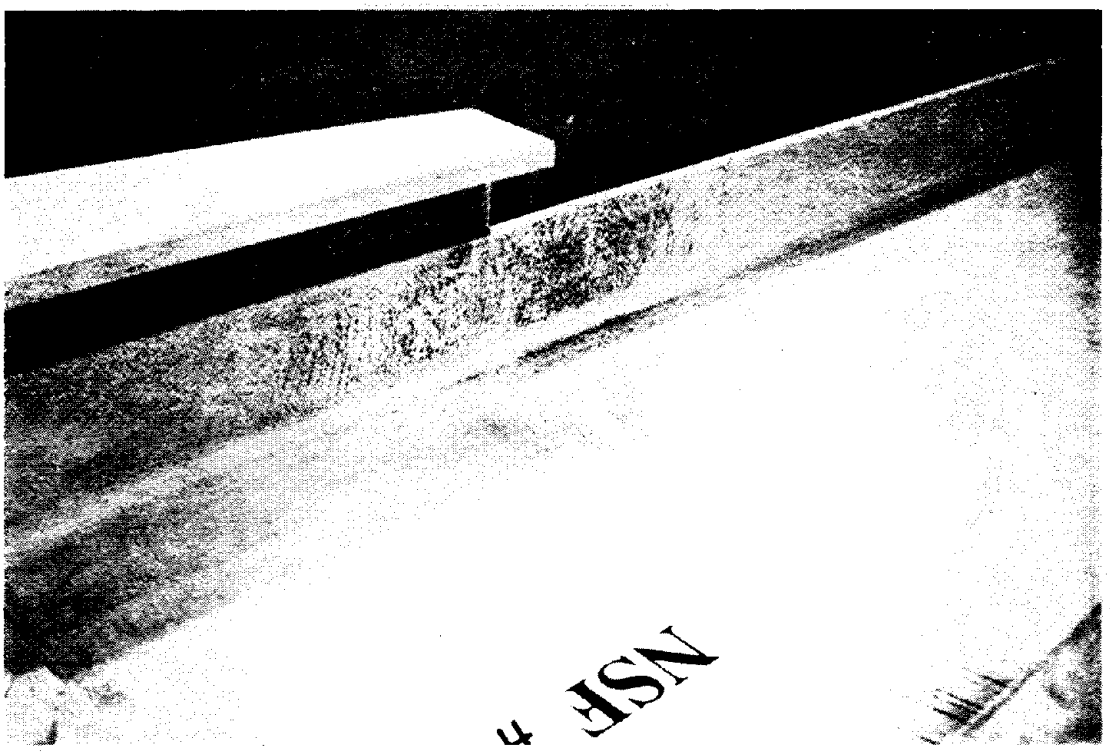

Figure 4-34. Yielding of Bottom Beam Flange and Web at 2-in. Displacement, Cycle 1

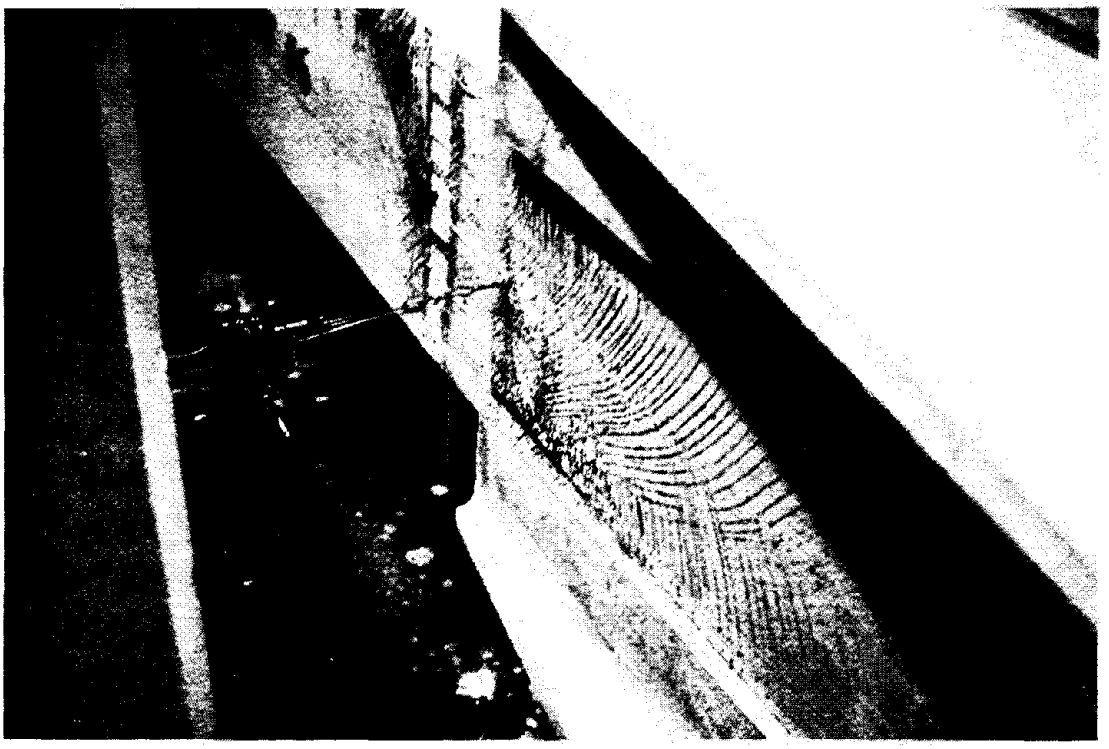

Figure 4-35. Yield Pattern of Bottom Beam Flange and Separation Between Beam Flange and Tee at 2-in. Displacement, Cycle 2 (caused by 3-in. long weld tear)

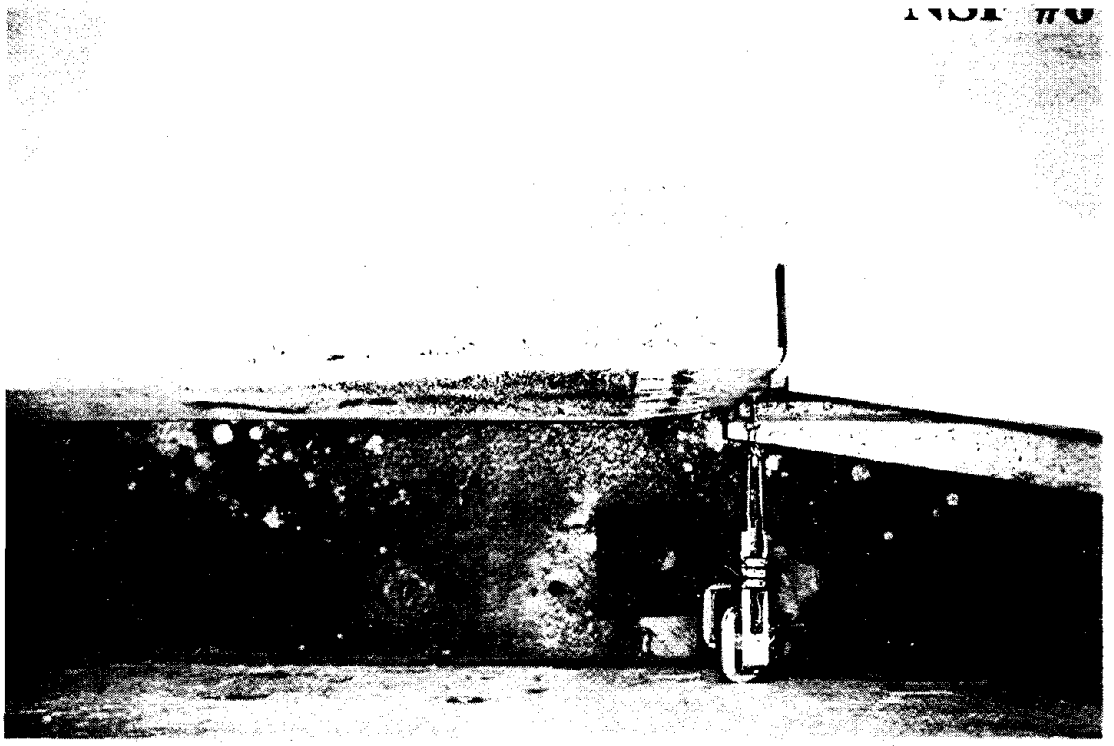

Figure 4-36. Buckling of Bottom Beam Flange and Web at 3-in. Displacement, Cycle 2

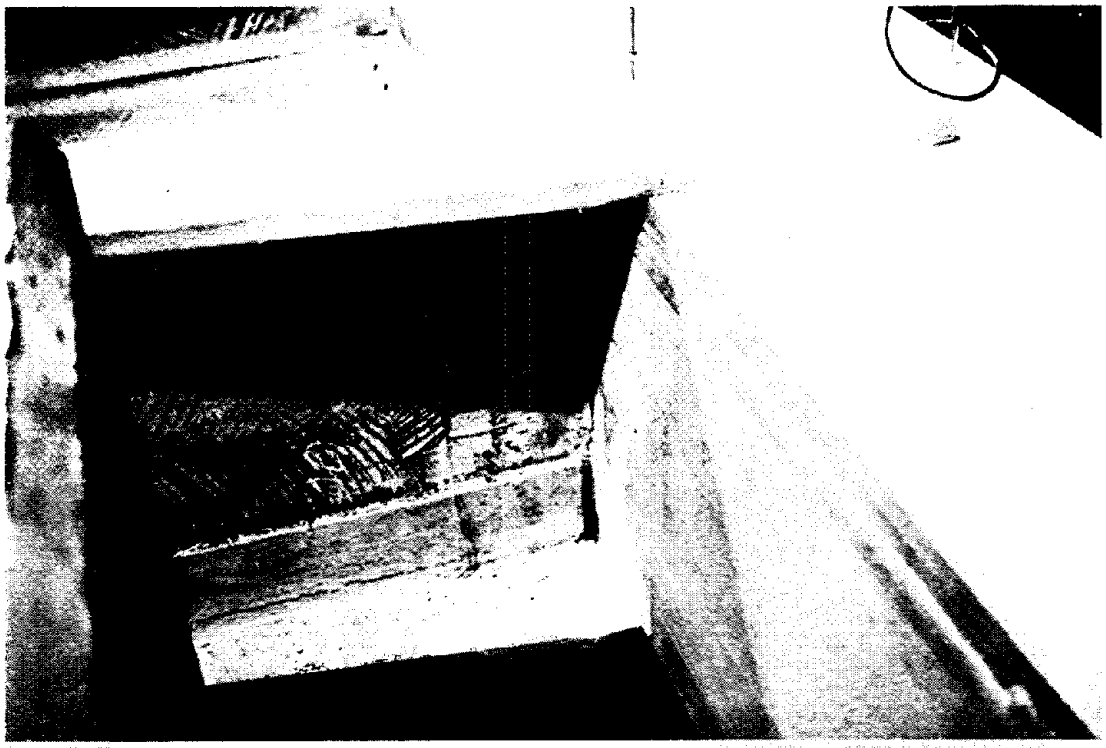

Figure 4-37. Propagation of Tee-to-Beam Flange Weld Tear (to length = 21 in.) and Subsequent Fracture Within the Column Flange Material (partial "divot") at 4-in. Displacement, Cycle 1

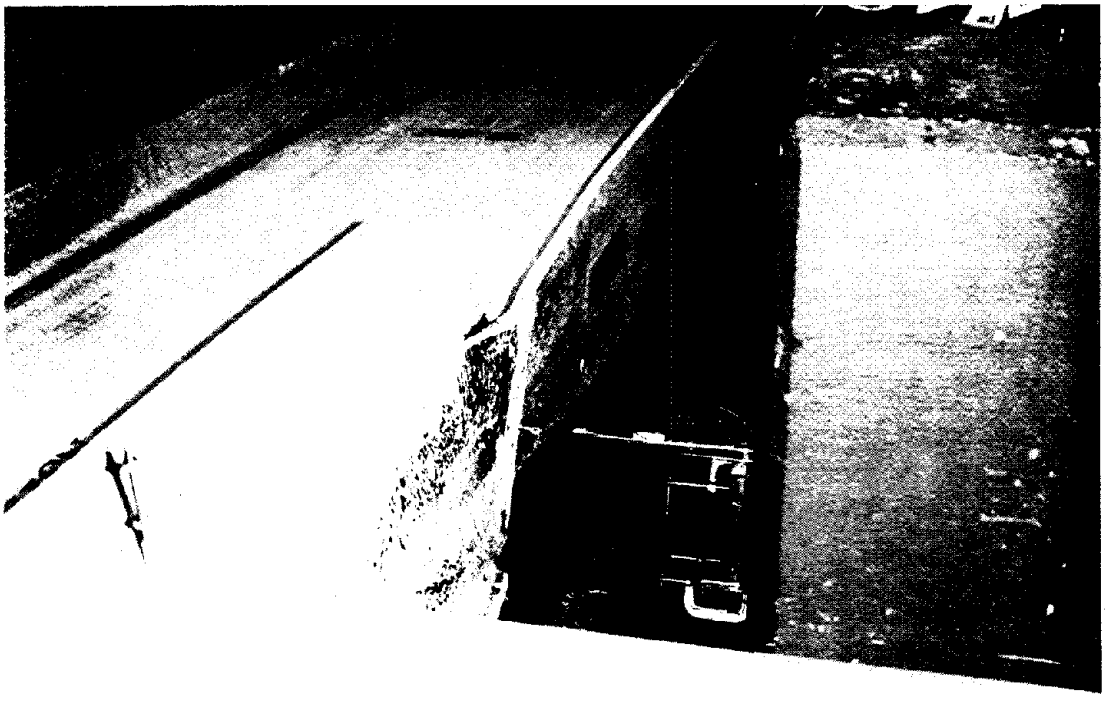

Figure 4-38. Yield Pattern and Buckling of Top Beam Flange and Subsequent Weld Tear at 4-in. Displacement, Cycle 1

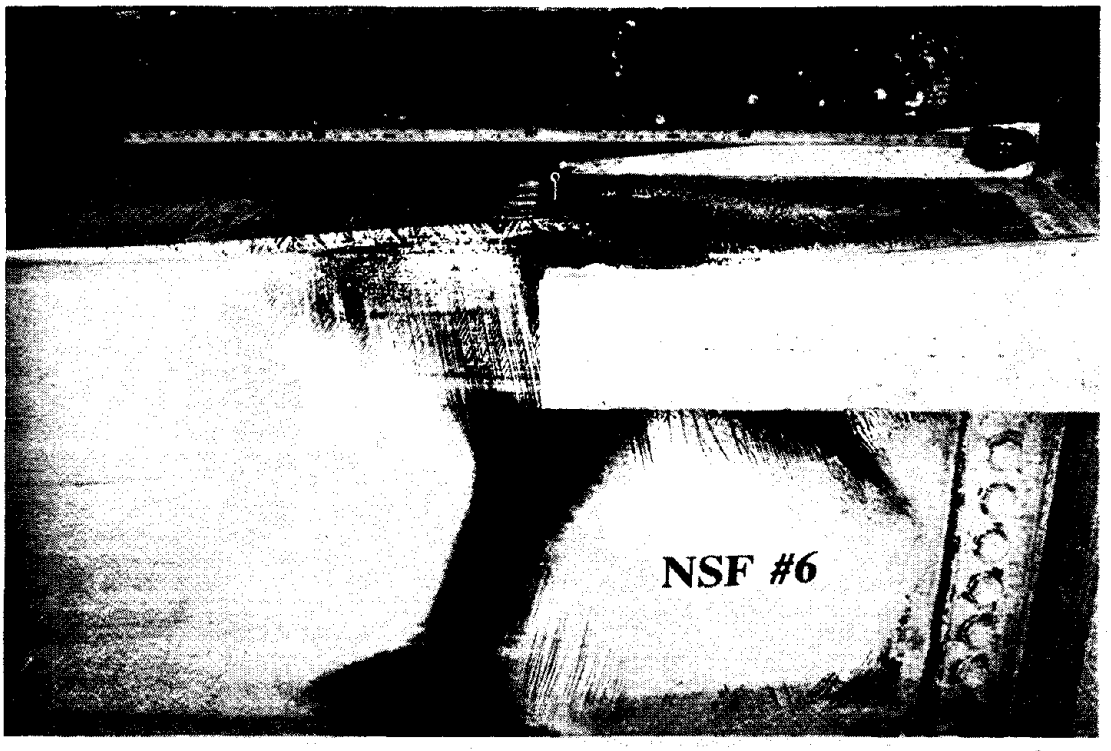

Figure 4-39. Yield Pattern over 4-ft. Length of Top Beam Flange at End of Test

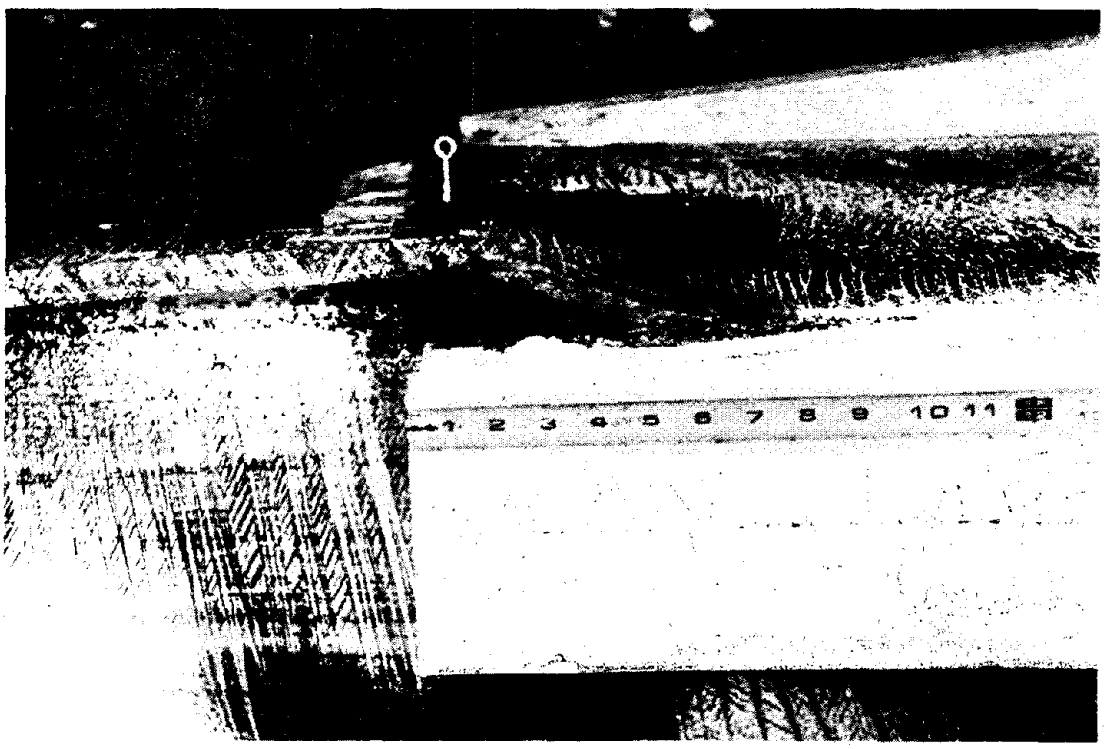

Figure 4-40. Weld Tear (7 in.) due to Buckling of Top Beam Flange Adjacent to Tee after Test

Figure 4-41. Yield Pattern and Buckling of Bottom Beam Flange after Test

Figure 4-42. Damage and Yield Pattern of Shear Tab and Adjacent Areas after Test

Figure 4-43. Complete Tear of Bottom Beam Flange-to-Tee Weld and "Divot" of Column Flange Material after Test

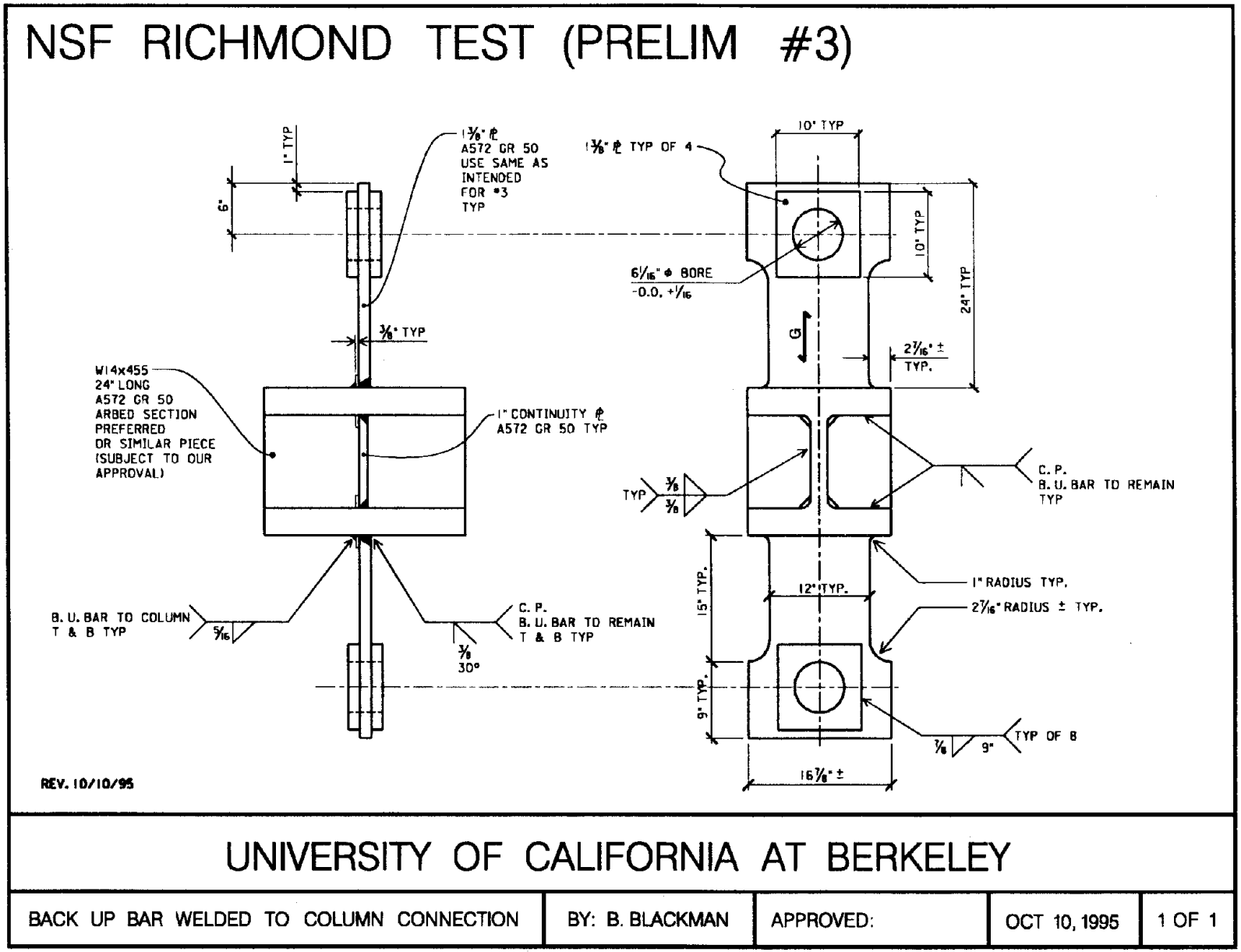

Figure 5-1. Backup Bar Welded to Column Testion Test Specimen

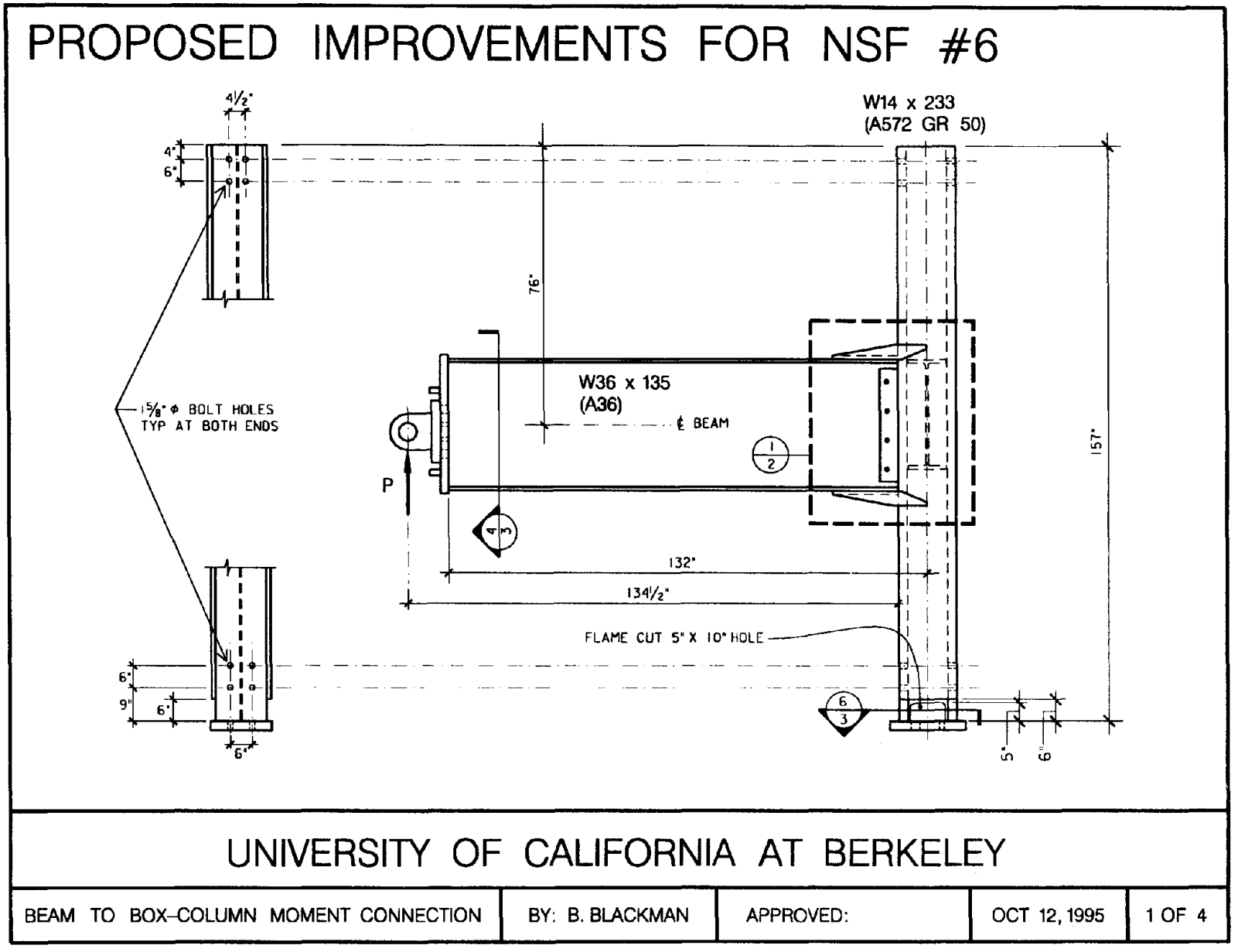

Figure 5-2. Beam-to-Box Column Connection with External Angle Stiffeners

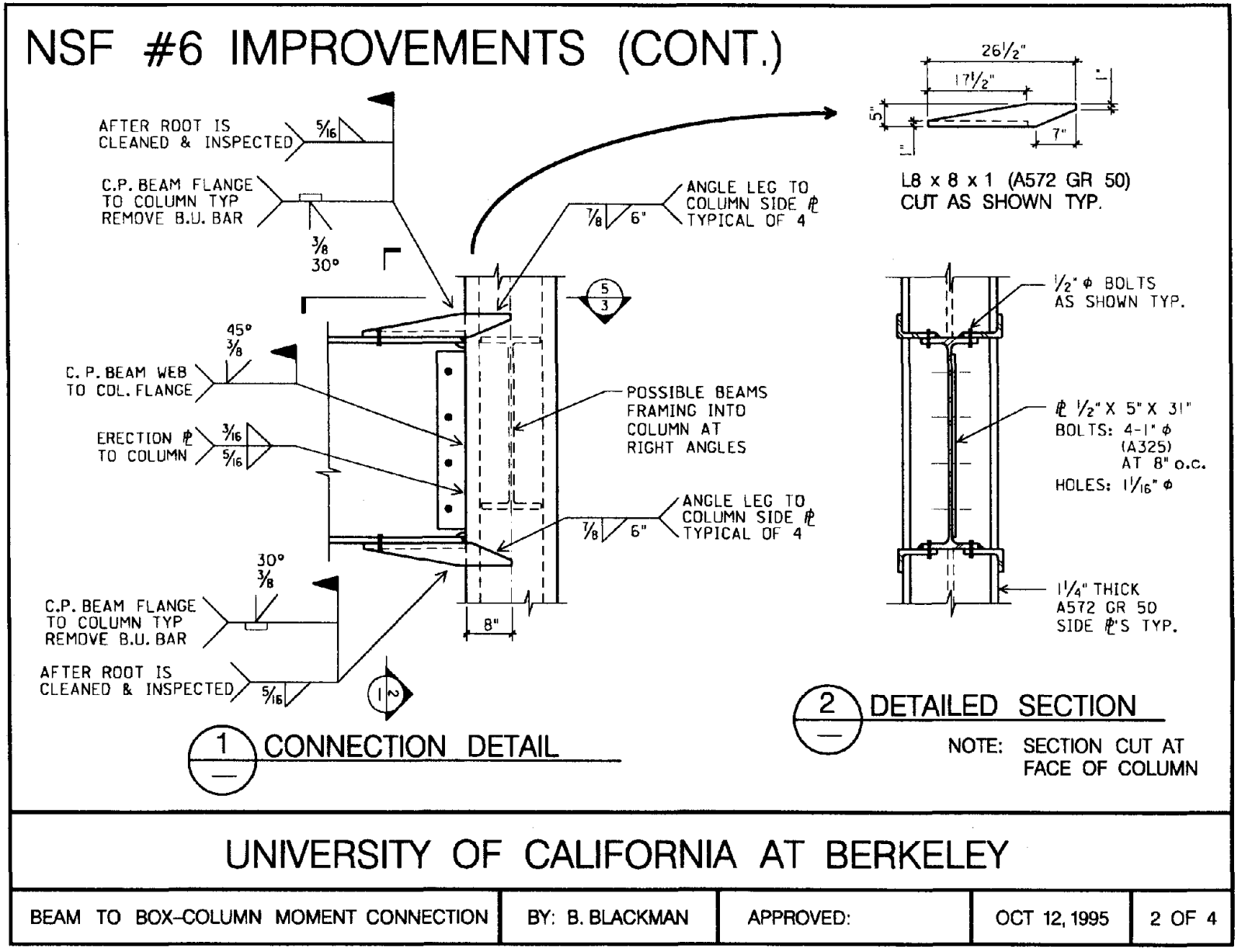

Figure 5-3. Beam-to-Box Column Connection Details

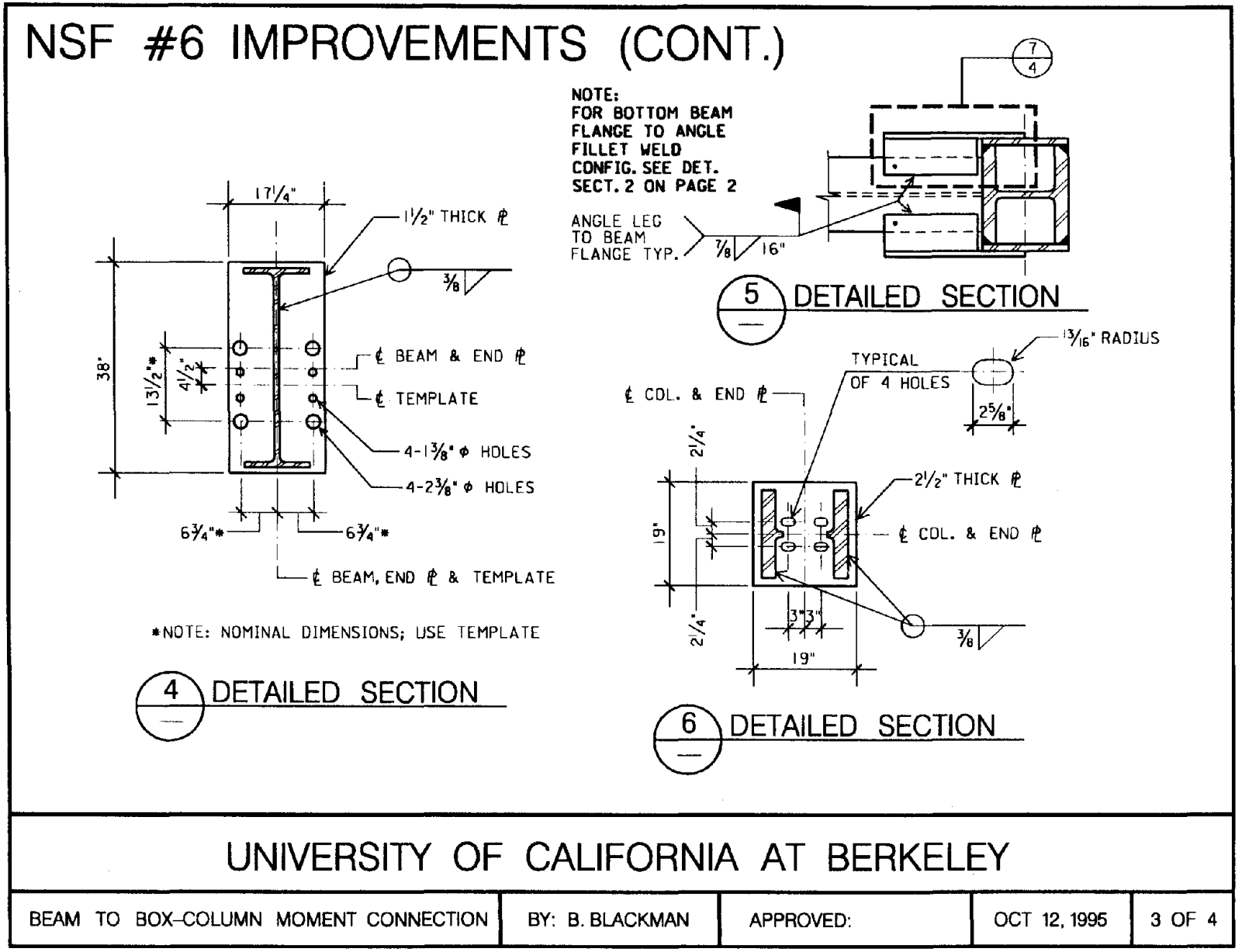

UNIVERSITY OF CALIFORNIA AT BERKELEY				
BEAM TO BOX-COLUMN MOMENT CONNECTION	BY: B. BLACKMAN	APPROVED:	OCT 12, 1995	3 OF 4

Figure 5-4. Beam-to-Box Column Detailed Sections

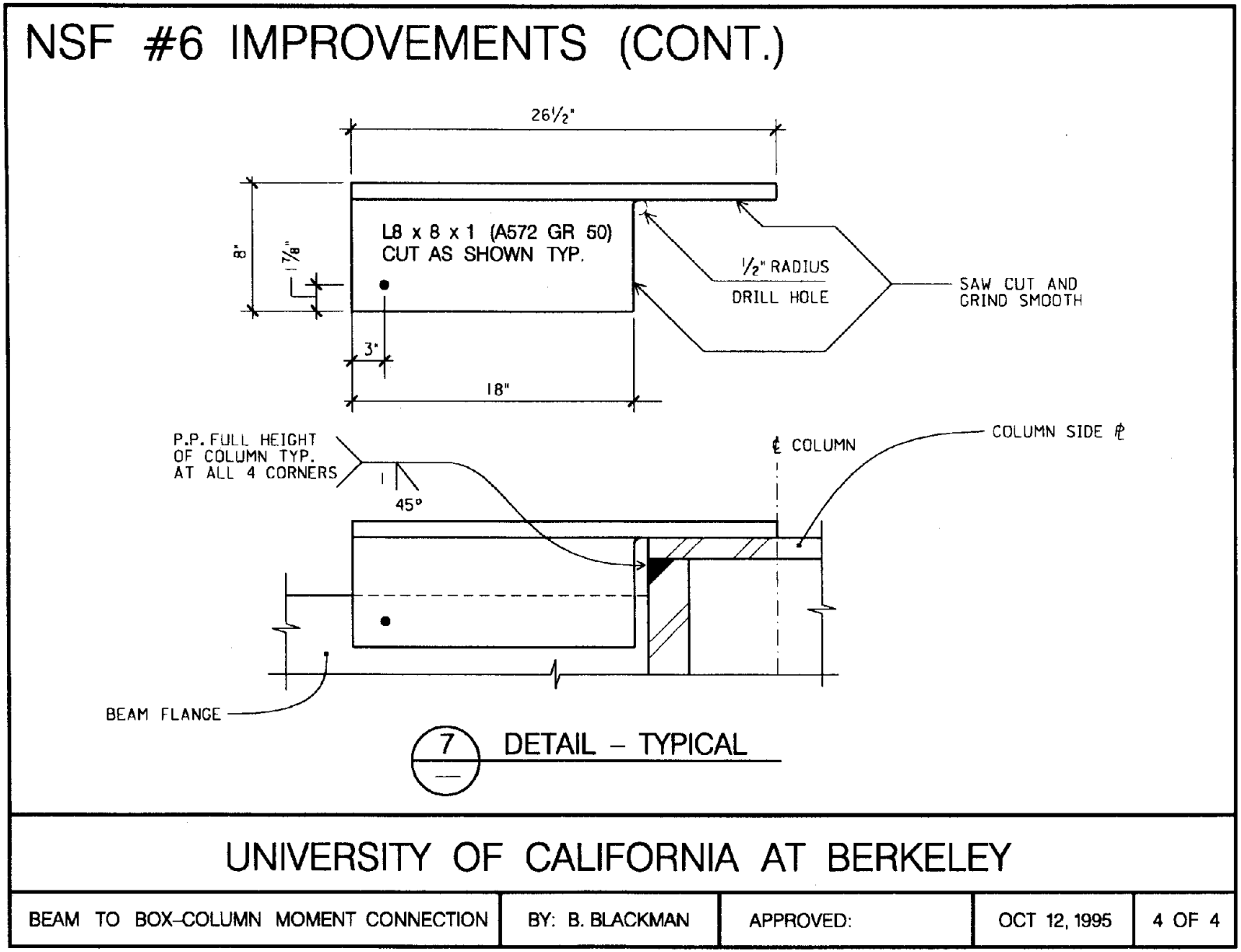

Figure 5-5. Beam-to-Box Column Angle and Weld Details

REFERENCES

[1] Structural Engineers Association of California, *Recommended Lateral Force Requirements and Commentary*, Seismology Committee, San Francisco, 1990.

[2] Anil K. Chopra, *Dynamics of Structures*, 1st ed., Prentice-Hall, Inc., 1995.

[3] International Conference of Building Officials, *Uniform Building Code*, Whittier, California, 1994.

[4] Roger M. Di Julio, Jr., "Static Lateral-Force Procedures," contained in: *The Seismic Design Handbook*, edited by Farzad Naeim, Van Nostrand Reinhold, New York, 1989.

[5] Robert E. Englekirk, "Design Implications Derived from the University of Texas, Austin, Test Program," *Northridge Steel Update 1*, AISC Publication, October, 1994.

[6] The British Broadcasting Corporation, "The City that Waits to Die," special program on San Francisco, 1979.

[7] Joseph Kendall Freitag, *Architectural Engineering with Special Reference to High Building Construction*, John Wiley and Sons, New York, 1895.

[8] Henry H. Quimby, "Wind Bracing in High Buildings," *Transactions of the American Society of Civil Engineers*, Vol. 36, 1892.

[9] Guy B. Waite, "Discussion on the Effect of Earthquake Shock," *Transactions of the American Society of Civil Engineers*, Vol. 61, 1908.

[10] R. S. Chew, "Effect of Earthquake Shock on High Buildings," *Transactions of the American Society of Civil Engineers*, Vol. 61, 1908.

[11] E. G. Walker, "Discussion on the Effect of Earthquake Shock," *Transactions of the American Society of Civil Engineers*, Vol. 61, 1908.

[12] International Conference of Building Officials, *Uniform Building Code*, Whittier, California, 1927.

[13] Carl W. Condit, *Rise of the Skyscraper*, Chicago, 1952.

[14] Carl W. Condit, *American Building, Materials and Techniques from the Beginning of the Colonial Settlements to the Present*, Chicago, 1968.

[15] Stephen Tobriner, first draft of: *Fate of the Phoenix, A History of Safety and Reconstruction after Earthquakes and Fires in San Francisco 1849-1915*, University of California at Berkeley, 1995.

[16] F. Robert Preece and Alvaro L. Collin, "Structural Steel Construction in the '90s," *Steel Tips*, Structural Steel Education Council, 1993.

[17] Charles G. Salmon and John E. Johnson, *Steel Structures, Design and Behavior*, Third Edition, New York, 1990.

[18] E. P. Popov and R. M. Stephen, "Cyclic Loading of Full-Scale Steel Connections," *Report No. UCB/EERC-70/03*, Earthquake Engineering Research Center, University of California, Berkeley, 1970.

[19] H. Krawinkler, V. V. Bertero, and E. P. Popov, "Inelastic Behavior of Steel Beam-to-Column Subassemblages," *Report No. UCB/EERC-71/07*, Earthquake Engineering Research Center, University of California, Berkeley, 1971.

[20] V. V. Bertero, E. P. Popov, and H. Krawinkler, "Further Studies on Seismic Behavior of Steel Beam-Column Subassemblages," *Report No. UCB/EERC-73/27*, Earthquake Engineering Research Center, University of California, Berkeley, 1973.

[21] J. E. Rogec, J. S. Huang, and W. F. Chen, "Test of a Fully-Welded Beam-to-Column Connection," *Publication No. 188*, Welding Research Council, 1973.

[22] E. P. Popov, "Seismic Moment Connections for Moment-Resisting Steel Frames," *Report No. UCB/EERC-83/02*, Earthquake Engineering Research Center, University of California, Berkeley, 1983.

[23] K. C. Tsai, "Steel Beam-Column Joints in Seismic Moment Resisting Frames," Ph.D. Dissertation, Department of Civil Engineering, University of California, Berkeley, 1988.

[24] Thomas A. Sabol and Michael D. Engelhardt, "Steel Moment Resisting Frame Connection Details and Geometry," *Invitational Workshop on Steel Seismic Issues*, Session 5, September 9, 1994.

[25] Michael D. Engelhardt and Thomas A. Sabol, Research Progress Report, "Testing of Welded Steel Moment Connections in Response to the Northridge Earthquake," *Northridge Steel Update I*, American Institute of Steel Construction, October 1, 1994.

[26] Alvarado L. Collin, "SAC Joint Venture Workshop Meeting No. 3 Summary and Commentary," December 2, 1994, reproduced in: *Steel Moment Frame Connection Advisory No. 3*, SAC Joint Venture, February 1, 1995.

[27] California Department of State Architects, "Interpretation of Regulations (Title 24, CCR)," *DSA/OSHPD Emergency Code Change for Steel Moment Frame Girder-to-Column Connection*, January, 1995, reproduced in: *Steel Moment Frame Connection Advisory No. 3*, SAC Joint Venture, February 1, 1995.

[28] T-S. Yang, "Experimental and Analytical Studies of Steel Connections and Energy Dissipators," Ph.D. Dissertation, Department of Civil Engineering, University of California, Berkeley, 1995.

[29] E. P. Popov and R. M. Stephen, "Cyclic Loading of Full-Size Steel Connections," *Bulletin No. 21, Steel Research for Construction*, American Iron and Steel Institute, New York, February, 1972.

[30] M. M. Frocht, "Factors of Stress Concentration Photoelastically Determined," *Transactions, ASME*, vol. 75, 1935.

[31] L-C. Ting, N. E. Shanmugam, and S-L. Lee, "Design of I-Beam to Box-Column Connections Stiffened Externally," *Engineering Journal / American Institute of Steel Construction*, Fourth Quarter, 1993.

[32] N. E. Shanmugam and L-C. Ting, "Welded Interior I-Beam to Box-Column Connections," *ASCE Journal of Structural Engineering*, vol. 121, no. 5, May, 1995.

[33] Mark Jokerst, "Lawrence Berkeley National Laboratory, Steel Joint Test," a technical brief available from Forell/Elsesser Engineers, 160 Pine Street #600, San Francisco, CA 94111, July 20, 1995.

[34] Y-S. Yang and E. P. Popov, "Behavior of Pre-Northridge Moment Resisting Steel Connections," *Report No. UCB/EERC-95/08*, Earthquake Engineering Research Center, University of California, Berkeley, 1995.

EARTHQUAKE ENGINEERING RESEARCH CENTER REPORT SERIES

EERC reports are available from the National Information Service for Earthquake Engineering (NISEE) and from the National Technical Information Service (NTIS). Numbers in parentheses are Accession Numbers assigned by the National Technical Information Service; these are followed by a price code. Contact NTIS, 5285 Port Royal Road, Springfield Virginia, 22161 for more information. Reports without Accession Numbers were not available from NTIS at the time of printing. For a current complete list of EERC reports (from EERC 67-1) and availablity information, please contact University of California, EERC, NISEE, 1301 South 46th Street, Richmond, California 94804-4698.

UCB/EERC-84/01 "Pseudodynamic Test Method for Seismic Performance Evaluation: Theory and Implementation," by Shing, P.-S.B. and Mahin, S.A., January 1984, (PB84 190 644)A08.

UCB/EERC-84/02 "Dynamic Response Behavior of Kiang Hong Dian Dam," by Clough, R.W., Chang, K.-T., Chen, H.-Q. and Stephen, R.M., April 1984, (PB84 209 402)A08.

UCB/EERC-84/03 "Refined Modelling of Reinforced Concrete Columns for Seismic Analysis," by Kaba, S.A. and Mahin, S.A., April 1984, (PB84 234 384)A06.

UCB/EERC-84/04 "A New Floor Response Spectrum Method for Seismic Analysis of Multiply Supported Secondary Systems," by Asfura, A. and Der Kiureghian, A., June 1984, (PB84 239 417)A06.

UCB/EERC-84/05 "Earthquake Simulation Tests and Associated Studies of a 1/5th-scale Model of a 7-Story R/C Frame-Wall Test Structure," by Bertero, V.V., Aktan, A.E., Charney, F.A. and Sause, R., June 1984, (PB84 239 409)A09.

UCB/EERC-84/06 "Unassigned," by Unassigned, 1984.

UCB/EERC-84/07 "Behavior of Interior and Exterior Flat-Plate Connections Subjected to Inelastic Load Reversals," by Zee, H.L. and Moehle, J.P., August 1984, (PB86 117 629/AS)A07.

UCB/EERC-84/08 "Experimental Study of the Seismic Behavior of a Two-Story Flat-Plate Structure," by Moehle, J.P. and Diebold, J.W., August 1984, (PB86 122 553/AS)A12.

UCB/EERC-84/09 "Phenomenological Modeling of Steel Braces under Cyclic Loading," by Ikeda, K., Mahin, S.A. and Dermitzakis, S.N., May 1984, (PB86 132 198/AS)A08.

UCB/EERC-84/10 "Earthquake Analysis and Response of Concrete Gravity Dams," by Fenves, G.L. and Chopra, A.K., August 1984, (PB85 193 902/AS)A11.

UCB/EERC-84/11 "EAGD-84: A Computer Program for Earthquake Analysis of Concrete Gravity Dams," by Fenves, G.L. and Chopra, A.K., August 1984, (PB85 193 613/AS)A05.

UCB/EERC-84/12 "A Refined Physical Theory Model for Predicting the Seismic Behavior of Braced Steel Frames," by Ikeda, K. and Mahin, S.A., July 1984, (PB85 191 450/AS)A09.

UCB/EERC-84/13 "Earthquake Engineering Research at Berkeley - 1984," by EERC, August 1984, (PB85 197 341/AS)A10.

UCB/EERC-84/14 "Moduli and Damping Factors for Dynamic Analyses of Cohesionless Soils," by Seed, H.B., Wong, R.T., Idriss, I.M. and Tokimatsu, K., September 1984, (PB85 191 468/AS)A04.

UCB/EERC-84/15 "The Influence of SPT Procedures in Soil Liquefaction Resistance Evaluations," by Seed, H.B., Tokimatsu, K., Harder, L.F. and Chung, R.M., October 1984, (PB85 191 732/AS)A04.

UCB/EERC-84/16 "Simplified Procedures for the Evaluation of Settlements in Sands Due to Earthquake Shaking," by Tokimatsu, K. and Seed, H.B., October 1984, (PB85 197 887/AS)A03.

UCB/EERC-84/17 "Evaluation of Energy Absorption Characteristics of Highway Bridges Under Seismic Conditions - Volume I (PB90 262 627)A16 and Volume II (Appendices) (PB90 262 635)A13," by Imbsen, R.A. and Penzien, J., September 1986.

UCB/EERC-84/18 "Structure-Foundation Interactions under Dynamic Loads," by Liu, W.D. and Penzien, J., November 1984, (PB87 124 889/AS)A11.

UCB/EERC-84/19 "Seismic Modelling of Deep Foundations," by Chen, C.-H. and Penzien, J., November 1984, (PB87 124 798/AS)A07.

UCB/EERC-84/20 "Dynamic Response Behavior of Quan Shui Dam," by Clough, R.W., Chang, K.-T., Chen, H.-Q., Stephen, R.M., Ghanaat, Y. and Qi, J.-H., November 1984, (PB86 115177/AS)A07.

UCB/EERC-85/01 "Simplified Methods of Analysis for Earthquake Resistant Design of Buildings," by Cruz, E.F. and Chopra, A.K., February 1985, (PB86 112299/AS)A12.

UCB/EERC-85/02 "Estimation of Seismic Wave Coherency and Rupture Velocity using the SMART 1 Strong-Motion Array Recordings," by Abrahamson, N.A., March 1985, (PB86 214 343)A07.

UCB/EERC-85/03 "Dynamic Properties of a Thirty Story Condominium Tower Building," by Stephen, R.M., Wilson, E.L. and Stander, N., April 1985, (PB86 118965/AS)A06.

UCB/EERC-85/04 "Development of Substructuring Techniques for On-Line Computer Controlled Seismic Performance Testing," by Dermitzakis, S. and Mahin, S., February 1985, (PB86 132941/AS)A08.

UCB/EERC-85/05 "A Simple Model for Reinforcing Bar Anchorages under Cyclic Excitations," by Filippou, F.C., March 1985, (PB86 112 919/AS)A05.

UCB/EERC-85/06 "Racking Behavior of Wood-framed Gypsum Panels under Dynamic Load," by Oliva, M.G., June 1985, (PB90 262 643)A04.

UCB/EERC-85/07 "Earthquake Analysis and Response of Concrete Arch Dams," by Fok, K.-L. and Chopra, A.K., June 1985, (PB86 139672/AS)A10.

UCB/EERC-85/08 "Effect of Inelastic Behavior on the Analysis and Design of Earthquake Resistant Structures," by Lin, J.P. and Mahin, S.A., June 1985, (PB86 135340/AS)A08.

UCB/EERC-85/09 "Earthquake Simulator Testing of a Base-Isolated Bridge Deck," by Kelly, J.M., Buckle, I.G. and Tsai, H.-C., January 1986, (PB87 124 152/AS)A06.

UCB/EERC-85/10 "Simplified Analysis for Earthquake Resistant Design of Concrete Gravity Dams," by Fenves, G.L. and Chopra, A.K., June 1986, (PB87 124 160/AS)A08.

UCB/EERC-85/11 "Dynamic Interaction Effects in Arch Dams," by Clough, R.W., Chang, K.-T., Chen, H.-Q. and Ghanaat, Y., October 1985, (PB86 135027/AS)A05.

UCB/EERC-85/12 "Dynamic Response of Long Valley Dam in the Mammoth Lake Earthquake Series of May 25-27, 1980," by Lai, S. and Seed, H.B., November 1985, (PB86 142304/AS)A05.

UCB/EERC-85/13 "A Methodology for Computer-Aided Design of Earthquake-Resistant Steel Structures," by Austin, M.A., Pister, K.S. and Mahin, S.A., December 1985, (PB86 159480/AS)A10 .

UCB/EERC-85/14 "Response of Tension-Leg Platforms to Vertical Seismic Excitations," by Liou, G.-S., Penzien, J. and Yeung, R.W., December 1985, (PB87 124 871/AS)A08.

UCB/EERC-85/15 "Cyclic Loading Tests of Masonry Single Piers: Volume 4 - Additional Tests with Height to Width Ratio of 1," by Sveinsson, B., McNiven, H.D. and Sucuoglu, H., December 1985, (PB87 165031/AS)A08.

UCB/EERC-85/16 "An Experimental Program for Studying the Dynamic Response of a Steel Frame with a Variety of Infill Partitions," by Yanev, B. and McNiven, H.D., December 1985, (PB90 262 676)A05.

UCB/EERC-86/01 "A Study of Seismically Resistant Eccentrically Braced Steel Frame Systems," by Kasai, K. and Popov, E.P., January 1986, (PB87 124 178/AS)A14.

UCB/EERC-86/02 "Design Problems in Soil Liquefaction," by Seed, H.B., February 1986, (PB87 124 186/AS)A03.

UCB/EERC-86/03 "Implications of Recent Earthquakes and Research on Earthquake-Resistant Design and Construction of Buildings," by Bertero, V.V., March 1986, (PB87 124 194/AS)A05.

UCB/EERC-86/04 "The Use of Load Dependent Vectors for Dynamic and Earthquake Analyses," by Leger, P., Wilson, E.L. and Clough, R.W., March 1986, (PB87 124 202/AS)A12.

UCB/EERC-86/05 "Two Beam-To-Column Web Connections," by Tsai, K.-C. and Popov, E.P., April 1986, (PB87 124 301/AS)A04.

UCB/EERC-86/06 "Determination of Penetration Resistance for Coarse-Grained Soils using the Becker Hammer Drill," by Harder, L.F. and Seed, H.B., May 1986, (PB87 124 210/AS)A07.

UCB/EERC-86/07 "A Mathematical Model for Predicting the Nonlinear Response of Unreinforced Masonry Walls to In-Plane Earthquake Excitations," by Mengi, Y. and McNiven, H.D., May 1986, (PB87 124 780/AS)A06.

UCB/EERC-86/08 "The 19 September 1985 Mexico Earthquake: Building Behavior," by Bertero, V.V., July 1986.

UCB/EERC-86/09 "EACD-3D: A Computer Program for Three-Dimensional Earthquake Analysis of Concrete Dams," by Fok, K.-L., Hall, J.F. and Chopra, A.K., July 1986, (PB87 124 228/AS)A08.

UCB/EERC-86/10 "Earthquake Simulation Tests and Associated Studies of a 0.3-Scale Model of a Six-Story Concentrically Braced Steel Structure," by Uang, C.-M. and Bertero, V.V., December 1986, (PB87 163 564/AS)A17.

UCB/EERC-86/11 "Mechanical Characteristics of Base Isolation Bearings for a Bridge Deck Model Test," by Kelly, J.M., Buckle, I.G. and Koh, C.-G., November 1987, (PB90 262 668)A04.

UCB/EERC-86/12 "Effects of Axial Load on Elastomeric Isolation Bearings," by Koh, C.-G. and Kelly, J.M., November 1987, PB88-179015(A06).

UCB/EERC-87/01 "The FPS Earthquake Resisting System: Experimental Report," by Zayas, V.A., Low, S.S. and Mahin, S.A., June 1987, (PB88 170 287)A06.

UCB/EERC-87/02 "Earthquake Simulator Tests and Associated Studies of a 0.3-Scale Model of a Six-Story Eccentrically Braced Steel Structure," by Whittaker, A., Uang, C.-M. and Bertero, V.V., July 1987, (PB88 166 707/AS)A18.

UCB/EERC-87/03 "A Displacement Control and Uplift Restraint Device for Base-Isolated Structures," by Kelly, J.M., Griffith, M.C. and Aiken, I.D., April 1987, (PB88 169 933)A04.

UCB/EERC-87/04 "Earthquake Simulator Testing of a Combined Sliding Bearing and Rubber Bearing Isolation System," by Kelly, J.M. and Chalhoub, M.S., December 1990, PB92-192962(A09).

UCB/EERC-87/05 "Three-Dimensional Inelastic Analysis of Reinforced Concrete Frame-Wall Structures," by Moazzami, S. and Bertero, V.V., May 1987, (PB88 169 586/AS)A08.

UCB/EERC-87/06 "Experiments on Eccentrically Braced Frames with Composite Floors," by Ricles, J. and Popov, E., June 1987, (PB88 173 067/AS)A14.

UCB/EERC-87/07 "Dynamic Analysis of Seismically Resistant Eccentrically Braced Frames," by Ricles, J. and Popov, E., June 1987, (PB88 173 075/AS)A16.

UCB/EERC-87/08 "Undrained Cyclic Triaxial Testing of Gravels-The Effect of Membrane Compliance," by Evans, M.D. and Seed, H.B., July 1987, (PB88 173 257)A19.

UCB/EERC-87/09 "Hybrid Solution Techniques for Generalized Pseudo-Dynamic Testing," by Thewalt, C. and Mahin, S.A., July 1987, (PB 88 179 007)A07.

UCB/EERC-87/10 "Ultimate Behavior of Butt Welded Splices in Heavy Rolled Steel Sections," by Bruneau, M., Mahin, S.A. and Popov, E.P., September 1987, (PB90 254 285)A07.

UCB/EERC-87/11 "Residual Strength of Sand from Dam Failures in the Chilean Earthquake of March 3, 1985," by De Alba, P., Seed, H.B., Retamal, E. and Seed, R.B., September 1987, (PB88 174 321/AS)A03.

UCB/EERC-87/12 "Inelastic Seismic Response of Structures with Mass or Stiffness Eccentricities in Plan," by Bruneau, M. and Mahin, S.A., September 1987, (PB90 262 650/AS)A14.

UCB/EERC-87/13 "CSTRUCT: An Interactive Computer Environment for the Design and Analysis of Earthquake Resistant Steel Structures," by Austin, M.A., Mahin, S.A. and Pister, K.S., September 1987, (PB88 173 339/AS)A06.

UCB/EERC-87/14 "Experimental Study of Reinforced Concrete Columns Subjected to Multi-Axial Loading," by Low, S.S. and Moehle, J.P., September 1987, (PB88 174 347/AS)A07.

UCB/EERC-87/15 "Relationships between Soil Conditions and Earthquake Ground Motions in Mexico City in the Earthquake of Sept. 19, 1985," by Seed, H.B., Romo, M.P., Sun, J., Jaime, A. and Lysmer, J., October 1987, (PB88 178 991)A06.

UCB/EERC-87/16 "Experimental Study of Seismic Response of R. C. Setback Buildings," by Shahrooz, B.M. and Moehle, J.P., October 1987, (PB88 176 359)A16.

UCB/EERC-87/17 "The Effect of Slabs on the Flexural Behavior of Beams," by Pantazopoulou, S.J. and Moehle, J.P., October 1987, (PB90 262 700)A07.

UCB/EERC-87/18 "Design Procedure for R-FBI Bearings," by Mostaghel, N. and Kelly, J.M., November 1987, (PB90 262 718)A04.

UCB/EERC-87/19 "Analytical Models for Predicting the Lateral Response of R C Shear Walls: Evaluation of their Reliability," by Vulcano, A. and Bertero, V.V., November 1987, (PB88 178 983)A05.

UCB/EERC-87/20 "Earthquake Response of Torsionally-Coupled Buildings," by Hejal, R. and Chopra, A.K., December 1987, PB90-208638(A15).

UCB/EERC-87/21 "Dynamic Reservoir Interaction with Monticello Dam," by Clough, R.W., Ghanaat, Y. and Qiu, X-F., December 1987, (PB88 179 023)A07.

UCB/EERC-87/22 "Strength Evaluation of Coarse-Grained Soils," by Siddiqi, F.H., Seed, R.B., Chan, C.K., Seed, H.B. and Pyke, R.M., December 1987, (PB88 179 031)A04.

UCB/EERC-88/01 "Seismic Behavior of Concentrically Braced Steel Frames," by Khatib, I., Mahin, S.A. and Pister, K.S., January 1988, (PB91 210 898/AS)A11.

UCB/EERC-88/02 "Experimental Evaluation of Seismic Isolation of Medium-Rise Structures Subject to Uplift," by Griffith, M.C., Kelly, J.M., Coveney, V.A. and Koh, C.G., January 1988, (PB91 217 950/AS)A09.

UCB/EERC-88/03 "Cyclic Behavior of Steel Double Angle Connections," by Astaneh-Asl, A. and Nader, M.N., January 1988, (PB91 210 872)A05.

UCB/EERC-88/04 "Re-evaluation of the Slide in the Lower San Fernando Dam in the Earthquake of Feb. 9, 1971," by Seed, H.B., Seed, R.B., Harder, L.F. and Jong, H.-L., April 1988, (PB91 212 456/AS)A07.

UCB/EERC-88/05 "Experimental Evaluation of Seismic Isolation of a Nine-Story Braced Steel Frame Subject to Uplift," by Griffith, M.C., Kelly, J.M. and Aiken, I.D., May 1988, (PB91 217 968/AS)A07.

UCB/EERC-88/06 "DRAIN-2DX User Guide.," by Allahabadi, R. and Powell, G.H., March 1988, (PB91 212 530)A12.

UCB/EERC-88/07 "Theoretical and Experimental Studies of Cylindrical Water Tanks in Base-Isolated Structures," by Chalhoub, M.S. and Kelly, J.M., April 1988, (PB91 217 976/AS)A05.

UCB/EERC-88/08 "Analysis of Near-Source Waves: Separation of Wave Types Using Strong Motion Array Recording," by Darragh, R.B., June 1988, (PB91 212 621)A08.

UCB/EERC-88/09 "Alternatives to Standard Mode Superposition for Analysis of Non-Classically Damped Systems," by Kusainov, A.A. and Clough, R.W., June 1988, (PB91 217 992/AS)A04.

UCB/EERC-88/10 "The Landslide at the Port of Nice on October 16, 1979," by Seed, H.B., Seed, R.B., Schlosser, F., Blondeau, F. and Juran, I., June 1988, (PB91 210 914)A05.

UCB/EERC-88/11 "Liquefaction Potential of Sand Deposits Under Low Levels of Excitation," by Carter, D.P. and Seed, H.B., August 1988, (PB91 210 880)A15.

UCB/EERC-88/12 "Nonlinear Analysis of Reinforced Concrete Frames Under Cyclic Load Reversals," by Filippou, F.C. and Issa, A., September 1988, (PB91 212 589)A07.

UCB/EERC-88/13 "Implications of Recorded Earthquake Ground Motions on Seismic Design of Building Structures," by Uang, C.-M. and Bertero, V.V., November 1988, (PB91 212 548)A06.

UCB/EERC-88/14 "An Experimental Study of the Behavior of Dual Steel Systems," by Whittaker, A.S. , Uang, C.-M. and Bertero, V.V., September 1988, (PB91 212 712)A16.

UCB/EERC-88/15 "Dynamic Moduli and Damping Ratios for Cohesive Soils," by Sun, J.I., Golesorkhi, R. and Seed, H.B., August 1988, (PB91 210 922)A04.

UCB/EERC-88/16 "Reinforced Concrete Flat Plates Under Lateral Load: An Experimental Study Including Biaxial Effects," by Pan, A. and Moehle, J.P., October 1988, (PB91 210 856)A13.

UCB/EERC-88/17 "Earthquake Engineering Research at Berkeley - 1988," by EERC, November 1988, (PB91 210 864)A10.

UCB/EERC-88/18 "Use of Energy as a Design Criterion in Earthquake-Resistant Design," by Uang, C.-M. and Bertero, V.V., November 1988, (PB91 210 906/AS)A04.

UCB/EERC-88/19 "Steel Beam-Column Joints in Seismic Moment Resisting Frames," by Tsai, K.-C. and Popov, E.P., November 1988, (PB91 217 984/AS)A20.

UCB/EERC-88/20 "Base Isolation in Japan, 1988," by Kelly, J.M., December 1988, (PB91 212 449)A05.

UCB/EERC-89/01 "Behavior of Long Links in Eccentrically Braced Frames," by Engelhardt, M.D. and Popov, E.P., January 1989, (PB92 143 056)A18.

UCB/EERC-89/02 "Earthquake Simulator Testing of Steel Plate Added Damping and Stiffness Elements," by Whittaker, A., Bertero, V.V., Alonso, J. and Thompson, C., January 1989, (PB91 229 252/AS)A10.

UCB/EERC-89/03 "Implications of Site Effects in the Mexico City Earthquake of Sept. 19, 1985 for Earthquake-Resistant Design Criteria in the San Francisco Bay Area of California," by Seed, H.B. and Sun, J.I., March 1989, (PB91 229 369/AS)A07.

UCB/EERC-89/04 "Earthquake Analysis and Response of Intake-Outlet Towers," by Goyal, A. and Chopra, A.K., July 1989, (PB91 229 286/AS)A19.

UCB/EERC-89/05 "The 1985 Chile Earthquake: An Evaluation of Structural Requirements for Bearing Wall Buildings," by Wallace, J.W. and Moehle, J.P., July 1989, (PB91 218 008/AS)A13.

UCB/EERC-89/06 "Effects of Spatial Variation of Ground Motions on Large Multiply-Supported Structures," by Hao, H., July 1989, (PB91 229 161/AS)A08.

UCB/EERC-89/07 "EADAP - Enhanced Arch Dam Analysis Program: Users's Manual," by Ghanaat, Y. and Clough, R.W., August 1989, (PB91 212 522)A06.

UCB/EERC-89/08 "Seismic Performance of Steel Moment Frames Plastically Designed by Least Squares Stress Fields," by Ohi, K. and Mahin, S.A., August 1989, (PB91 212 597)A05.

UCB/EERC-89/09 "Feasibility and Performance Studies on Improving the Earthquake Resistance of New and Existing Buildings Using the Friction Pendulum System," by Zayas, V., Low, S., Mahin, S.A. and Bozzo, L., July 1989, (PB92 143 064)A14.

UCB/EERC-89/10 "Measurement and Elimination of Membrane Compliance Effects in Undrained Triaxial Testing," by Nicholson, P.G., Seed, R.B. and Anwar, H., September 1989, (PB92 139 641/AS)A13.

UCB/EERC-89/11 "Static Tilt Behavior of Unanchored Cylindrical Tanks," by Lau, D.T. and Clough, R.W., September 1989, (PB92 143 049)A10.

UCB/EERC-89/12 "ADAP-88: A Computer Program for Nonlinear Earthquake Analysis of Concrete Arch Dams," by Fenves, G.L., Mojtahedi, S. and Reimer, R.B., September 1989, (PB92 139 674/AS)A07.

UCB/EERC-89/13 "Mechanics of Low Shape Factor Elastomeric Seismic Isolation Bearings," by Aiken, I.D., Kelly, J.M. and Tajirian, F.F., November 1989, (PB92 139 732/AS)A09.

UCB/EERC-89/14 "Preliminary Report on the Seismological and Engineering Aspects of the October 17, 1989 Santa Cruz (Loma Prieta) Earthquake," by EERC, October 1989, (PB92 139 682/AS)A04.

UCB/EERC-89/15 "Experimental Studies of a Single Story Steel Structure Tested with Fixed, Semi-Rigid and Flexible Connections," by Nader, M.N. and Astaneh-Asl, A., August 1989, (PB91 229 211/AS)A10.

UCB/EERC-89/16 "Collapse of the Cypress Street Viaduct as a Result of the Loma Prieta Earthquake," by Nims, D.K., Miranda, E., Aiken, I.D., Whittaker, A.S. and Bertero, V.V., November 1989, (PB91 217 935/AS)A05.

UCB/EERC-90/01 "Mechanics of High-Shape Factor Elastomeric Seismic Isolation Bearings," by Kelly, J.M., Aiken, I.D. and Tajirian, F.F., March 1990.

UCB/EERC-90/02 "Javid's Paradox: The Influence of Preform on the Modes of Vibrating Beams," by Kelly, J.M., Sackman, J.L. and Javid, A., May 1990, (PB91 217 943/AS)A03.

UCB/EERC-90/03 "Earthquake Simulator Testing and Analytical Studies of Two Energy-Absorbing Systems for Multistory Structures," by Aiken, I.D. and Kelly, J.M., October 1990, (PB92 192 988)A13.

UCB/EERC-90/04 "Unassigned," by Unassigned, 1990.

UCB/EERC-90/05 "Preliminary Report on the Principal Geotechnical Aspects of the October 17, 1989 Loma Prieta Earthquake," by Seed, R.B., Dickenson, S.E., Riemer, M.F., Bray, J.D., Sitar, N., Mitchell, J.K., Idriss, I.M., Kayen, R.E., Kropp, A., Harder, L.F., Jr. and Power, M.S., April 1990, (PB 192 970)A08.

UCB/EERC-90/06 "Models of Critical Regions in Reinforced Concrete Frames Under Seismic Excitations," by Zulfiqar, N. and Filippou, F.C., May 1990.

UCB/EERC-90/07 "A Unified Earthquake-Resistant Design Method for Steel Frames Using ARMA Models," by Takewaki, I., Conte, J.P., Mahin, S.A. and Pister, K.S., June 1990, PB92-192947(A06).

UCB/EERC-90/08 "Soil Conditions and Earthquake Hazard Mitigation in the Marina District of San Francisco," by Mitchell, J.K., Masood, T., Kayen, R.E. and Seed, R.B., May 1990, (PB 193 267/AS)A04.

UCB/EERC-90/09 "Influence of the Earthquake Ground Motion Process and Structural Properties on Response Characteristics of Simple Structures," by Conte, J.P., Pister, K.S. and Mahin, S.A., July 1990, (PB92 143 064)A15.

UCB/EERC-90/10 "Experimental Testing of the Resilient-Friction Base Isolation System," by Clark, P.W. and Kelly, J.M., July 1990, (PB92 143 072)A08.

UCB/EERC-90/11 "Seismic Hazard Analysis: Improved Models, Uncertainties and Sensitivities," by Araya, R. and Der Kiureghian, A., March 1988, PB92-193010(A08).

UCB/EERC-90/12 "Effects of Torsion on the Linear and Nonlinear Seismic Response of Structures," by Sedarat, H. and Bertero, V.V., September 1989, (PB92 193 002/AS)A15.

UCB/EERC-90/13 "The Effects of Tectonic Movements on Stresses and Deformations in Earth Embankments," by Bray, J. D., Seed, R. B. and Seed, H. B., September 1989, PB92-192996(A18).

UCB/EERC-90/14 "Inelastic Seismic Response of One-Story, Asymmetric-Plan Systems," by Goel, R.K. and Chopra, A.K., October 1990, (PB93 114 767)A11.

UCB/EERC-90/15 "Dynamic Crack Propagation: A Model for Near-Field Ground Motion.," by Seyyedian, H. and Kelly, J.M., 1990.

UCB/EERC-90/16 "Sensitivity of Long-Period Response Spectra to System Initial Conditions," by Blasquez, R., Ventura, C. and Kelly, J.M., 1990.

UCB/EERC-90/17 "Behavior of Peak Values and Spectral Ordinates of Near-Source Strong Ground-Motion over a Dense Array," by Niazi, M., June 1990, (PB93 114 833)A07.

UCB/EERC-90/18 "Material Characterization of Elastomers used in Earthquake Base Isolation," by Papoulia, K.D. and Kelly, J.M., 1990, PB94-190063(A08).

UCB/EERC-90/19 "Cyclic Behavior of Steel Top-and-Bottom Plate Moment Connections," by Harriott, J.D. and Astaneh-Asl, A., August 1990, (PB91 229 260/AS)A05.

UCB/EERC-90/20 "Seismic Response Evaluation of an Instrumented Six Story Steel Building," by Shen, J.-H. and Astaneh-Asl, A., December 1990, (PB91 229 294/AS)A04.

UCB/EERC-90/21 "Observations and Implications of Tests on the Cypress Street Viaduct Test Structure," by Bollo, M., Mahin, S.A., Moehle, J.P., Stephen, R.M. and Qi, X., December 1990, (PB93 114 775)A13.

UCB/EERC-91/01 "Experimental Evaluation of Nitinol for Energy Dissipation in Structures," by Nims, D.K., Sasaki, K.K. and Kelly, J.M., 1991.

UCB/EERC-91/02 "Displacement Design Approach for Reinforced Concrete Structures Subjected to Earthquakes," by Qi, X. and Moehle, J.P., January 1991, (PB93 114 569/AS)A09.

UCB/EERC-91/03 "A Long-Period Isolation System Using Low-Modulus High-Damping Isolators for Nuclear Facilities at Soft-Soil Sites," by Kelly, J.M., March 1991, (PB93 114 577/AS)A10.

UCB/EERC-91/04 "Dynamic and Failure Characteristics of Bridgestone Isolation Bearings," by Kelly, J.M., April 1991, (PB93 114 528)A05.

UCB/EERC-91/05 "Base Sliding Response of Concrete Gravity Dams to Earthquakes," by Chopra, A.K. and Zhang, L., May 1991, (PB93 114 544/AS)A05.

UCB/EERC-91/06 "Computation of Spatially Varying Ground Motion and Foundation-Rock Impedance Matrices for Seismic Analysis of Arch Dams," by Zhang, L. and Chopra, A.K., May 1991, (PB93 114 825)A07.

UCB/EERC-91/07 "Estimation of Seismic Source Processes Using Strong Motion Array Data," by Chiou, S.-J., July 1991, (PB93 114 551/AS)A08.

UCB/EERC-91/08 "A Response Spectrum Method for Multiple-Support Seismic Excitations," by Der Kiureghian, A. and Neuenhofer, A., August 1991, (PB93 114 536)A04.

UCB/EERC-91/09 "A Preliminary Study on Energy Dissipating Cladding-to-Frame Connection," by Cohen, J.M. and Powell, G.H., September 1991, (PB93 114 510)A05.

UCB/EERC-91/10 "Evaluation of Seismic Performance of a Ten-Story RC Building During the Whittier Narrows Earthquake," by Miranda, E. and Bertero, V.V., October 1991, (PB93 114 783)A06.

UCB/EERC-91/11 "Seismic Performance of an Instrumented Six-Story Steel Building," by Anderson, J.C. and Bertero, V.V., November 1991, (PB93 114 809)A07.

UCB/EERC-91/12 "Performance of Improved Ground During the Loma Prieta Earthquake," by Mitchell, J.K. and Wentz, Jr., F.J., October 1991, (PB93 114 791)A06.

UCB/EERC-91/13 "Shaking Table - Structure Interaction," by Rinawi, A.M. and Clough, R.W., October 1991, (PB93 114 917)A13.

UCB/EERC-91/14 "Cyclic Response of RC Beam-Column Knee Joints: Test and Retrofit," by Mazzoni, S., Moehle, J.P. and Thewalt, C.R., October 1991, (PB93 120 277)A03.

UCB/EERC-91/15 "Design Guidelines for Ductility and Drift Limits: Review of State-of-the-Practice and State-of-the-Art in Ductility and Drift-Based Earthquake-Resistant Design of Buildings," by Bertero, V.V., Anderson, J.C., Krawinkler, H., Miranda, E. and The CUREe and The Kajima Research Teams, July 1991, (PB93 120 269)A08.

UCB/EERC-91/16 "Evaluation of the Seismic Performance of a Thirty-Story RC Building," by Anderson, J.C., Miranda, E., Bertero, V.V. and The Kajima Project Research Team, July 1991, (PB93 114 841)A12.

UCB/EERC-91/17 "A Fiber Beam-Column Element for Seismic Response Analysis of Reinforced Concrete Structures," by Taucer, F., Spacone, E. and Filippou, F.C., December 1991, (PB94 117 629AS)A07.

UCB/EERC-91/18 "Investigation of the Seismic Response of a Lightly-Damped Torsionally-Coupled Building," by Boroschek, R. and Mahin, S.A., December 1991, (PB93 120 335)A13.

UCB/EERC-92/01 "Studies of a 49-Story Instrumented Steel Structure Shaken During the Loma Prieta Earthquake," by Chen, C.-C., Bonowitz, D. and Astaneh-Asl, A., February 1992, (PB93 221 778)A08.

UCB/EERC-92/02 "Response of the Dumbarton Bridge in the Loma Prieta Earthquake," by Fenves, G.L., Filippou, F.C. and Sze, D.T., January 1992, (PB93 120 319)A09.

UCB/EERC-92/03 "Models for Nonlinear Earthquake Analysis of Brick Masonry Buildings," by Mengi, Y., McNiven, H.D. and Tanrikulu, A.K., March 1992, (PB93 120 293)A08.

UCB/EERC-92/04 "Shear Strength and Deformability of RC Bridge Columns Subjected to Inelastic Cyclic Displacements," by Aschheim, M. and Moehle, J.P., March 1992, (PB93 120 327)A06.

UCB/EERC-92/05 "Parameter Study of Joint Opening Effects on Earthquake Response of Arch Dams," by Fenves, G.L., Mojtahedi, S. and Reimer, R.B., April 1992, (PB93 120 301)A04.

UCB/EERC-92/06 "Seismic Behavior and Design of Semi-Rigid Steel Frames," by Nader, M.N. and Astaneh-Asl, A., May 1992, PB93-221760(A17).

UCB/EERC-92/07 "A Beam Element for Seismic Damage Analysis," by Spacone, E., Ciampi, V. and Filippou, F.C., August 1992, (PB95-192126)A06.

UCB/EERC-92/08 "Nonlinear Static and Dynamic Analysis of Reinforced Concrete Subassemblages," by Filippou, F.C., D'Ambrisi, A. and Issa, A., August 1992, PB95-192175(A09).

UCB/EERC-92/09 "Evaluation of Code Accidental-Torsion Provisions Using Earthquake Records from Three Nominally Symmetric-Plan Buildings," by De la Llera, J.C. and Chopra, A.K., September 1992, (PB94 117 611)A08.

UCB/EERC-92/10 "Slotted Bolted Connection Energy Dissipators," by Grigorian, C.E., Yang, T.-S. and Popov, E.P., July 1992, (PB92 120 285)A03.

UCB/EERC-92/11 "Mechanical Characteristics of Neoprene Isolation Bearings," by Kelly, J.M. and Quiroz, E., August 1992, (PB93 221 729)A07.

UCB/EERC-92/12 "Application of a Mass Damping System to Bridge Structures," by Hasegawa, K. and Kelly, J.M., August 1992, (PB93 221 786)A06.

UCB/EERC-92/13 "Earthquake Engineering Research at Berkeley - 1992," by EERC, October 1992, PB93-223709(A10).

UCB/EERC-92/14 "Earthquake Risk and Insurance," by Brillinger, D.R., October 1992, (PB93 223 352)A03.

UCB/EERC-92/15 "A Friction Mass Damper for Vibration Control," by Inaudi, J.A. and Kelly, J.M., October 1992, (PB93 221 745)A04.

UCB/EERC-92/16 "Tall Reinforced Concrete Buildings: Conceptual Earthquake-Resistant Design Methology," by Bertero, R.D. and Bertero, V.V., December 1992, (PB93 221 695)A12.

UCB/EERC-92/17 "Performance of Tall Buildings During the 1985 Mexico Earthquakes," by Terán-Gilmore, A. and Bertero, V.V., December 1992, (PB93 221 737)A11.

UCB/EERC-92/18 "Dynamic Analysis of Nonlinear Structures using State-Space Formulation and Partitioned Integration Schemes," by Inaudi, J.A. and De la Llera, J.C., December 1992, (PB94 117 702/AS/A05.

UCB/EERC-93/01 "Seismic Performance of an Instrumented Six-Story Reinforced-Concrete Building," by Anderson, J.C. and Bertero, V.V., 1993.

UCB/EERC-93/02 "Evaluation of an Active Variable-Damping-Structure," by Polak, E., Meeker, G., Yamada, K. and Kurata, N., 1993, (PB93 221 711)A05.

UCB/EERC-93/03 "An Experimental Study of Flat-Plate Structures under Vertical and Lateral Loads," by Hwang, S.-H. and Moehle, J.P., February 1993, (PB94 157 690/AS)A13.

UCB/EERC-93/04 "Seismic Performance of a 30-Story Building Located on Soft Soil and Designed According to UBC 1991," by Terán-Gilmore, A. and Bertero, V.V., 1993, (PB93 221 703)A17.

UCB/EERC-93/05 "Multiple-Support Response Spectrum Analysis of the Golden Gate Bridge," by Nakamura, Y., Der Kiureghian, A. and Liu, D., May 1993, (PB93 221 752)A05.

UCB/EERC-93/06 "On the Analysis of Structures with Viscoelastic Dampers," by Inaudi, J.A., Zambrano, A. and Kelly, J.M., August 1993, PB94-165867(A06).

UCB/EERC-93/07 "Earthquake Analysis and Response of Concrete Gravity Dams Including Base Sliding," by Chávez, J.W. and Fenves, G.L., December 1993, (PB94 157 658/AS)A10.

UCB/EERC-93/08 "Model for Anchored Reinforcing Bars under Seismic Excitations," by Monti, G., Spacone, E. and Filippou, F.C., December 1993, PB95-192183(A05).

UCB/EERC-93/09 "A Methodology for Design of Viscoelastic Dampers in Earthquake-Resistant Structures," by Abbas, H. and Kelly, J.M., November 1993, PB94-190071(A10).

UCB/EERC-93/10 "Tuned Mass Dampers Using Viscoelastic Dampers," by Inaudi, J.A., Lopez-Almansa, F. and Kelly, J.M., December 1993.

UCB/EERC-93/11 "Nonlinear Homogeneous Dynamical Systems," by Inaudi, J.A. and Kelly, J.M., December 1993.

UCB/EERC-93/12 "Synthesized Strong Ground Motions for the Seismic Condition Assessment of the Eastern Portion of the San Francisco Bay Bridge," by Bolt, B.A. and Gregor, N.J., December 1993, PB94-165842(A10).

UCB/EERC-93/13 "On the Analysis of Structures with Energy Dissipating Restraints," by Inaudi, J.A., Nims, D.K. and Kelly, J.M., December 1993, PB94-203619(A07).

UCB/EERC-94/01 "Preliminary Report on the Seismological and Engineering Aspects of the January 17, 1994 Northridge Earthquake," by EERC, January 1994, (PB94 157 666/AS)A05.

UCB/EERC-94/02 "Energy Dissipation with Slotted Bolted Connections," by Grigorian, C.E. and Popov, E.P., February 1994, PB94-164605.

UCB/EERC-94/03 "The Influence of Plate Flexibility on the Buckling Load of Elastomeric Isolators," by Kelly, J.M., March 1994, PB95-192134(A04).

UCB/EERC-94/04 "Insitu Test Results from Four Loma Prieta Earthquake Liquefaction Sites: SPT, CPT, DMT and Shear Wave Velocity," by Mitchell, J.K., Lodge, A.L., Coutinho, R.Q., Kayen, R.E., Seed, R.B., Nishio, S. and Stokoe II, K.H., April 1994, PB94-190089(A09).

UCB/EERC-94/05 "Seismic Response of Steep Natural Slopes," by Sitar, N. and Ashford, S.A., May 1994, PB94-203643(A10).

UCB/EERC-94/06 "Small-Scale Testing of a Self-Centering Friction Energy Dissipator for Structures," by Nims, D.K. and Kelly, J.M., August 1994.

UCB/EERC-94/07 "Accidental and Natural Torsion in Earthquake Response and Design of Buildings," by De la Llera, J.C. and Chopra, A.K., June 1994, PB94-203627(A14).

UCB/EERC-94/08 "Preliminary Report on the Principal Geotechnical Aspects of the January 17, 1994 Northridge Earthquake," by Stewart, J.P., Bray, J.D., Seed, R.B. and Sitar, N., June 1994, PB94203635(A12).

UCB/EERC-94/09 "Performance of Steel Building Structures During the Northridge Earthquake," by Bertero, V.V., Anderson, J.C. and Krawinkler, H., August 1994, PB95-112025(A10).

UCB/EERC-94/10 "Manual for Menshin Design of Highway Bridges: Ministry of Construction, Japan," by Sugita, H. and Mahin, S., August 1994, PB95-192100(A08).

UCB/EERC-94/11 "Earthquake Analysis and Response of Two-Level Viaducts," by Singh, S.P. and Fenves, G.L., October 1994, (A09).

UCB/EERC-94/12 "Response of the Northwest Connector in the Landers and Big Bear Earthquakes," by Fenves, G.L. and Desroches, R., December 1994, PB95-192001(A08).

UCB/EERC-95/01 "Geotechnical Reconnaissance of the Effects of the January 17, 1995, Hyogoken-Nanbu Earthquake, Japan," by , August 1995.

UCB/EERC-95/02 "The Attenuation of Strong Ground Motion Displacement," by Gregor, N.J., June 1995.

UCB/EERC-95/03 "Upgrading Bridge Outrigger Knee Joint Systems," by Stojadinovic, B. and Thewalt, C.R., June 1995.

UCB/EERC-95/04 "Earthquake Hazard Reduction in Historical Buildings Using Seismic Isolation," by Garevski, M., June 1995.

UCB/EERC-95/05 "Final Report on the International Workshop on the Use of Rubber-Based Bearings for the Earthquake Protection of Building," by Kelly, J.M., May 1995.

UCB/EERC-95/06 "Seismic Rehabilitation of Framed Buildings Infilled with Unreinforced Masonry Walls Using Post-Tensioned Steel Braces," by Terán-Gilmore, A., Bertero, V.V. and Youssef, N., June 1995.

UCB/EERC-95/07 "Earthquake Analysis and Response of Concrete Arch Dams," by Tan, H. and Chopra, A.K., August 1995.

UCB/EERC-95/08 "Behavior of Pre-Northridge Moment Resisting Steel Connections," by Yang, T.-S. and Popov, E.P., August 1995.

UCB/EERC-95/09 "Seismic Behavior and Retrofit of Older Reinforced Concrete Bridge T-Joints," by Lowes, L.N. and Mochle, J.P., September 1995.

UCB/EERC-95/10 "Seismological and Engineering Aspects of the 1995 Hyogoken-Nanbu (Kobe) Earthquake," by EERC, November 1995.

UCB/EERC-95/11 "Studies in Steel Moment Resisting Beam-to-Column Connections for Seismic-Resistant Design," by Blackman, B. and Popov, E.P., October 1995.